NTI

MAY 1968

RECEIVED
NASA STI FACILITY
INPUT BRANCH

GPO PRICE $ _____

CFSTI PRICE(S) $ _____

Hard copy (HC) _3.00_

Microfiche (MF) _.65_

ff 653 July 65

N 68-26741
(ACCESSION NUMBER)

_120_
(PAGES)

(THRU)

(CODE)

_30_
(CATEGORY)

CR 61816
(NASA CR OR TMX OR AD NUMBER)

FACILITY FORM 602

CLUSTER A MISSION STUDIES

Augmentation Task No. 23

LMSC-A842318   5 September 1967

Prepared Under Contract No. NAS8-21003 by

LOCKHEED MISSILES & SPACE COMPANY
A Group Division of Lockheed Aircraft Corporation
Sunnyvale, California

for

NATIONAL AERONAUTICS AND SPACE ADMINISTRATION
GEORGE C. MARSHALL SPACE FLIGHT CENTER
Huntsville, Alabama

Prepared by: _____   Approved by: _____

LOCKHEED MISSILES & SPACE COMPANY

LMSC-A842318

CONTENTS

LOCKHEED MISSILES & SPACE COMPANY

LOCKHEED MISSILES & SPACE COMPANY

ILLUSTRATIONS

LOCKHEED MISSILES & SPACE COMPANY

LOCKHEED MISSILES & SPACE COMPANY

LOCKHEED MISSILES & SPACE COMPANY

TABLES

Part I
56-DAY-TIMELINE STUDY

I.1 INTRODUCTION

The 56-day mission has two primary objectives: (1) the intensive observation of the sun with a manned observatory in space, ATM; and (2) the measurement of the effects on men and vehicles of prolonged periods in space. As secondary objectives, the mission has certain biological, astronomical, and geophysical experiments.

Groundrules and assumptions are as follows:

- Launch of AAP-3 and AAP-4 is from Cape Kennedy in mid-1969 at an inclination angle of 28.5 deg.

- At the time of launch, the Cluster is at an altitude of 250 nm.

- The Cluster weight of AAP-2, AAP-3, and AAP-4 is constant at 105,000 lb; its area in the line of flight is constant at 2,700 sq ft.

- Days 1 − 6 inclusive are reserved for launch; days 55 and 56 are reserved for reentry.

- Days 7, 14, 21, 28, 35, 42, and 49 are reserved for rest and recreation. Days 17, 26, 39, and 54 are reserved for EVA.

- EVA is scheduled when the vehicle is over the U.S., but not in the South Atlantic Anomaly.

- No experiments are scheduled during reserved days.

- The command module, CM, is occupied at all times, although the occupant can be asleep.

- No more than one repetition of a particular experiment can be scheduled simultaneously.

- Each man has 12 to 12.5 hr per day for sleep, eating, hygiene, and personal duties; 2 to 4 manhours per day are scheduled for housekeeping.

I.2 TIMELINE TABLES

Table I-1 is the timeline for the first 6 days, including launch of AAP-3, launch of AAP-4, rendezvous of AAP-3 with AAP-4, rendezvous of AAP-3/-4 with the Cluster, AAP-2, and activation of the Cluster. Table I-2 is a timeline for days 7 to 54 inclusive, giving the day, the revolution within the day, and, where necessary, the 30 min period within the revolution during which each of the three crewmen is performing a particular activity. In Table I-2, references are made to a typical R&R day (Table I-4) and typical EVA day (Table I-5). These are in the same format as Table I-2. Table I-3 is the timeline for days 55 and 56, reentry and recovery. Like Table I-1, it assigns each activity to all three crewmen and has the time in blocks.

The following is an explanation of the listing codes appearing in Tables I-2, I-4, and I-5:

ATM-A	manned solar observatory experiments in active mode (two men)
ATM-P	manned solar observatory experiments in patrol mode (one man)
CM	activity specifically designed to ensure that the command module is occupied at all times
DACT	deactivation of the Lunar Module – Telescope Module
EHK	1-1/2 hr period, scheduled once per day per man, for eating, hygiene, and personal housekeeping
EVA	specific 3-hr period during which one crewman is outside the AM
M18	Vectorcardiogram Experiment – the dash numbers indicate the subject astronaut
M50	Metabolic Cost – with the second crewman as subject, performed during the first half of the mission
M51	Cardiovascular Function – the dash numbers indicate the subject

I-2

M52	Bone and Muscle Changes, and with it the Mass Measuring Device, M56, and Body Mass Measuring System, M58. Each man performs these experiments on himself.
M53	Human Vestibular Function – divided into three experiments A, B, C performed on crewmen 3, 2, and 1, respectively.
M57	Total Body Exercise System – performed by each crewman on himself, three times during the mission.
PREP	3-hr period during which two crewmen prepare in AM for EVA
POST	1-1/2 hr period after EVA during which two crewmen doff suits in AM
RES	approximately 1 manhr per experiment day for experiments involving photography and/or targets
R&R	Specific time during R&R days reserved for each crewman's rest and recreation
SEH	10-1/2 hr period for each crewman each day, during which he has 8 hrs continuous sleep, two meals, and hygiene and personal housekeeping time
S19	UV Stellar Astronomy – performed throughout the whole mission
S363	UV Airglow Horizon Photography
S69	X-ray Astronomy, formerly S17
S70	UV X-ray Solar Astronomy, formerly S20
VHK	Vehicle Housekeeping, with approximately 1 manhr per day scheduled.

LOCKHEED MISSILES & SPACE COMPANY

Table I-1

LAUNCH AND ACTIVATION

Time; Hours, Minutes	Activity, Assigned to all 3 Men
DAY 1	
1200 - 1210	Launch of AAP-3 from KSC complex 34, includes S-IVB, IU, SLA, CSM
1210 - 1330	Insertion into elliptical orbit, start insertion checklist
1330 - 1350	Verify orbit, finish checklist
1350 - 1420	Jettison S-IVB, prepare for circularization
1420 - 1600	Circularization at 110 nm, start vehicle systems checklist
1600 - 1700	Verify orbit, mission lifetime, complete vehicle checklist and navigation checks
1700 - 1800	AAP-4 launch preparations
1800 - 2000	Eat, hygiene
2000 - 2400	First 4 hr of 10-hr sleep – hygiene period
DAY 2	
0000 - 0600	Simultaneous sleep and hygiene
0600 - 0800	Eat, hygiene
0800 - 1100	Review and preparation for AAP-4 launch, in communications with KSC
1100 - 1200	Eat, hygiene, housekeeping
1200 - 1300	Immediate preparation for AAP-4 launch
1300 - 1310	Launch of AAP-4 from KSC complex 37, includes S-IVB, IU, SLA, LM, ATM

LOCKHEED MISSILES & SPACE COMPANY

1310 - 1430	Insertion of AAP-4 into circular orbit, 160 nm
1430	CSM phase adjust (NC1)
1515	CSM height and plane adjust (NCC)
1600	CSM circularization (NSR) at 150 nm, below and behind AAP-4
1630	CSM TPI
1700 - 1730	CSM braking, 160-nm circular orbit
1730 - 1900	Dock CSM to AAP-4, remove probe and drogue, check hatches, pressurize LM
1900 - 2025	CSM/LM/ATM withdrawal from S-IVB of AAP-4, jettison S-IVB
2025	CSM/LM/ATM phase maneuver, NCH1, HAW
2030 - 2130	Eat, hygiene
2130 - 2400	First 2-1/2 hr of 10-hr sleep-hygiene

DAY 3

0000 - 0730	Balance of 10-hr sleep-hygiene period
0730 - 0830	Eat, housekeeping
0830 - 1230	Prepare to renezvous with Cluster
1230	Height and plane adjust manuever
1330	LM/ATM/CSM coelliptic with Cluster
1400 - 1500	Eat, hygiene
1500 - 1600	Two men enter LM/ATM
1600 - 1900	LM/ATM checkout
1900 - 2100	CSM/LM/ATM system checkout
2100 - 2400	First 3 hr of 10-hr sleep-hygiene period

DAY 4

0000 – 0700	7 hr of 10-hr sleep hygiene
0700 – 0800	Eat, housekeeping
0800 – 1030	Prepare for docking with Cluster
1040	LM/ATM/CSM correction (NCC)
1110	LM/ATM/CSM coelliptic
1215	LM/ATM/CSM TPI
1300	LM/ATM/CSM braking
1330	LM/ATM docking, port 1
1400	CSM docking, port 5
1500 – 1800	Activate MDA, deploy solar panels
1800 – 1900	LM crew return to CSM
1900 – 2000	Eat, housekeeping
2000 – 2400	First 3 hr of 10-hr sleep-hygiene period

DAY 5

0000 – 0700	7 remaining hr of sleep-hygiene period
0700 – 0800	Eat, housekeeping
0800 – 1200	Two men activate Airlock Module
1200 – 1300	Eat
1300 – 1800	Prepare Cluster
1800 – 2000	Eat, housekeeping
2000 – 2400	First 4 hr of 10-hr sleep-hygiene period

DAY 6

0000 - 0600	6 hr of 10-hr sleep-hygiene period
0600 - 0800	Eat, housekeeping
0800 - 1200	Prepare Cluster, including OWS
1200 - 1300	Eat
1300 - 1800	Prepare Cluster, including OWS
1800 - 1900	Eat
1900 - 2400	Final checkout, Experiment M439, prepare for phasing with experiment schedule, days 7 through 53

Table I-2

DAYS 7-54 INCLUSIVE

DAY 7

This day was reserved for rest and recreation. A typical R & R day is given in Table I-4.

DAY 8

Rev	Crew 1	Crew 2	Crew 3	Rev	Crew 1	Crew 2	Crew 3
1	SEH	VHK	M52	9	ATM-P	SEH	SEH
	SEH	M18-2	M18-2	10	EHK	SEH	SEH
	SEH	M18-3	M18-3	11		M52	SEH
2	SEH	M51-3	M51-3		M18-1	M18-1	SEH
	SEH	M51-3	M51-3		M51-2	M51-2	SEH
	SEH	M52	VHK	12	M51-2	M51-2	SEH
3	SEH				M53B	M53B	SEH
	SEH	M53A	M53A		M53B	M53B	SEH
	SEH		EHK	13	VHK	EHK	SEH
4	SEH	SEH	EHK			EHK	SEH
	SEH	SEH	EHK		M52	EHK	SEH
	SEH	SEH	M52	14	ATM-P	M52	CM
5	SEH	SEH	ATM-P		ATM-P	CM	M52
6	SEH	SEH	ATM-P		ATM-P	CM	
7	SEH	SEH	SEH	15	ATM-A	ATM-A	CM
8	ATM-P	SEH	SEH	16	ATM-A	ATM-A	CM

DAY 9

Rev	Crew 1	Crew 2	Crew 3	Rev	Crew 1	Crew 2	Crew 3
1	SEH	ATM-A	ATM-A	10	ATM-P	SEH	SEH
2	SEH	ATM-A	ATM-A	11	EHK	ATM-P	SEH
3	SEH	ATM-A	ATM-A	12	M52	ATM-P	SEH
4	SEH	SEH	EHK			ATM-P	SEH
5	SEH	SEH	ATM-P		VHK	ATM-P	SEH
6	SEH	SEH	ATM-P	13		EHK	SEH
7	SEH	SEH	SEH	14		VHK	CM
8	M52	SEH	SEH		M53C	M53C	CM
	VHK	SEH	SEH		M53C	M53C	CM
		SEH	SEH	15	CM	ATM-A	ATM-A
9	ATM-P	SEH	SEH	16	CM	ATM-A	ATM-A

DAY 10

Rev	Crew 1	Crew 2	Crew 3	Rev	Crew 1	Crew 2	Crew 3
1	SEH	ATM-A	ATM-A	9	ATM-P	SEH	SEH
2	SEH	ATM-A	ATM-A	10	EHK	SEH	SEH
3	SEH	M57	VHK	11	S19	S19	SEH
	SEH	M57		12		VHK	SEH
	SEH	M53A	M53A		M53B	M53B	SEH
4	SEH	SEH	EHK		M53B	M53B	SEH
5	SEH	SEH	ATM-P	13	ATM-P	EHK	SEH
6	SEH	SEH	ATM-P	14	ATM-A	ATM-A	CM
7	SEH	SEH	SEH	15	ATM-A	ATM-A	CM
8	ATM-P	SEH	SEH				

LOCKHEED MISSILES & SPACE COMPANY

DAY 11

Rev	Crew 1	Crew 2	Crew 3	Rev	Crew 1	Crew 2	Crew 3
1	SEH	ATM-A	ATM-A	11	VHK		SEH
2	SEH	ATM-A	ATM-A			VHK	SEH
3	SEH	ATM-A	ATM-A		M53C	M53C	SEH
4	SEH	SEH	EHK	12	M53C	M53C	SEH
5	SEH	SEH	ATM-P		M51-1	M51-1	SEH
6	SEH	SEH	ATM-P		M51-1	M51-1	SEH
7	SEH	SEH	SEH	13	ATM-P	EHK	SEH
8	ATM-P	SEH	SEH	14	ATM-A	ATM-A	CM
9	ATM-P	SEH	SEH	15	ATM-A	ATM-A	CM
10	EHK	SEH	SEH				

DAY 12

Rev	Crew 1	Crew 2	Crew 3	Rev	Crew 1	Crew 2	Crew 3
1	SEH	ATM-A	ATM-A	9	ATM-P	SEH	SEH
2	SEH	ATM-A	ATM-A	10	EHK	SEH	SEH
3	SEH	M50	M50	11	S19	S19	SEH
	SEH	M50	M50	12	VHK		SEH
	SEH	M53A	M53A		M53B	M53B	SEH
4	SEH	SEH	EHK		M53B	M53B	SEH
5	SEH	SEH	ATM-P	13	ATM-P	EHK	SEH
6	SEH	SEH	ATM-P	14	ATM-A	ATM-A	CM
7	SEH	SEH	SEH	15	ATM-A	ATM-A	CM
8	ATM-P	SEH	SEH	16	SEH	ATM-A	ATM-A

DAY 13

Rev	Crew 1	Crew 2	Crew 3		Rev	Crew 1	Crew 2	Crew 3
1	SEH	ATM-A	ATM-A		10	M50	M50	SEH
2	SEH	ATM-A	ATM-A			M50	M50	SEH
3	SEH	SEH	EHK			VHK		SEH
4	SEH	SEH	ATM-P		11		VHK	SEH
5	SEH	SEH	ATM-P			M53C	M53C	SEH
6	SEH	SEH	SEH			M53C	M53C	SEH
7	ATM-P	SEH	SEH		12	ATM-P	EHK	SEH
8	ATM-P	SEH	SEH		13	ATM-A	ATM-A	CM
9	EHK	SEH	SEH		14	ATM-A	ATM-A	CM
					15	CM	ATM-A	ATM-A
					16	CM	ATM-A	ATM-A

DAY 14

This day was reserved for rest and recreation. A typical R & R day is given in Table I-4.

DAY 15

Rev	Crew 1	Crew 2	Crew 3		Rev	Crew 1	Crew 2	Crew 3
1	SEH	M18-2	M18-2		9	ATM-P	SEH	SEH
	SEH	M18-3	M18-3		10	EHK	SEH	SEH
	SEH	VHK			11	M50	M50	SEH
2	SEH	S19	S19			M50	M50	SEH
3	SEH		VHK			M18-1	M18-1	SEH
	SEH	M51-3	M51-3		12	M51-2	M51-2	SEH
	SEH	M51-3	M51-3			M51-2	M51-2	SEH
4	SEH	SEH	EHK					SEH
5	SEH	SEH	ATM-P		13	ATM-P	EHK	SEH
6	SEH	SEH	ATM-P		14	ATM-A	ATM-A	CM
7	SEH	SEH	SEH		15	ATM-A	ATM-A	CM
8	ATM-P	SEH	SEH		16	SEH	ATM-A	ATM-A

DAY 16

Rev	Crew 1	Crew 2	Crew 3		Rev	Crew 1	Crew 2	Crew 3
1	SEH	ATM-A	ATM-A		9	EHK	SEH	SEH
2	SEH	ATM-A	ATM-A		10	S19	S19	SEH
3	SEH	SEH	EHK		11	VHK		SEH
4	SEH	SEH	ATM-P		12	ATM-P	EHK	SEH
5	SEH	SEH	ATM-P		13	ATM-A	ATM-A	CM
6	SEH	SEH	SEH		14	ATM-A	ATM-A	CM
7	ATM-P	SEH	SEH		15	CM	ATM-A	ATM-A
8	ATM-P	SEH	SEH		16	CM	ATM-A	ATM-A

DAY 17

This day was reserved for EVA. A typical EVA day is given in Table I-5.

DAY 18

Rev	Crew 1	Crew 2	Crew 3		Rev	Crew 1	Crew 2	Crew 3
1	SEH	VHK	M52		9	ATM-P	SEH	SEH
	SEH		M57		10	EHK	SEH	SEH
	SEH		M57		11		M52	SEH
2	SEH	M52				M50	M50	SEH
	SEH		VHK			M50	M50	SEH
	SEH	S19	S19		12	M51-1	M51-1	SEH
3	SEH	S19	S19			M51-1	M51-1	SEH
	SEH	S19	S19					SEH
	SEH		EHK		13		EHK	SEH
4	SEH	SEH	EHK				EHK	SEH
	SEH	SEH	EHK			M52	EHK	SEH
	SEH	SEH	M52		14	ATM-P	M52	CM
5	SEH	SEH	ATM-P			ATM-P	CM	M52
6	SEH	SEH	ATM-P			ATM-P	CM	VHK
7	SEH	SEH	SEH		15	ATM-A	ATM-A	CM
8	ATM-P	SEH	SEH		16	ATM-A	ATM-A	CM

DAY 19

Rev	Crew 1	Crew 2	Crew 3	Rev	Crew 1	Crew 2	Crew 3
1	SEH	ATM-A	ATM-A	11	EHK	VHK	SEH
2	SEH	ATM-A	ATM-A		M50	M50	SEH
3	SEH	ATM-A	ATM-A		M50	M50	SEH
4	SEH	SEH	EHK	12			SEH
5	SEH	SEH	ATM-P	13	M52	EHK	SEH
6	SEH	SEH	ATM-P		VHK	EHK	SEH
7	SEH	SEH	SEH			EHK	SEH
8	ATM-P	SEH	SEH	14	ATM-P	VHK	CM
9	ATM-P	SEH	SEH	15	ATM-A	ATM-A	CM
10	M52	SEH	SEH	16	ATM-A	ATM-A	CM
	EHK	SEH	SEH				
	EHK	SEH	SEH				

DAY 20

Rev	Crew 1	Crew 2	Crew 3	Rev	Crew 1	Crew 2	Crew 3
1	SEH	ATM-A	ATM-A	10	EHK	SEH	SEH
2	SEH	ATM-A	ATM-A	11	ATM-A	ATM-A	SEH
3	SEH	ATM-A	ATM-A	12	ATM-A	ATM-A	SEH
4	SEH	SEH	EHK	13	ATM-A	ATM-A	SEH
5	SEH	SEH	ATM-P	14	ATM-A	ATM-A	CM
6	SEH	SEH	ATM-P	15	ATM-P	EHK	CM
7	SEH	SEH	SEH	16	VHK		CM
8	ATM-P	SEH	SEH		M50	M50	CM
9	ATM-P	SEH	SEH		M50	M50	CM

DAY 21

This day was reserved for rest and recreation. A typical R & R day is given in Table 2-4.

DAY 22

Rev	Crew 1	Crew 2	Crew 3
1	SEH	VHK	M52
	SEH	M18-2	M18-2
	SEH	M52	VHK
2	SEH	ATM-P	
3	SEH	ATM-P	
4	SEH	SEH	EHK
5	SEH	SEH	ATM-P
6	SEH	SEH	ATM-P
7	SEH	SEH	SEH
8	ATM-P	SEH	SEH
9	ATM-P	SEH	SEH

Rev	Crew 1	Crew 2	Crew 3
10	EHK	SEH	SEH
11	M50	M50	SEH
	M50	M50	SEH
	M52	VHK	SEH
12	M18-1	M18-1	SEH
	M51-1	M51-1	SEH
	M51-1	M51-1	SEH
13	ATM-P	EHK	SEH
14	ATM-A	ATM-A	CM
15	ATM-A	ATM-A	CM

DAY 23

Rev	Crew 1	Crew 2	Crew 3
1	SEH	ATM-A	ATM-A
2	SEH	ATM-A	ATM-A
3	SEH	ATM-A	ATM-A
4	SEH	SEH	EHK
5	SEH	SEH	M52
	SEH	SEH	VHK
	SEH	SEH	
6	SEH	SEH	
7	SEH	SEH	SEH
8	ATM-P	SEH	SEH

Rev	Crew 1	Crew 2	Crew 3
9	ATM-P	SEH	SEH
10	EHK	SEH	SEH
11	M52		SEH
	VHK	M52	SEH
		VHK	SEH
12	ATM-P		SEH
13	ATM-P	EHK	SEH
14	ATM-A	ATM-A	CM
15	ATM-A	ATM-A	CM

DAY 24

Rev	Crew 1	Crew 2	Crew 3	Rev	Crew 1	Crew 2	Crew 3
1	SEH	ATM-A	ATM-A	10	EHK	SEH	SEH
2	SEH	ATM-A	ATM-A	11	M50	M50	SEH
3	SEH	M18-3	M18-3		M50	M50	SEH
	SEH	M51-3	M51-3		M18-1	M18-1	SEH
	SEH	M51-3	M51-3	12	VHK	M52	SEH
4	SEH	SEH	EHK		M51-2	M51-2	SEH
5	SEH	SEH	M52		M51-2	M51-2	SEH
	SEH	SEH	VHK	13	M52	EHK	SEH
	SEH	SEH			M57	EHK	SEH
6	SEH	SEH			M57	EHK	SEH
7	SEH	SEH	SEH	14	ATM-A	ATM-A	CM
8	ATM-P	SEH	SEH	15	ATM-A	ATM-A	CM
9	ATM-P	SEH	SEH	16	SEH	ATM-A	ATM-A

DAY 25

Rev	Crew 1	Crew 2	Crew 3	Rev	Crew 1	Crew 2	Crew 3
1	SEH	ATM-A	ATM-A	11	VHK	M52	SEH
2	SEH	ATM-A	ATM-A		M51-1	M51-1	SEH
3	SEH	SEH	EHK		M51-1	M51-1	SEH
4	SEH	SEH	M52	12	M52	EHK	SEH
	SEH	SEH	VHK			EHK	SEH
	SEH	SEH			VHK	EHK	SEH
5	SEH	SEH		13	ATM-A	ATM-A	CM
6	SEH	SEH	SEH	14	ATM-A	ATM-A	CM
7	ATM-P	SEH	SEH	15	CM	ATM-A	ATM-A
8	ATM-P	SEH	SEH	16	CM	ATM-A	ATM-A
9	EHK	SEH	SEH				
10	M50	M50	SEH				
	M50	M50	SEH				
	M18-2	M18-2	SEH				

DAY 26

This day was reserved for EVA. A typical EVA day is given in Table I-5.

DAY 27

Rev	Crew 1	Crew 2	Crew 3	Rev	Crew 1	Crew 2	Crew 3
1	SEH	M50	M50	7	SEH	SEH	SEH
	SEH	M50	M50	8	ATM-P	SEH	SEH
	SEH	M52	VHK	9	ATM-P	SEH	SEH
2	SEH	VHK	M52	10	EHK	SEH	SEH
	SEH	M18-3	M18-3	11	ATM-A	ATM-A	SEH
	SEH	M51-3	M51-3	12	ATM-A	ATM-A	SEH
3	SEH	M51-3	M51-3	13	ATM-A	ATM-A	SEH
	SEH	M51-2	M51-2	14	ATM-A	ATM-A	CM
	SEH	M51-2	M51-2	15	M52	EHK	CM
4	SEH	SEH	EHK		VHK	EHK	CM
5	SEH	SEH	ATM-P			EHK	CM
6	SEH	SEH	ATM-P				

DAY 28

This day was reserved for rest and recreation. A typical R & R day is given in Table I-4.

DAY 29

Rev	Crew 1	Crew 2	Crew 3		Rev	Crew 1	Crew 2	Crew 3
1	SEH	M52	S63		9	ATM-P	SEH	SEH
	SEH	M18-3	M18-3		10	EHK	SEH	SEH
	SEH	S69	S69		11	M52	ATM-P	SEH
2	SEH	ATM-P	M52			VHK	ATM-P	SEH
	SEH	ATM-P	VHK			VHK	ATM-P	SEH
	SEH	ATM-P			12		ATM-P	SEH
3	SEH	ATM-P	EHK		13	RES	EHK	SEH
4	SEH	SEH	RES		14	M51-1	M51-1	CM
5	SEH	SEH	ATM-P			M51-1	M51-1	CM
6	SEH	SEH	ATM-P			M18-1	M18-1	CM
7	SEH	SEH	SEH		15	CM	ATM-A	ATM-A
8	ATM-P	SEH	SEH					

DAY 30

Rev	Crew 1	Crew 2	Crew 3		Rev	Crew 1	Crew 2	Crew 3
1	SEH	ATM-A	ATM-A		12	ATM-P	M52	SEH
2	SEH	ATM-A	ATM-A			ATM-P	VHK	SEH
3	SEH	ATM-A	ATM-A			ATM-P	EHK	SEH
4	SEH	SEH	EHK		13	RES	EHK	SEH
5	SEH	SEH	ATM-P			RES	EHK	SEH
6	SEH	SEH	ATM-P			M18-2	M18-2	SEH
7	SEH	SEH	SEH		14	M52	S69	CM
8	ATM-P	SEH	SEH			CM	M51-2	M51-2
9	ATM-P	SEH	SEH			CM	M51-2	M51-2
10	EHK	SEH	SEH		15	CM	M51-3	M51-3
11	ATM-P	VHK	SEH			CM	M51-3	M51-3
						CM	S69	M52

DAY 31

Rev	Crew 1	Crew 2	Crew 3		Rev	Crew 1	Crew 2	Crew 3
1	SEH	M52	RES		9	ATM-P	SEH	SEH
	SEH	RES	M52		10	EHK	SEH	SEH
	SEH	S69	S69		11	M52	ATM-P	SEH
2	SEH	VHK	ATM-P			VHK	ATM-P	SEH
3	SEH		ATM-P				ATM-P	SEH
4	SEH	SEH	EHK		12		ATM-P	SEH
5	SEH	SEH	ATM-P		13	ATM-P	EHK	SEH
6	SEH	SEH	ATM-P		14	ATM-P	VHK	CM
7	SEH	SEH	SEH		15	CM	ATM-A	ATM-A
8	ATM-P	SEH	SEH					

DAY 32

Rev	Crew 1	Crew 2	Crew 3		Rev	Crew 1	Crew 2	Crew 3
1	SEH	ATM-A	ATM-A		11	ATM-P	VHK	SEH
2	SEH	ATM-A	ATM-A		12	ATM-P	EHK	SEH
3	SEH	ATM-A	ATM-A		13	S19	S19	SEH
4	SEH	SEH	EHK		14	M52	S69	CM
5	SEH	SEH	ATM-P			M51-1	M51-1	CM
6	SEH	SEH	ATM-P			M51-1	M51-1	CM
7	SEH	SEH	SEH		15	M18-1	M18-1	CM
8	ATM-P	SEH	SEH			S69	M52	CM
9	ATM-P	SEH	SEH			S63	CM	M52
10	EHK	SEH	SEH					

DAY 33

Rev	Crew 1	Crew 2	Crew 3
1	SEH	M52	RES
	SEH	S69	S69
	SEH	M51-2	M51-2
2	SEH	M51-2	M51-2
	SEH	M51-3	M51-3
	SEH	M51-3	M51-3
3	SEH	M18-3	M18-3
	SEH	S69	S69
	SEH	S63	M52
4	SEH	SEH	EHK
5	SEH	SEH	ATM-P
6	SEH	SEH	ATM-P
7	SEH	SEH	SEH

Rev	Crew 1	Crew 2	Crew 3
8	ATM-P	SEH	SEH
9	ATM-P	SEH	SEH
10	EHK	SEH	SEH
11	ATM-P	VHK	SEH
12	ATM-P		SEH
	ATM-P	VHK	SEH
	ATM-P	EHK	SEH
13	M52	EHK	SEH
	RES	EHK	SEH
	M18-2	M18-2	SEH
14	S19	S19	CM
15	CM	ATM-A	ATM-A

DAY 34

Rev	Crew 1	Crew 2	Crew 3
1	SEH	ATM-A	ATM-A
2	SEH	ATM-A	ATM-A
3	SEH	ATM-A	ATM-A
4	SEH	SEH	EHK
5	SEH	SEH	ATM-P
6	SEH	SEH	ATM-P
7	SEH	SEH	SEH
8	ATM-P	SEH	SEH
9	ATM-P	SEH	SEH
10	EHK	SEH	SEH

Rev	Crew 1	Crew 2	Crew 3
11	M52	ATM-P	SEH
	VHK	ATM-P	SEH
		ATM-P	SEH
12		ATM-P	SEH
13	ATM-P	EHK	SEH
14	ATM-P	M52	CM
	ATM-P	VHK	CM
	ATM-P		CM
15	CM	S69	VHK
	CM		RES
	CM	S69	M52

DAY 35

This day was reserved for rest and recreation. A typical R & R day is given in Table I-4.

DAY 36

Rev	Crew 1	Crew 2	Crew 3	Rev	Crew 1	Crew 2	Crew 3
1	SEH	M52	RES	8	ATM-P	SEH	SEH
	SEH	S63	M52	9	ATM-P	SEH	SEH
	SEH	M51-2	M51-2	10	EHK	SEH	SEH
2	SEH	M51-2	M51-2	11	M52	ATM-P	SEH
	SEH	M51-3	M51-3		M57	ATM-P	SEH
	SEH	M51-3	M51-3		M57	ATM-P	SEH
3	SEH	M18-2	M18-2	12	VHK	ATM-P	SEH
	SEH	RES	VHK	13	RES	EHK	SEH
	SEH	S69	S69	14	M51-1	M51-1	CM
4	SEH	SEH	EHK		M51-1	M51-1	CM
5	SEH	SEH	ATM-P		M18-1	M18-1	CM
6	SEH	SEH	ATM-P	15	CM	ATM-A	ATM-A
7	SEH	SEH	SEH				

DAY 37

Rev	Crew 1	Crew 2	Crew 3	Rev	Crew 1	Crew 2	Crew 3
1	SEH	ATM-A	ATM-A	11	M52	ATM-P	SEH
2	SEH	ATM-A	ATM-A		VHK	ATM-P	SEH
3	SEH	ATM-A	ATM-A			ATM-P	SEH
4	SEH	SEH	EHK	12	VHK	ATM-P	SEH
5	SEH	SEH	ATM-P	13	ATM-P	EHK	SEH
6	SEH	SEH	ATM-P	14	ATM-P	S69	CM
7	SEH	SEH	SEH		ATM-P	M57	CM
8	ATM-P	SEH	SEH		ATM-P	M57	CM
9	ATM-P	SEH	SEH	15	CM	M18-3	M18-3
10	EHK	SEH	SEH		CM	M52	S69
					CM	S69	M52

DAY 38

Rev	Crew 1	Crew 2	Crew 3	Rev	Crew 1	Crew 2	Crew 3
1	SEH	ATM-P	VHK	11	M52	ATM-P	SEH
2	SEH	ATM-P				ATM-P	SEH
3	SEH	RES			VHK	ATM-P	SEH
4	SEH	SEH	EHK	12		ATM-P	SEH
5	SEH	SEH	ATM-P	13	RES	EHK	SEH
6	SEH	SEH	ATM-P	14	M18-2	M18-2	CM
7	SEH	SEH	SEH		M51-1	M51-1	CM
8	ATM-P	SEH	SEH		M51-1	M51-1	CM
9	ATM-P	SEH	SEH	15	CM	M52	M57
10	EHK	SEH	SEH		CM	S69	M57
					CM	S63	M52

DAY 39

This day was reserved for EVA. A typical EVA day is given in Table I-5.

DAY 40

Rev	Crew 1	Crew 2	Crew 3	Rev	Crew 1	Crew 2	Crew 3
1	SEH	M52	RES	8	ATM-P	SEH	SEH
	SEH	S69	S69	9	ATM-P	SEH	SEH
	SEH	M51-2	M51-2	10	EHK	SEH	SEH
2	SEH	M51-2	M51-2	11	M52	ATM-P	SEH
	SEH	M51-3	M51-3		VHK	ATM-P	SEH
	SEH	M51-3	M51-3		VHK	ATM-P	SEH
3	SEH	M18-3	M18-3	12		ATM-P	SEH
	SEH	S69	S69	13	RES	EHK	SEH
	SEH	RES	M52	14	M18-1	M18-1	CM
4	SEH	SEH	EHK			S69	CM
5	SEH	SEH	ATM-P		VHK	S63	CM
6	SEH	SEH	ATM-P	15	CM	ATM-A	ATM-A
7	SEH	SEH	SEH				

DAY 41

Rev	Crew 1	Crew 2	Crew 3		Rev	Crew 1	Crew 2	Crew 3
1	SEH	ATM-A	ATM-A		11	M52	ATM-P	SEH
2	SEH	ATM-A	ATM-A			VHK	ATM-P	SEH
3	SEH	ATM-A	ATM-A			VHK	ATM-P	SEH
4	SEH	SEH	EHK		12		ATM-P	SEH
5	SEH	SEH	ATM-P		13	ATM-P	EHK	SEH
6	SEH	SEH	ATM-P		14	ATM-P	M52	CM
7	SEH	SEH	SEH			ATM-P	CM	M52
8	ATM-P	SEH	SEH			ATM-P	CM	VHK
9	ATM-P	SEH	SEH		15	M18-2	M18-2	CM
10	EHK	SEH	SEH			M51-1	M51-1	CM
						M51-1	M51-1	CM

DAY 42

This day was reserved for rest and recreation. A typical R & R day is given in Table I-4.

DAY 43

Rev	Crew 1	Crew 2	Crew 3		Rev	Crew 1	Crew 2	Crew 3
1	SEH	M52	RES		9	ATM-P	SEH	SEH
	SEH	S69	S69		10	EHK	SEH	SEH
	SEH	M51-2	M51-2		11	ATM-P	VHK	SEH
2	SEH	M51-2	M51-2		12	ATM-P	VHK	SEH
	SEH	M51-3	M51-3			ATM-P	EHK	SEH
	SEH	M51-3	M51-3			ATM-P	EHK	SEH
3	SEH	M18-3	M18-3		13	M52	EHK	SEH
	SEH	S69	S69			M18-1	M18-1	SEH
	SEH	RES	M52			S19	S19	SEH
4	SEH	SEH	EHK		14	S19	S19	CM
5	SEH	SEH	ATM-P			S19	S19	CM
6	SEH	SEH	ATM-P			VHK	S69	CM
7	SEH	SEH	SEH		15	CM	ATM-A	ATM-A
8	ATM-P	SEH	SEH					

DAY 44

Rev	Crew 1	Crew 2	Crew 3
1	SEH	ATM-A	ATM-A
2	SEH	ATM-A	ATM-A
3	SEH	ATM-A	ATM-A
4	SEH	SEH	EHK
5	SEH	SEH	ATM-P
6	SEH	SEH	ATM-P
7	SEH	SEH	SEH
8	ATM-P	SEH	SEH
9	ATM-P	SEH	SEH
10	EHK	SEH	SEH
11	M52	ATM-P	SEH
	VHK	ATM-P	SEH
	VHK	ATM-P	SEH
12		ATM-P	SEH
13	ATM-P	EHK	SEH
14	ATM-P	M52	CM
	ATM-P	CM	M52
	ATM-P	CM	S69
15	S63	VHK	CM
	M51-1	M51-1	CM
	M51-1	M51-1	CM

DAY 45

Rev	Crew 1	Crew 2	Crew 3
1	SEH	M52	RES
	SEH	RES	M52
	SEH	S69	S69
2	SEH	ATM-P	VHK
3	SEH	ATM-P	
4	SEH	SEH	EHK
5	SEH	SEH	ATM-P
6	SEH	SEH	ATM-P
7	SEH	SEH	SEH
8	ATM-P	SEH	SEH
9	ATM-P	SEH	SEH
10	EHK	SEH	SEH
11	M52	ATM-P	SEH
		ATM-P	SEH
	VHK	ATM-P	SEH
12		ATM-P	SEH
13	ATM-P	EHK	SEH
14	ATM-P	VHK	CM
15	CM	ATM-A	ATM-A

DAY 46

Rev	Crew 1	Crew 2	Crew 3	Rev	Crew 1	Crew 2	Crew 3
1	SEH	ATM-A	ATM-A	11	M52	ATM-P	SEH
2	SEH	ATM-A	ATM-A		VHK	ATM-P	SEH
3	SEH	ATM-A	ATM-A			ATM-P	SEH
4	SEH	SEH	EHK	12	VHK	ATM-P	SEH
5	SEH	SEH	ATM-P	13	RES	EHK	SEH
6	SEH	SEH	ATM-P	14	CM	M52	RES
7	SEH	SEH	SEH		CM	M51-2	M51-2
8	ATM-P	SEH	SEH		CM	M51-2	M51-2
9	ATM-P	SEH	SEH	15	CM	M51-3	M51-3
10	EHK	SEH	SEH		CM	M51-3	M51-3
					CM	S69	M52

DAY 47

Rev	Crew 1	Crew 2	Crew 3	Rev	Crew 1	Crew 2	Crew 3
1	SEH	M52	RES	10	EHK	SEH	SEH
	SEH	S63	M52	11	ATM-P	VHK	SEH
	SEH	S69	S69	12	ATM-P	EHK	SEH
2	SEH	ATM-P	VHK	13	M51-1	M51-1	SEH
3	SEH	ATM-P			M51-1	M51-1	SEH
4	SEH	SEH	EHK		S19	S19	SEH
5	SEH	SEH	ATM-P	14	S19	S19	CM
6	SEH	SEH	ATM-P		S19	S19	CM
7	SEH	SEH	SEH		M52	S69	CM
8	ATM-P	SEH	SEH	15	CM	ATM-A	ATM-A
9	ATM-P	SEH	SEH				

DAY 48

Rev	Crew 1	Crew 2	Crew 3		Rev	Crew 1	Crew 2	Crew 3
1	SEH	ATM-A	ATM-A		11	M52	ATM-P	SEH
2	SEH	ATM-A	ATM-A			VHK	ATM-P	SEH
3	SEH	ATM-A	ATM-A				ATM-P	SEH
4	SEH	SEH	EHK		12	VHK	ATM-P	SEH
5	SEH	SEH	ATM-P		13	ATM-P	EHK	SEH
6	SEH	SEH	ATM-P		14	ATM-P	M52	CM
7	SEH	SEH	SEH			ATM-P	CM	M52
8	ATM-P	SEH	SEH			ATM-P	CM	VHK
9	ATM-P	SEH	SEH		15	CM	M51-3	M51-3
10	EHK	SEH	SEH			CM	M51-3	M51-3
						CM	M53A	M53A

DAY 49

This day was reserved for rest and recreation. A typical R & R day is given in Table I-4 .

DAY 50

Rev	Crew 1	Crew 2	Crew 3		Rev	Crew 1	Crew 2	Crew 3
1	SEH	M52	RES		8	ATM-P	SEH	SEH
	SEH	RES	M52		9	ATM-P	SEH	SEH
	SEH	M51-2	M51-2		10	EHK	SEH	SEH
2	SEH	M51-2	M51-2		11	M52	RES	SEH
	SEH	M53B	M53B			M51-1	M51-1	SEH
	SEH	M53B	M53B			M51-1	M51-1	SEH
3	SEH	S69	S69		12	ATM-P	VHK	SEH
	SEH	RES	VHK		13	ATM-P	EHK	SEH
	SEH	S69	S69		14	M53C	M53C	CM
4	SEH	SEH	EHK			M53C	M53C	CM
5	SEH	SEH	ATM-P			VHK	S69	CM
6	SEH	SEH	ATM-P		15	CM	ATM-A	ATM-A
7	SEH	SEH	SEH					

DAY 51

Rev	Crew 1	Crew 2	Crew 3
1	SEH	ATM-A	ATM-A
2	SEH	ATM-A	ATM-A
3	SEH	ATM-A	ATM-A
4	SEH	SEH	EHK
5	SEH	SEH	ATM-P
6	SEH	SEH	ATM-P
7	SEH	SEH	SEH
8	ATM-P	SEH	SEH
9	ATM-P	SEH	SEH
10	EHK	SEH	SEH

Rev	Crew 1	Crew 2	Crew 3
11	M52	ATM-P	SEH
	VHK	ATM-P	SEH
	VHK	ATM-P	SEH
12		ATM-P	SEH
13	ATM-P	EHK	SEH
14	ATM-P	M52	CM
	ATM-P	CM	M52
	ATM-P	CM	VHK
15	CM	M51-3	M51-3
	CM	M51-3	M51-3
	CM	M53A	M53A

DAY 52

Rev	Crew 1	Crew 2	Crew 3
1	SEH	M52	RES
	SEH	RES	M52
	SEH	M53B	M53B
2	SEH	M53B	M53B
	SEH	S69	S69
	SEH	RES	VHK
3	SEH	S19	S19
4	SEH	SEH	EHK
5	SEH	SEH	ATM-P
6	SEH	SEH	ATM-P
7	SEH	SEH	SEH
8	ATM-P	SEH	SEH

Rev	Crew 1	Crew 2	Crew 3
9	ATM-P	SEH	SEH
10	EHK	SEH	SEH
11	M52	ATM-P	SEH
	VHK	ATM-P	SEH
		ATM-P	SEH
12		ATM-P	SEH
13	RES	EHK	SEH
14	M53C	M53C	CM
	M53C	M53C	CM
	VHK	S69	CM
15	CM	ATM-A	ATM-A

DAY 53

Rev	Crew 1	Crew 2	Crew 3	Rev	Crew 1	Crew 2	Crew 3
1	SEH	ATM-A	ATM-A	11	M52	ATM-P	SEH
2	SEH	ATM-A	ATM-A		M57	ATM-P	SEH
3	SEH	ATM-A	ATM-A		M57	ATM-P	SEH
4	SEH	SEH	EHK	12	VHK	ATM-P	SEH
5	SEH	SEH	ATM-P	13	RES	EHK	SEH
6	SEH	SEH	ATM-P	14	CM	M53A	M53A
7	SEH	SEH	SEH		CM	M57	M52
8	ATM-P	SEH	SEH		CM	M57	M57*
9	ATM-P	SEH	SEH	15	CM	M52	M57
10	EHK	SEH	SEH		CM	M51-2	M51-2
					CM	M51-2	M51-2

*As M57 is 45 min long, it could be scheduled this way.

The following period, between days 53 and 54, was reserved for scheduling the UV-x ray Solar Photography Experiment (code S70) and deactivation of the LM/ATM (code DACT). As it is 10 revolutions in length, it was not considered a separate day.

Rev	Crew 1	Crew 2	Crew 3	Rev	Crew 1	Crew 2	Crew 3
1	SEH	EHK	DACT	6	S70	SEH	DACT
2	SEH	DACT	DACT	7	S70	SEH	SEH
3	SEH	DACT	DACT	8	S70	DACT	SEH
4	SEH	SEH	EHK	9	S70	DACT	SEH
5	SEH	SEH	DACT	10	S70	DACT	SEH

DAY 54

This day was reserved for EVA. A typical EVA day is given in Table I-5.

Table I-3

DAYS 55 AND 56

Time; Hours, Minutes | Activity, Assigned to all 3 Men

DAY 55

0000 - 1000   Simultaneous sleep, eat, and hygiene

1000 - 1430   S-IVB and AM deactivation

(a) Secure waste management systems

(b) Transfer returnable data to CM

(c) Service LiOH cannisters, water condensate tank and PCO_2 sensors in aft portion of AM

(d) Replace launch covers on ECS package

(e) Secure electrical power

1430 - 1745   (a) Donn space suits

(b) Initiate S-IVB venting

(c) Activate CM ECS

(d) Close aft AM hatch

(e) Close and lock equalization valve

(f) Service suit heat exchanger and cooling systems

(g) Doff space suits

1745 - 1900   Simultaneous eat and hygiene

1900 - 2400   MDA deactivation

(a) Replace launch and dust covers

(b) Deactivate electrical systems

(c) Transfer returnable equipment and experiment data to the CM

(d) Replace CSM/MDA probe and drogue assembly

(e) Replace thermal and pressure hatch

(f) Maneuver and stabilize cluster in gravity gradient mode

I-28

DAY 56

000

0000 - 1000	Simultaneous sleep, eat, hygiene
1000 - 1000	(a) CSM/MDA separation
	(b) CSM/recovery area phasing
	(c) Reentry and recovery

Table I-4
TYPICAL R & R DAY

Rev	Crew 1	Crew 2	Crew 3	Rev	Crew 1	Crew 2	Crew 3
1	SEH	R & R	R & R	9	R & R	SEH	SEH
2	SEH	R & R	R & R	10	EHK	SEH	SEH
3	SEH	VHK	EHK	11	R & R	R & R	SEH
4	SEH	SEH	R & R	12	R & R	R & R	SEH
5	SEH	SEH	R & R	13	VHK	EHK	SEH
6	SEH	SEH	VHK	14	Review experiment		
7	SEH	SEH	SEH	15	status and plans, to		
8	R & R	SEH	SEH		be done in the CM		

Table I-5
TYPICAL EVA DAY

Rev	Crew 1	Crew 2	Crew 3	Rev	Crew 1	Crew 2	Crew 3
1	SEH	EHK	EHK	9	VHK	SEH	SEH
2	SEH	VHK		10	EHK	VHK	SEH
3	SEH	SEH	VHK	11	PREP	PREP	VHK
4	SEH	SEH	SEH	12	PREP	PREP	CM
5	SEH	SEH	SEH	13	EVA	EVA	CM
6	SEH	SEH	SEH	14	EVA	EVA	CM
7	SEH	SEH	SEH	15	POST	POST	CM
8		SEH	SEH				

I.3 POWER AND DATA

I.3.1 Data

A typical 2-day period was taken from each half, and the data vs. revolution graphed for 30 revolutions. Figure I-1 is a graph typical of days 7 through 28, and Fig. I-2 is a graph typical of days 29 through 53. For all experiment days, the data readout capability is 340 min/day with a ten-station net, 190 min/day with a four-station net, and 78 min/day with a two-station net.

I.3.2 Power

A typical 2-day period was taken from each half of the mission, and the power requirements/revolution graphed for 30 revolutions in Figs. I-3 and I-4.

I.4 UNCITED REFERENCES

NASA/MFSC, Mission Requirement Document, 23 May 1967

NASA/MFSC, Recommended Flight Assignments of Approved Experiments for Missions AAP-1/AAP-2 and AAP-3/AAP-4, 10 March 1967

NASA/MFSC, AAP-2 Design Reference Flight Sequence, 21 June 1967

NASA/MSC, Reference Flight Plan, AAP-1/AAP-2, 1 June 1967

NASA/MSC, AAP-3/AAP-4 Flight Plan, 6 July 1967

LMSC, Cluster A Design Reference Manual, 11 March 1967

LMSC, Final Report for Augmentation Task No. 6, Man-Machine Engineering and Docking Aids, 26 June 1967
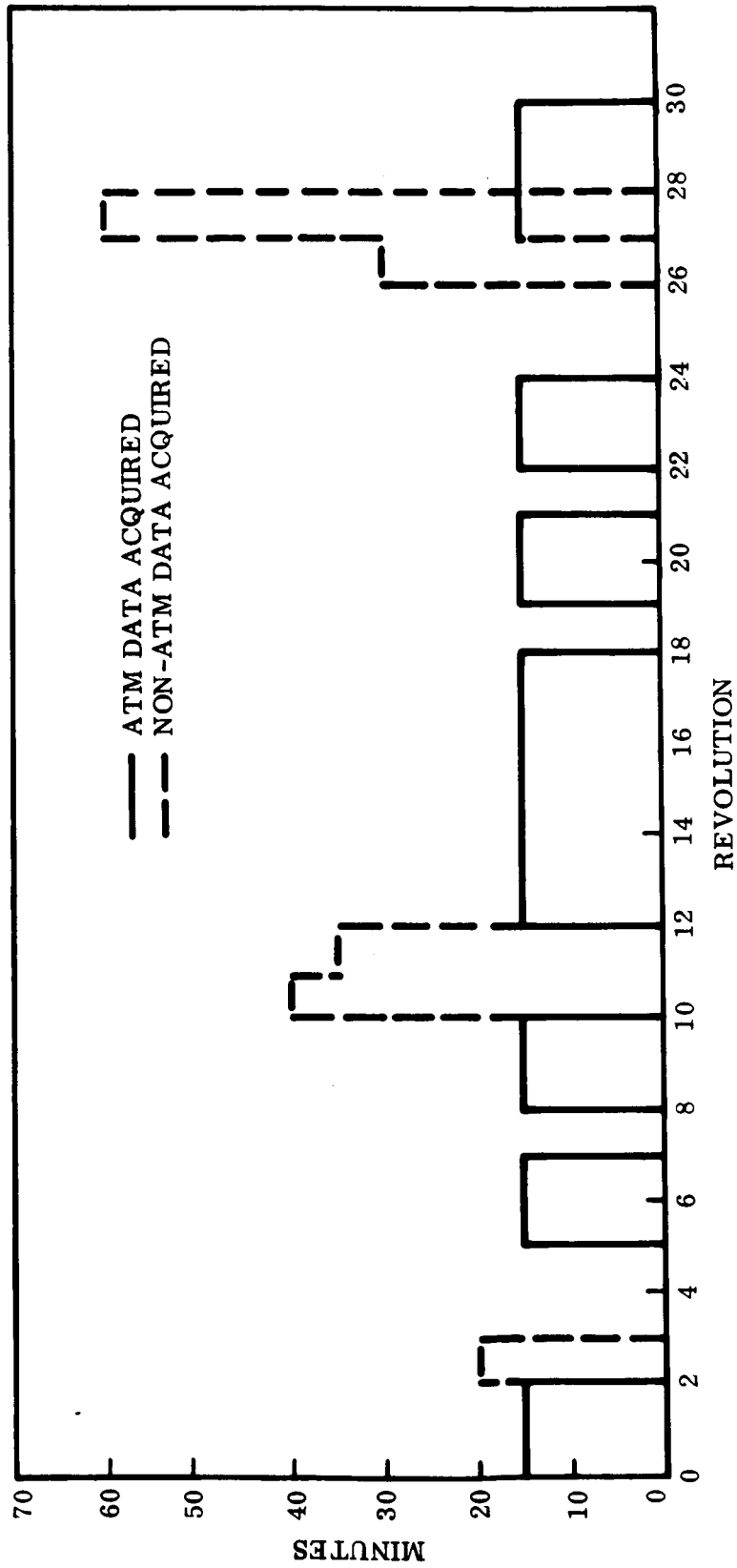
Fig. I-1 Experiment Data Handling, Typical 2-Day Period for Days 7 – 28
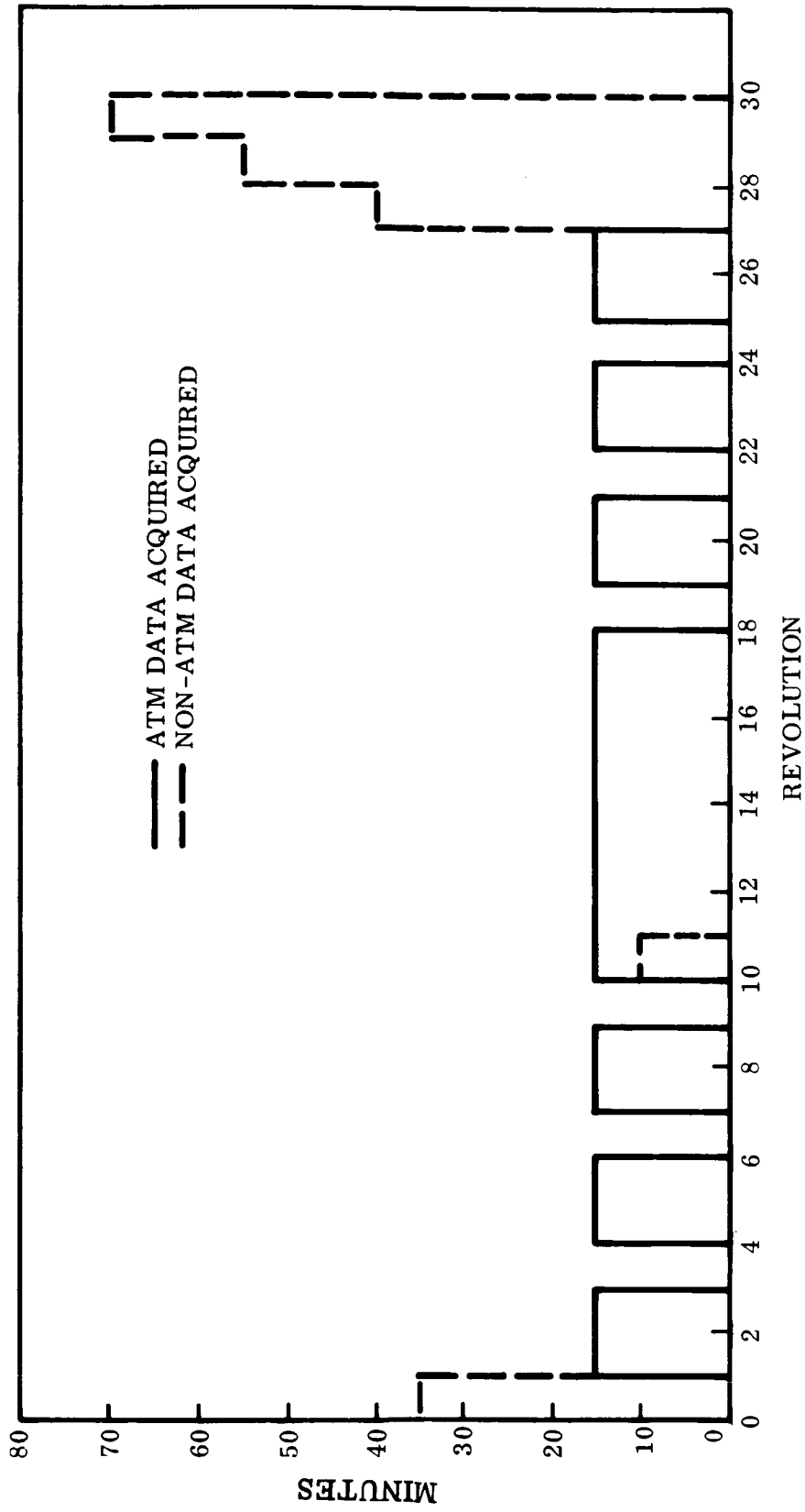
Fig. I-2 Experiment Data Handling, Representative 2-Day Period for Days 29 – 53

PEAK POWER   = 4.2 KW
MIN. POWER   = 1.5 KW
TOTAL ENERGY = 128.9 KWH/2 DAYS
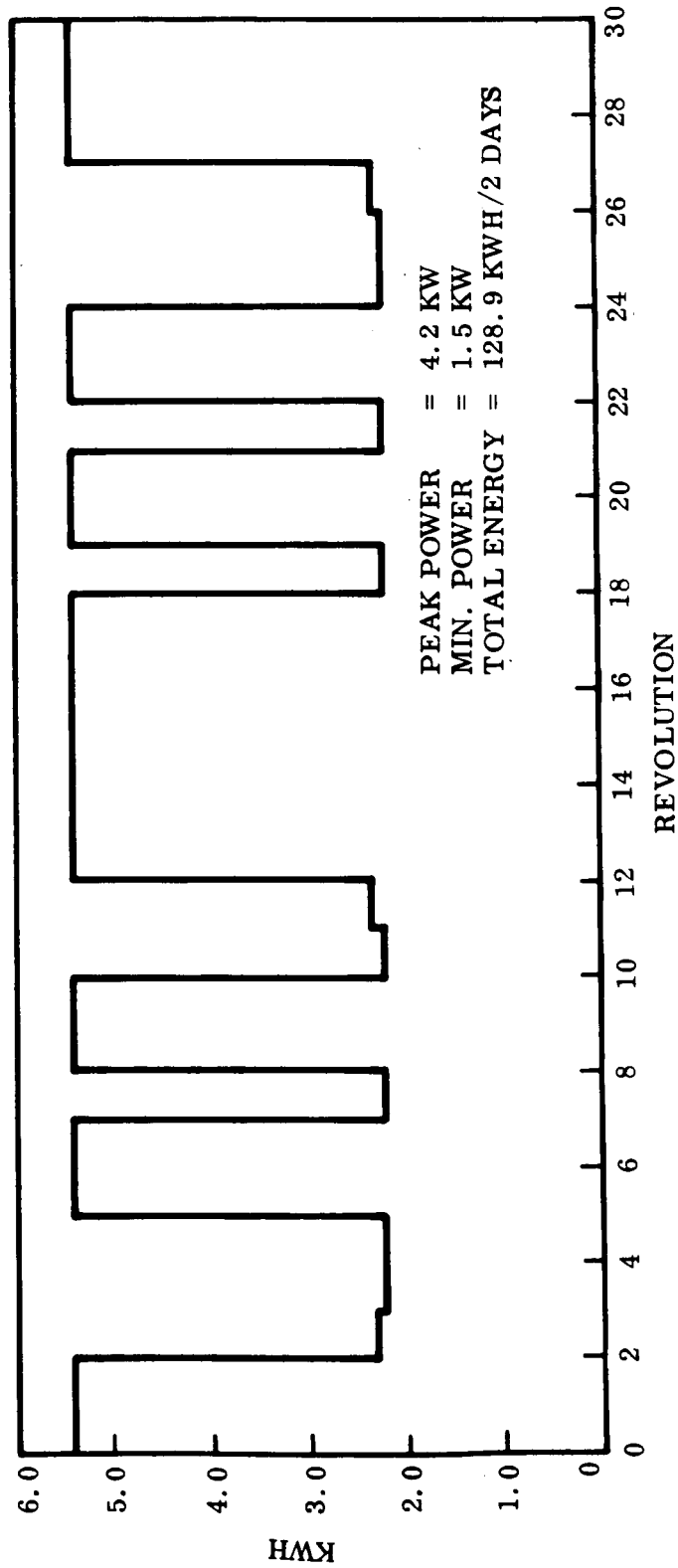
Fig. I-3 Experiment Power Profile, Typical 2-Day Period for Days 7 – 28

LOCKHEED MISSILES & SPACE COMPANY
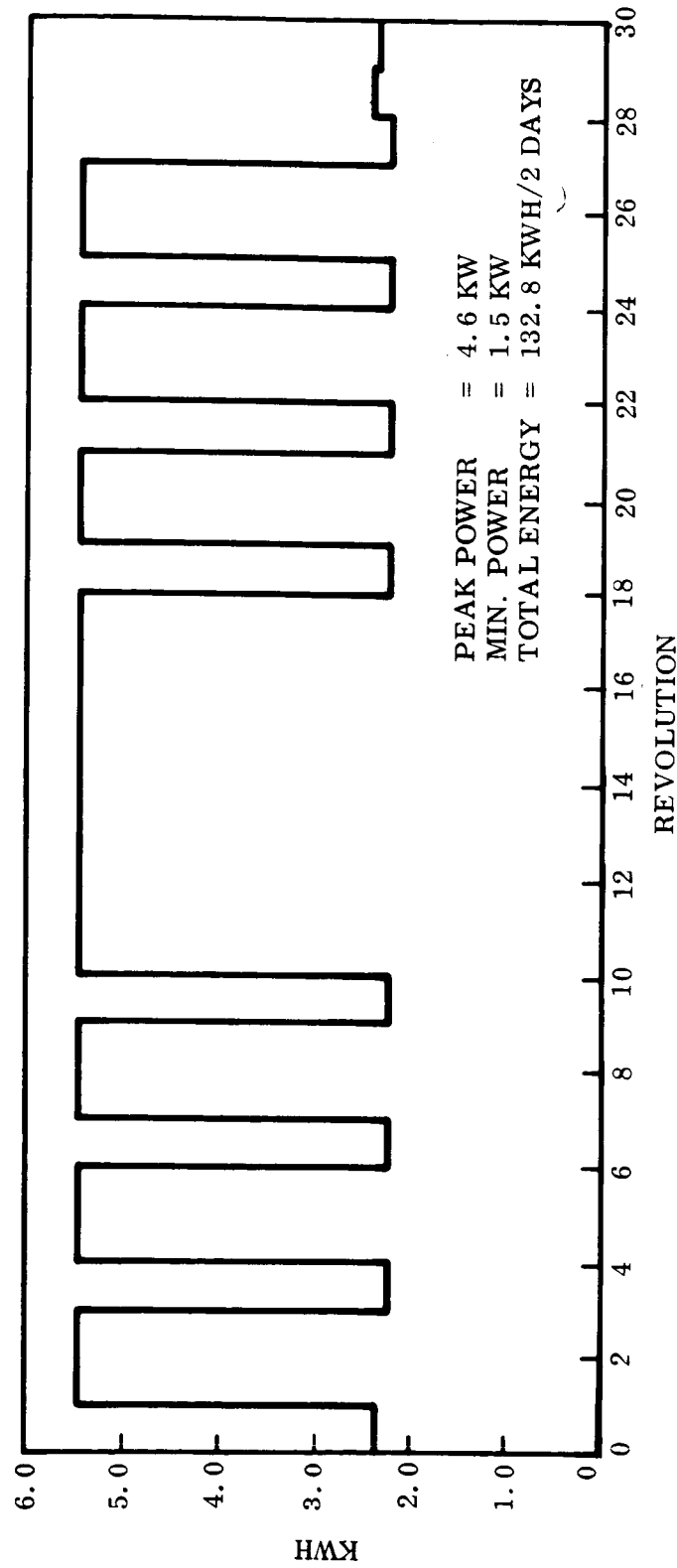
Fig. I-4 Experiment Power Profile, Representative 2-Day Period for Days 29 – 53

PEAK POWER = 4.6 KW
MIN. POWER = 1.5 KW
TOTAL ENERGY = 132.8 KWH/2 DAYS

LOCKHEED MISSILES & SPACE COMPANY

Part II

CLUSTER A ATTITUDE STABILIZATION REQUIREMENTS

II.1 INTRODUCTION

During the AAP-1 and AAP-2 (and possibly AAP-3A) missions, the solar panels on the OWS must be pointed at the sun. Because of disturbances such as aerodynamic and gravity gradient torques, the vehicle will not remain pointed at the sun if it is not attitude controlled. If it does deviate from the sun line (i.e., pointing at the sun), then a loss of power results that is directly proportional to the cosine of the angle of deviation. While a control system can limit this deviation from the sun line (and thus reduce the power loss), the cost, reliability, etc., of such a control system must be weighed against the increase in solar panels required if the deviation is left uncontrolled.

If a control system is to be used, then the question arises as to the best system to use. One of the more obvious possibilities is the CSM system since it will "be there." Before any decision of the best system can be made (assuming one is used), the requirements of the system must be determined as well as the consequences of leaving the vehicle uncontrolled. This report is directed primarily to these two problems – uncontrolled motion and control impulse required to counter the disturbances. The report is divided into three main parts. The first defines the vehicle characteristics and the analytical representation used (coordinate system, equations, etc.). The second part develops the uncontrolled motion and the control impulse requirements for various conditions. The third part considers how these control requirements might be met.

II.2 STATEMENT OF THE PROBLEM

During the orbit operations of the AAP-1, AAP-2, and AAP-3, the OWS solar panels must be pointed at the sun in order to collect power, i.e., the plane of the panels must

be normal to the line of sight to the sun. (Herein the notation LOS will be used to denote the line-of-sight to the sun.) Any deviation from the LOS results in a collected power loss equal to $1-\cos \alpha_2$, where α_2 is the angle of deviation. Both gravity gradient and aerodynamic torques can be expected to force such deviations. Other disturbances are considered negligible compared to these two.

Orienting to always face the sun is approximately the same as establishing an inertially fixed attitude. However, the missions are planned to last 28 to 56 days, and over these periods the regression of nodes would lead to prohibitively large α_2's if a truly inertial attitude were established. Thus, the regression of nodes may also be viewed as a disturbance upon the system although it is a unidirectional disturbance of a precise known amount. To compensate for the regression of nodes will be a requirement of any system selected and is thus not considered further herein.

Solar radiation torques have been estimated to be orders of magnitude less than the aerodynamic and gravity gradient torques and are not considered herein.

During each orbit, the satellite spends roughly equal times in sunlight and in darkness.* Assuming a control system is required, the problem of loss of the sun and reacquisition each orbit must be considered. A further requirement arises at reacquisition where the time that can be allocated to reacquisition is not currently specified. However, the longer the time used in reacquiring the sun the greater the power loss.

Insofar as power losses are concerned, rotation about the LOS has no effect and thus does not lead directly to any control requirement. However, operation requirements are for the vehicle to operate with its longitudinal axis in the orbit plane. Thus, some control will be required to maintain this orientation in the presence of aerodynamic torques.

---

*For an orbit altitude of 260 to 250 nm, the period is on the order of 94 min. About 54 min is spent in sunlight and about 40 min in darkness.

II.3 BASIC DATA

II.3.1 Reference Systems

Figure II-1 shows a sun-referenced coordinate system (X_1, Y_1, Z_1) defined so that Z_1 points toward the sun and lies along the earth-sun line, X_1 lies along the radius vector at the terminator, and Y_1 completes the right-handed orthogonal coordinate system. Figure 3-1 also shows an orbital coordinate system (X_o, Y_o, Z_o). This system is produced from the sun-referenced axes by a single rotation about the negative X_1-axis through the sun angle λ. The sun angle is the angle between the earth-sun line and the projection of the earth-sun line onto the orbit plane. The true anomaly is measured from Z_o.

A body fixed geometric reference system (X, Y, Z) is shown in Fig. II-2. The origin of this system lies on the vehicle axis and is located at station number 966 in. in the Saturn IB coordinate system described below. The positive X-axis lies along the vehicle axis in the direction of the CSM, Z is normal to the plane of the solar panels in the direction of the sun, and Y completes the right-handed orthogonal coordinate system. In terms of these coordinates, the vehicle C.G. is located at X = 788 in., Y = -2.94 in., and Z = 4.97 in. The X-, Y-, and Z-axes are defined to be the vehicle roll, pitch, and yaw axes, respectively.

A second body fixed coordinate system (x, y, z), referred to as the Saturn IB Coordinate System, is also illustrated in Fig. II-2. The x-axis of the Saturn IB system is coincident with the X-axis of the geometric system described above. The y- and z-axes of the Saturn IB system are obtained by rotating the Y and Z geometric axes through a positive angle of 135 deg about the X axis.

Figure II-3 shows how the roll (α_1), pitch (α_2), and yaw (α_3) angles are defined in terms of the sun-referenced and geometric coordinate systems. The roll angle is defined to be the angle of rotation, about the positive X-axis, of the geometric axes
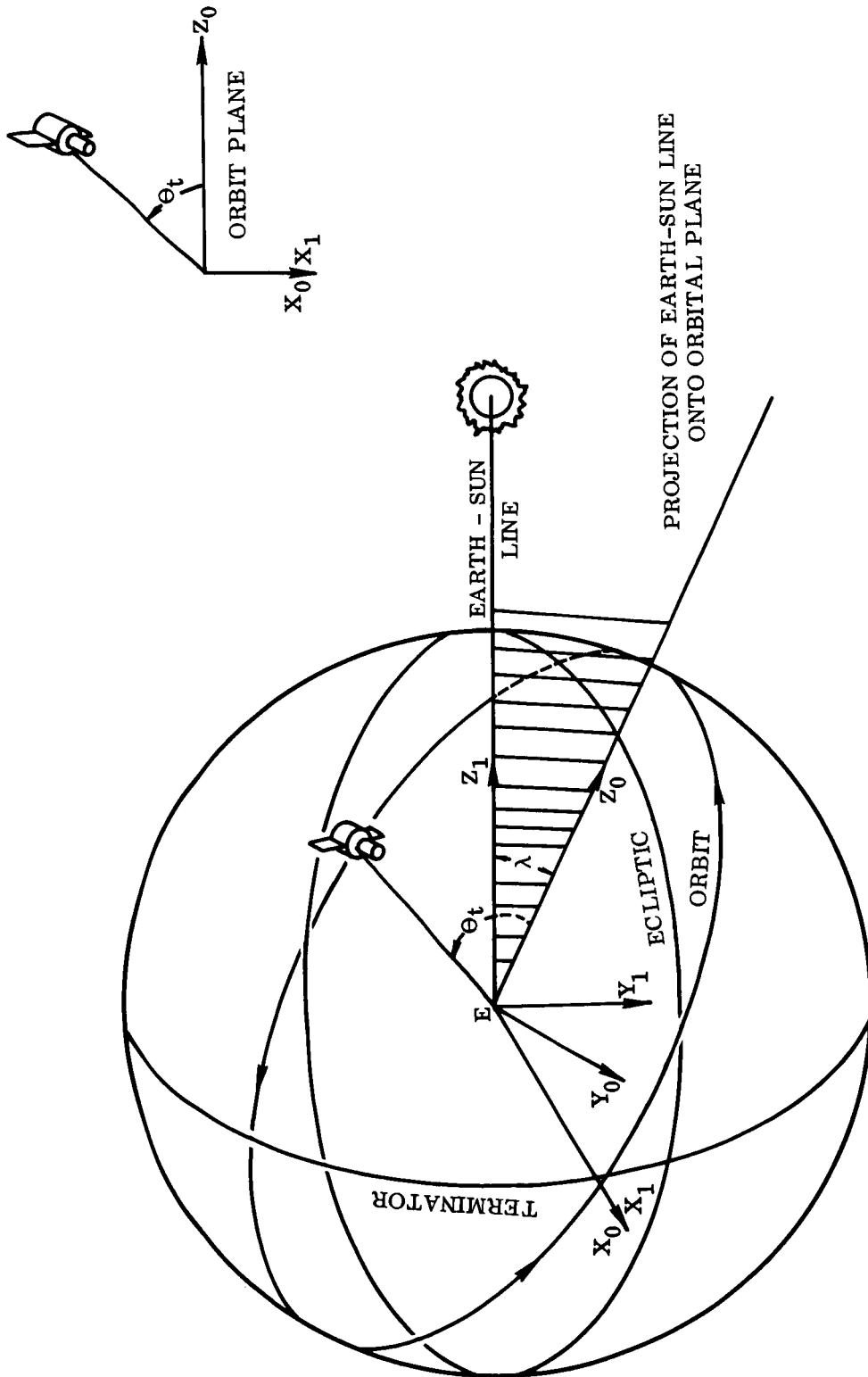
Fig. II-1 Sun-Referenced Axes

Fig. II-2 Body-Fixed Axes

LOCKHEED MISSILES & SPACE COMPANY
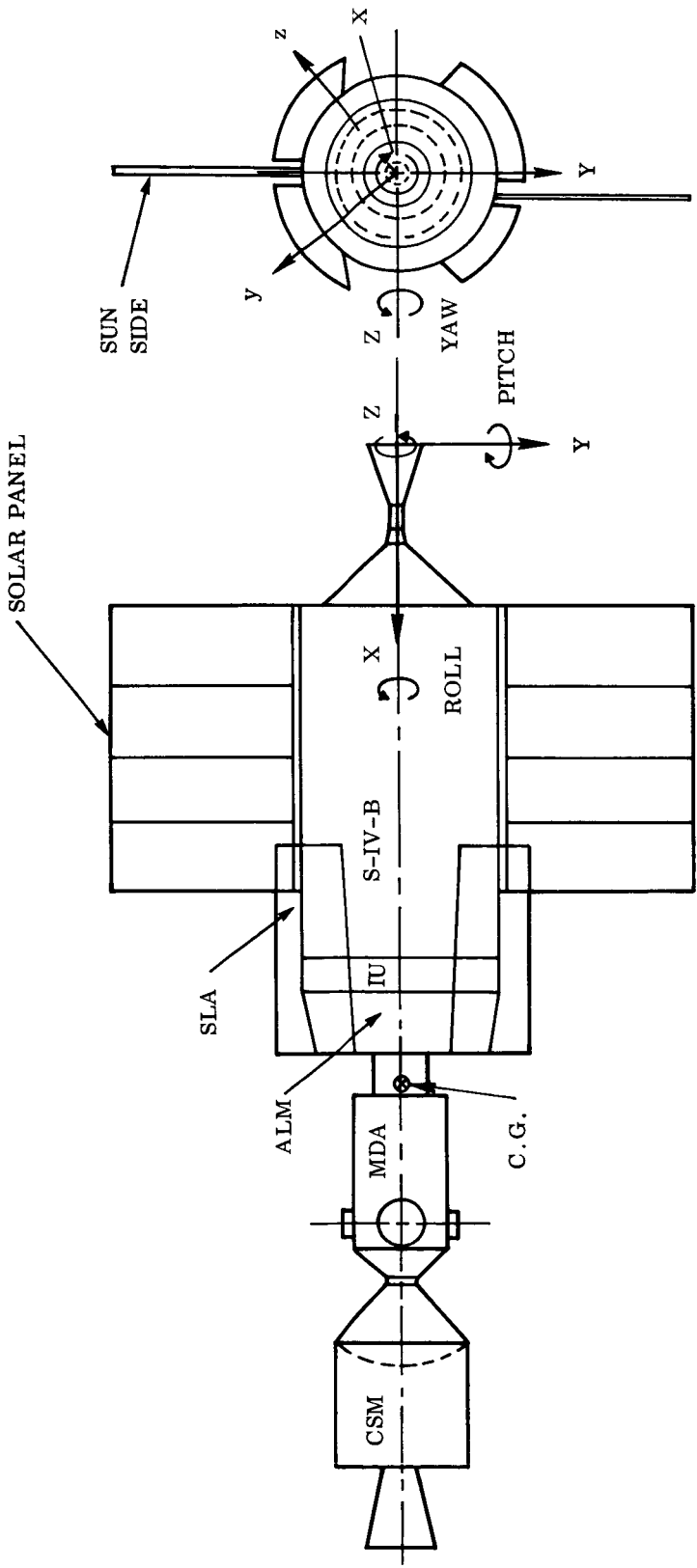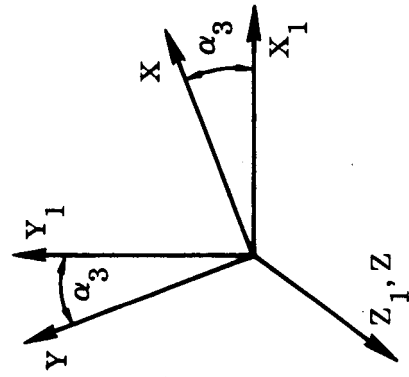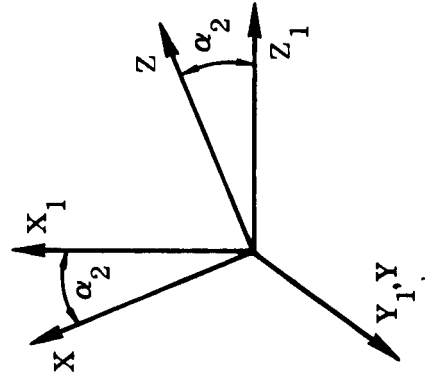
ROLL ANGLE
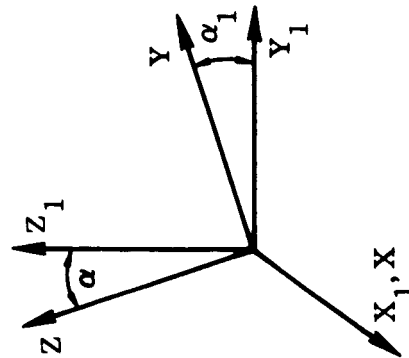
PITCH ANGLE

YAW ANGLE

Fig. II-3 Roll, Pitch, and Yaw Angles

referenced to the sun-referenced axes when the X_1-axis and X-axis are coincident. Similarly, the pitch and yaw angles are positive rotations about Y and Z of the (X, Y, Z) axes referenced to the (X_1, Y_1, Z_1) axes when Y and Z are coincident with Y_1 and Z_1, respectively. These angles may be considered to be three-axes Euler angles only for the special case in which two of the Euler angles are zero.

The nominal orientation of the vehicle is that in which the geometric and sun-referenced axes are coincident (i.e., $\alpha_1 = \alpha_2 = \alpha_3 = 0$). Any deviation from the sun-oriented flight mode is thus reflected in non-zero values of the roll, pitch, and yaw angles.

II.3.2 Orbital Elements

The vehicle is assumed to be in a circular orbit, having an altitude of 250 nm. It is also assumed that the orbital inclination is 28.5 deg. Because of the regression of the nodes between the orbit and ecliptic planes, the sun angle λ may vary between +52 deg and -52 deg. The rate of change of λ is sufficiently small, however, so that λ may be regarded as constant during any single orbit.

II.3.3 Vehicle Data

The vehicle configuration considered in this study is shown schematically in Fig. II-2. It consists of an OWS, solar panels, Instrument Unit (IU), Spacecraft-LM Adapter (SLA), Airlock Module (ALM), Multiple Docking Adapter (MDA), and an Apollo Command and Service Module (CSM).

The weights and inertias are derived from data presented in Ref. II-1 and are summarized below. All data are referenced to the Saturn IB coordinate system, described in subsection II.3.1.

- Total Weight   75,580 lb
- Center of Gravity   x = 1,754.45 in.

  y = 5.59 in.

  z = -1.43 in.

- Moments and Products of Inertia

$$J_x = 118,289 \text{ slug-ft}^2$$
$$J_y = 2,254,646 \text{ slug-ft}^2$$
$$J_z = 2,519,964 \text{ slug-ft}^2$$
$$J_{xy} = -4,105 \text{ slug-ft}^2$$
$$J_{xz} = 13,444 \text{ slug-ft}^2$$
$$J_{yz} = 28 \text{ slug-ft}^2$$

- Principal Inertias

$$J_1 \triangleq J_{xp} = 118,207 \text{ slug-ft}^2$$
$$J_2 \triangleq J_{yp} = 2,254,653 \text{ slug-ft}^2$$
$$J_3 \triangleq J_{zp} = 2,520,039 \text{ slug-ft}^2$$

The direction cosine matrix relating the principal axes to the Saturn IB axes is:

$$\begin{bmatrix} 0.99998286 & -0.00170613 & 0.00559775 \\ 0.00170083 & 0.99999793 & 0.00109498 \\ -0.00559961 & -0.00108545 & 0.99998371 \end{bmatrix}$$

II.4 AERODYNAMIC TORQUES

II.4.1 Method of Computation

The orbital aerodynamic characteristics of the given configuration and flight mode were obtained by utilzing the results of Sentman (Ref. II-2). These results are based upon the assumption that the flow regime is free molecule. The model of the cluster arrangement used to calculate the aerodynamic characteristics is composed of flat plates and cylinders (see Fig. II-4).
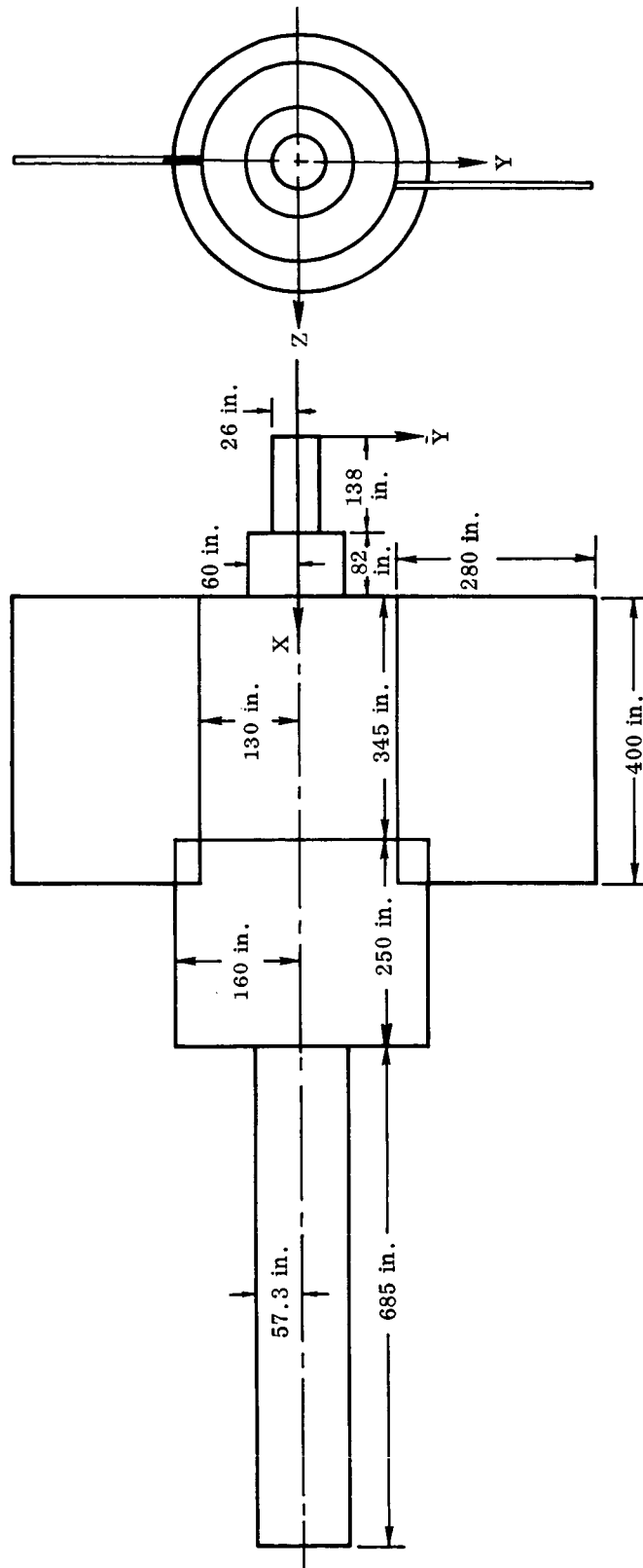
Fig. II-4 Vehicle Model Used in Aerodynamic Force and Moment Calculations

A reflected-to-incident molecular temperature ratio (Tr/Ti) of 0.247 and a molecular speed ratio S of 7.34 were obtained from Ref. II.3. In addition to these parameters, the results presented here are based on the following assumptions:

(1) Molecular reflection is completely diffuse.

(2) Tr is uniform over the body surface.

(3) The vehicle surface temperature Tw is uniform and equal to 300°K.

(4) The thermal accommodation coefficient (α) is unity (i.e., Tr = Tw).

(5) The dynamic pressure representation, in terms of orbital position, is

$$q = 10^{-6} \left[3.6 + 1.8 \cos (\theta_t - 30°) \right] \text{lb/ft}^2$$

In this expression, 3.6×10^{-6} lb/ft^2 is the mean dynamic pressure for the given flight mode, assuming the A1/A2 flights occur during near peak solar activity. The molecular density varies between a peak value in the day and a minimum value at night. From the data presented in Ref. II.4, the maximum density occurs approximately at a 30-deg lead angle from the earth-sun line. This accounts for the 30-deg phase shift in the periodic portion of the expression for q. Significant deviations from the results presented here may result if other density representations are used.

A shading technique is used to compensate for the shielding effect of one part of the vehicle upon another. This method is adequate only when the molecular speed ratio is high.

II.4.2 Results

The aerodynamic roll torques (T_{AX}), pitching torques (T_{AY}), and yaw torques (T_{AZ}) are shown as functions of orbital position and orientation in Figs. II-5, II-6, and II-7, respectively. These torques act about the body fixed axes and are referenced to the center of gravity of the cluster arrangement. Each torque component is presented for
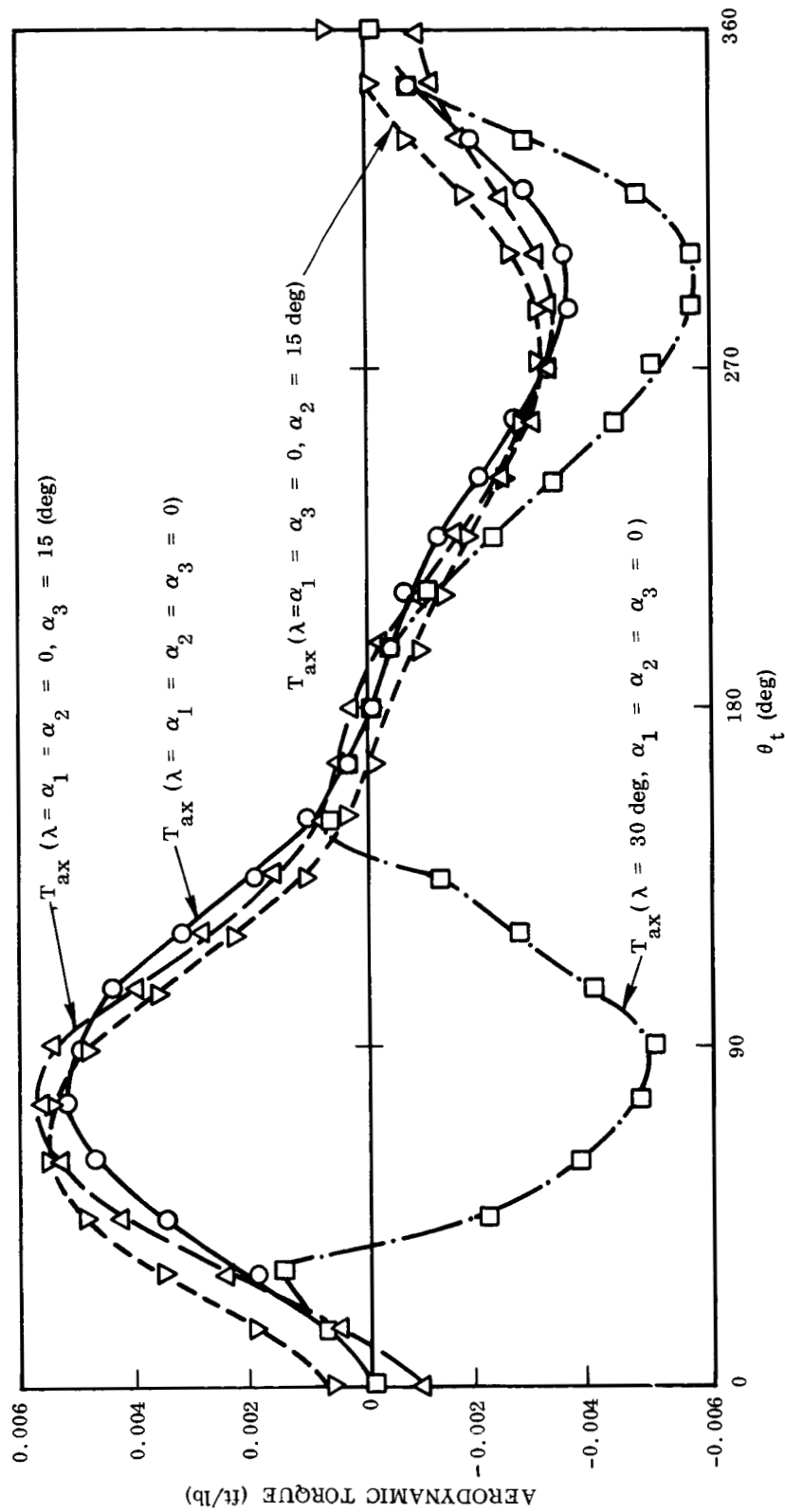
Fig. II-5 Aerodynamic Roll Torque as a Function of Orbital Position and Orientation
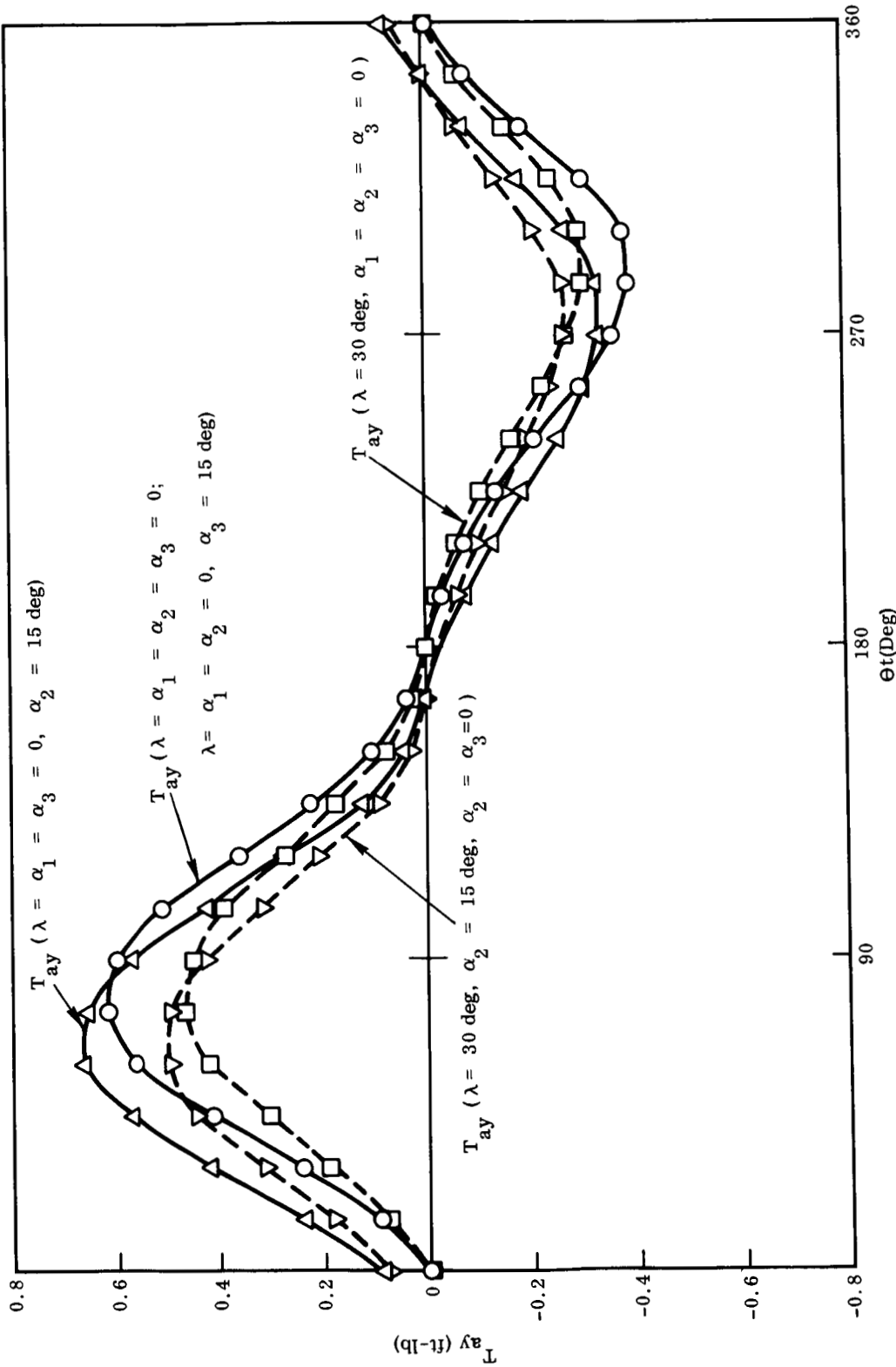
Fig. II-6 Aerodynamic Pitching Torque as a Function of Orbital Position and Orientation
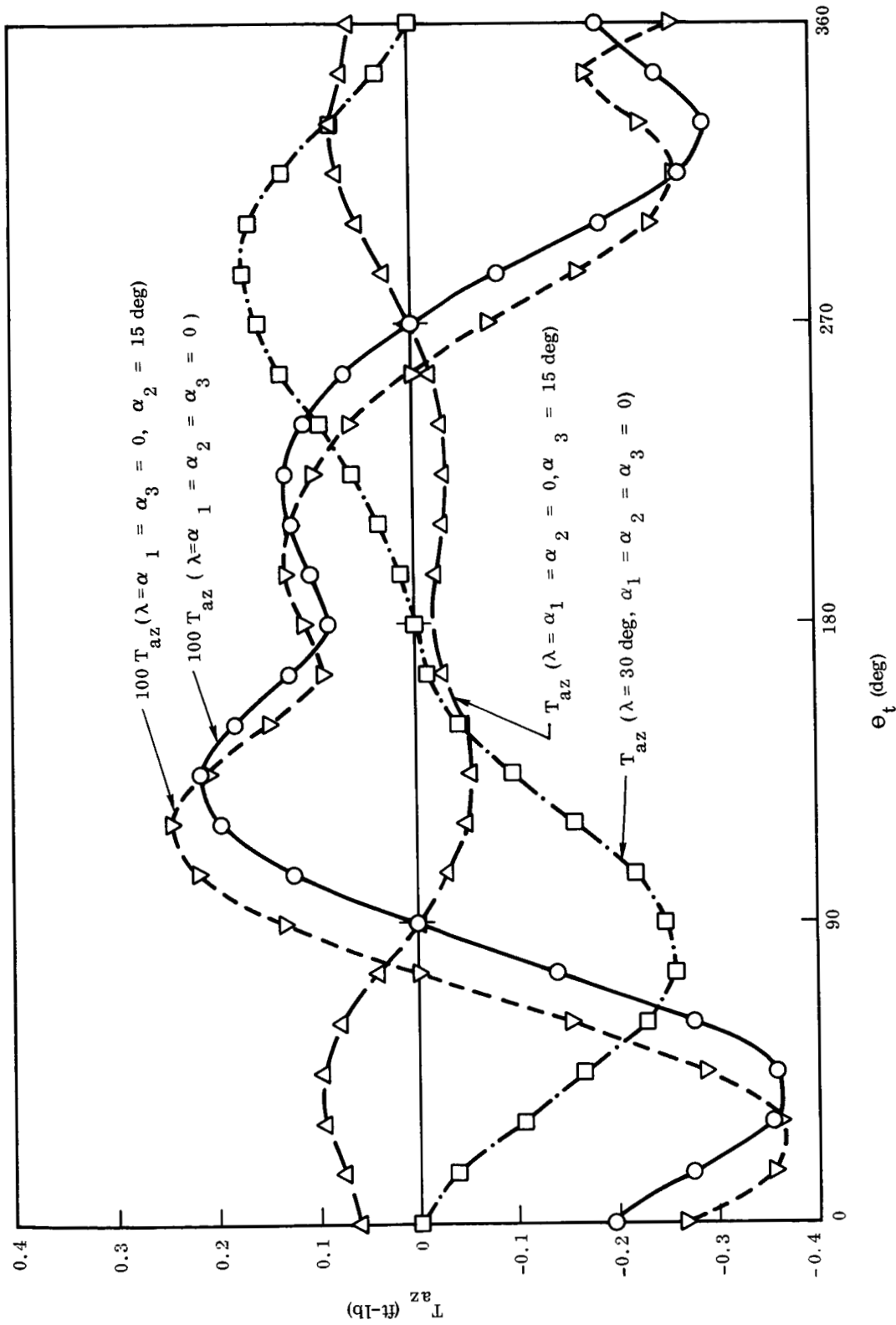
Fig. II-7 Aerodynamics Yaw Torque as a Function of Orbital Position Orientation

the case of nominal vehicle orientation and sun angle equal to 0 and 30-deg. In addition, the aerodynamic torques are shown for vehicle orientations having 15-deg pitch and yaw deviations from the nominal. The torques corresponding to 30-deg roll error and λ = 0-deg are exactly the torques corresponding to λ = 30-deg and nominal orientation. In each case, roll, pitch, and yaw errors are considered separately.

The aerodynamic pitch and yaw torques are even and odd functions of λ , respectively. The roll torques do not exhibit such a character due to the asymmetry of the solar panel locations. Tables of aerodynamic forces corresponding to the various vehicle orientations considered above are presented in Appendix A. These forces may be used to recalculate the aerodynamic moments if the vehicle center of gravity location is altered. F_{AX} and F_{AZ} are even functions of λ whereas F_{AY} is an odd function of λ .

It should be noted that the moments corresponding to a vehicle orientation having a 15-deg pitch error can be approximately represented by the moments corresponding to the nominal orientation with a 15-deg phase shift. A 15-deg yaw error has little effect upon T_{AX} and T_{AY} but does result in significant increases in T_{AZ}. Increasing λ tends to reduce the pitching torque and increase the yaw torque. This trend continues until λ = 45-deg and then the trend reverses. The magnitude of the resultant moment vector for any θ_t , however, is maximum when λ = 0. A change of λ does alter the shape of the T_{AX} curve, but does not significantly alter the magnitudes of the roll torques.

Orbital aerodynamic bias torques act about each vehicle axis for all nominal orientations. The shift of the maximum dynamic pressure from the projected earth-sun line (Z_o) is primarily responsible for these torques. Except for small shadowing effects, the C.P. shift with respect to the C.G. location is symmetrical about Z_o during an orbit. The slight asymmetry due to shadowing does not result in significant bias torques. The dynamic pressure, however, is asymmetrical with respect to Z_o and does result in significant bias torques acting about each vehicle axis. This is a direct consequence of the fact that the dynamic pressure, and hence aerodynamic forces, is greater for $+\theta_t$ ($0 \leq \theta_t \leq 180$-deg) (Fig. II-1) than for $-\theta_t$. Because the aerodynamic

moment coefficients are approximately equal at $\pm\theta_t$, a larger moment acts at $+\theta_t$. This, then, is the primary cause of the orbital aerodynamic bias torques acting on the vehicle.

The accuracy to which the bias torques may be calculated is directly related to the accuracy of the dynamic pressure representation. For the model used in this analysis the pitching bias torque is 0.075 ft-lb when λ is zero and the orientation nominal. In no case considered does the bias torque exceed 0.1 ft-lb and in all cases considered, the pitching bias torque is greater than the roll and yaw biases. All biases may be reduced by allowing the vehicle to have a negative pitch error of magnitude no greater than the offset angle, from Z_o , of the maximum dynamic pressure.

Although these bias torques are small compared to the oscillatory torques acting on the vehicle, their effect upon the vehicle attitude and motion is significant. For this reason, the choice of the dynamic pressure representation is critical in accurately determining the motion resulting from the action of the aerodynamic torques. However, the impulse needed to control these torques is relatively small, irrespective of the dynamic pressure representation used.

II.5 GRAVITY TORQUE ANALYSIS

Equations for the components of the gravity torque expressed in the sun reference system are derived in Part I of Ref. II.5. They are based on the assumptions that:

(1) The principal axes of the vehicle deviate from the geometric axes by a single rotation ν (not necessarily small) about the X-axis

(2) The geometric axes deviate from the sun system axes by small angles

The inertia data presented in subsection II.3 shows that for the vehicle under consideration assumption (1) is a good approximation. For this analysis, it is assumed that the geometric axes are coincident with the sun reference axes and the effects of misalignments are discussed at the end of this section. The equations for the gravity torques are thus reduced to the following:

$$T_{GX} = 3\Omega_o^2 \left[(\Delta_1 - \Delta_2) \, S\lambda \, C\lambda - \Delta_3 C \, (2\lambda) \right] C^2\theta$$

$$T_{GY} = 3\Omega_o^2 \left[\Delta_1 \, C\lambda + \Delta_3 \, S\lambda \right] S\theta \, C\theta \qquad\qquad \text{(II.1)}$$

$$T_{GZ} = 3\Omega_o^2 \left[\Delta_2 \, S\lambda + \Delta_3 \, C\lambda \right] S\theta \, C\theta$$

where

$$\Delta_1 \triangleq J_2 \sin^2 \nu + J_3 \cos^2 \nu - J_1$$

$$\Delta_2 \triangleq J_2 \cos^2 \nu + J_3 \sin^2 \nu - J_1 \qquad\qquad \text{(II.2)}$$

$$\Delta_3 \triangleq (J_2 - J_3) \sin \nu \cos \nu$$

$$S\theta \triangleq \sin \theta_t \qquad C\theta \triangleq \cos \theta_t$$

$$\qquad\qquad\qquad\qquad\qquad\qquad\qquad\qquad \text{(II.3)}$$

$$S\lambda \triangleq \sin \lambda \qquad C\lambda \triangleq \cos \lambda$$

In Figs. II-8 through II-10 the three components are plotted as a function of θ_t with λ as a parameter. It should be emphasized that the torque profiles presented are based on the assumption that the geometric axes remain aligned with the sun reference axes. If the vehicle is allowed to deviate significantly from the nominal attitude under the influence of the disturbing torques, the torque profiles will change.

Since J_2 and J_3 are nearly equal and the X-axis is constrained to lie in the orbit plane, the gravity torque is nearly normal to the orbit plane. This can be seen by letting $J_2 = J_3 \triangleq J$ in Eqs. (II.1) and (II.2) which results in

$$T_{GX} = 0$$

$$T_{GY} = \frac{3\Omega_o^2}{2} (J - J_1) \cos \lambda \sin 2\theta_t$$

$$T_{GZ} = \frac{-3\Omega_o^2}{2} (J - J_1) \sin \lambda \sin 2\theta_t$$
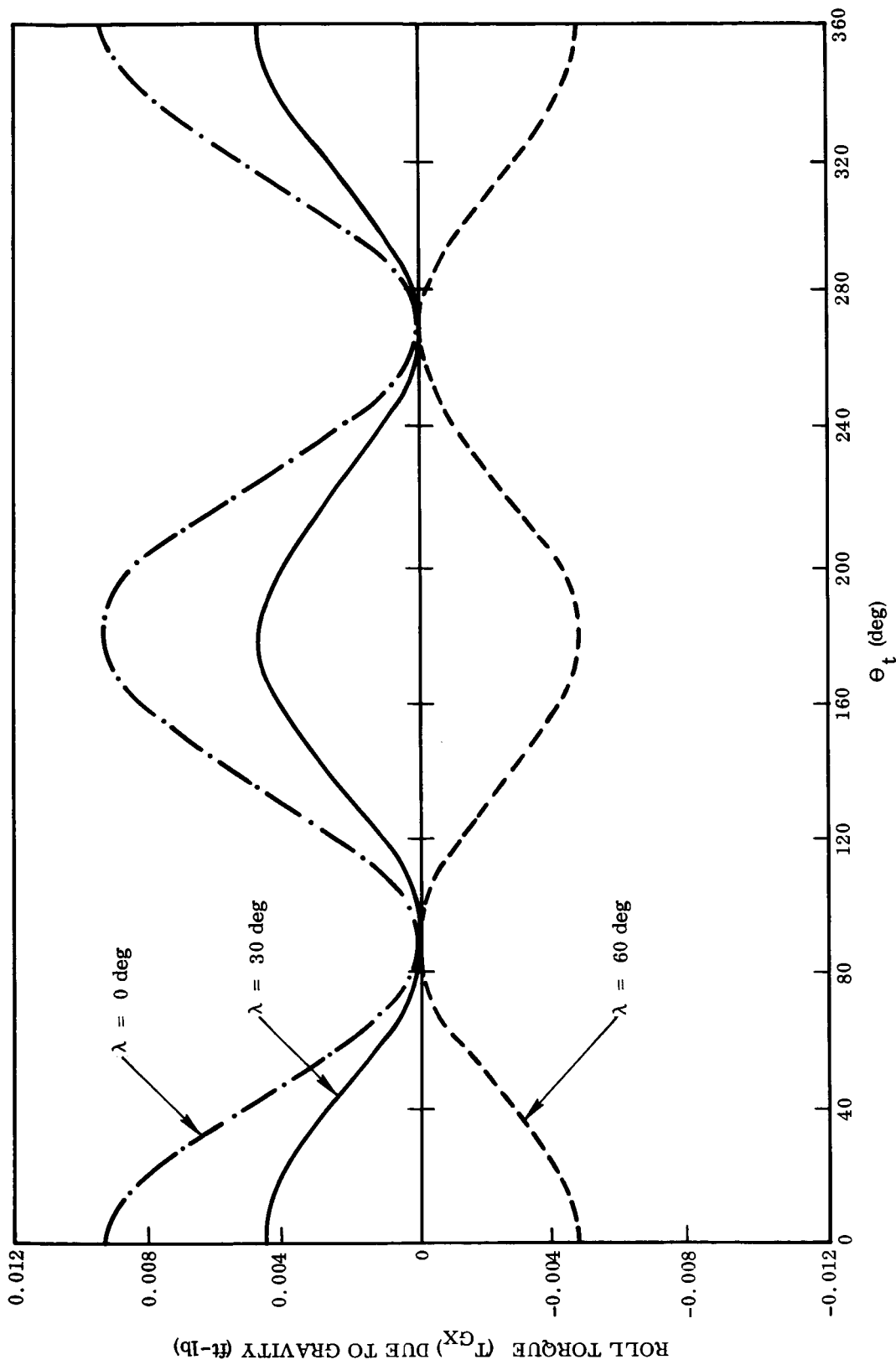
Fig. II-8 Roll Torque T_{GX} due to Gravity vs. θ_t for Ideal Orientation
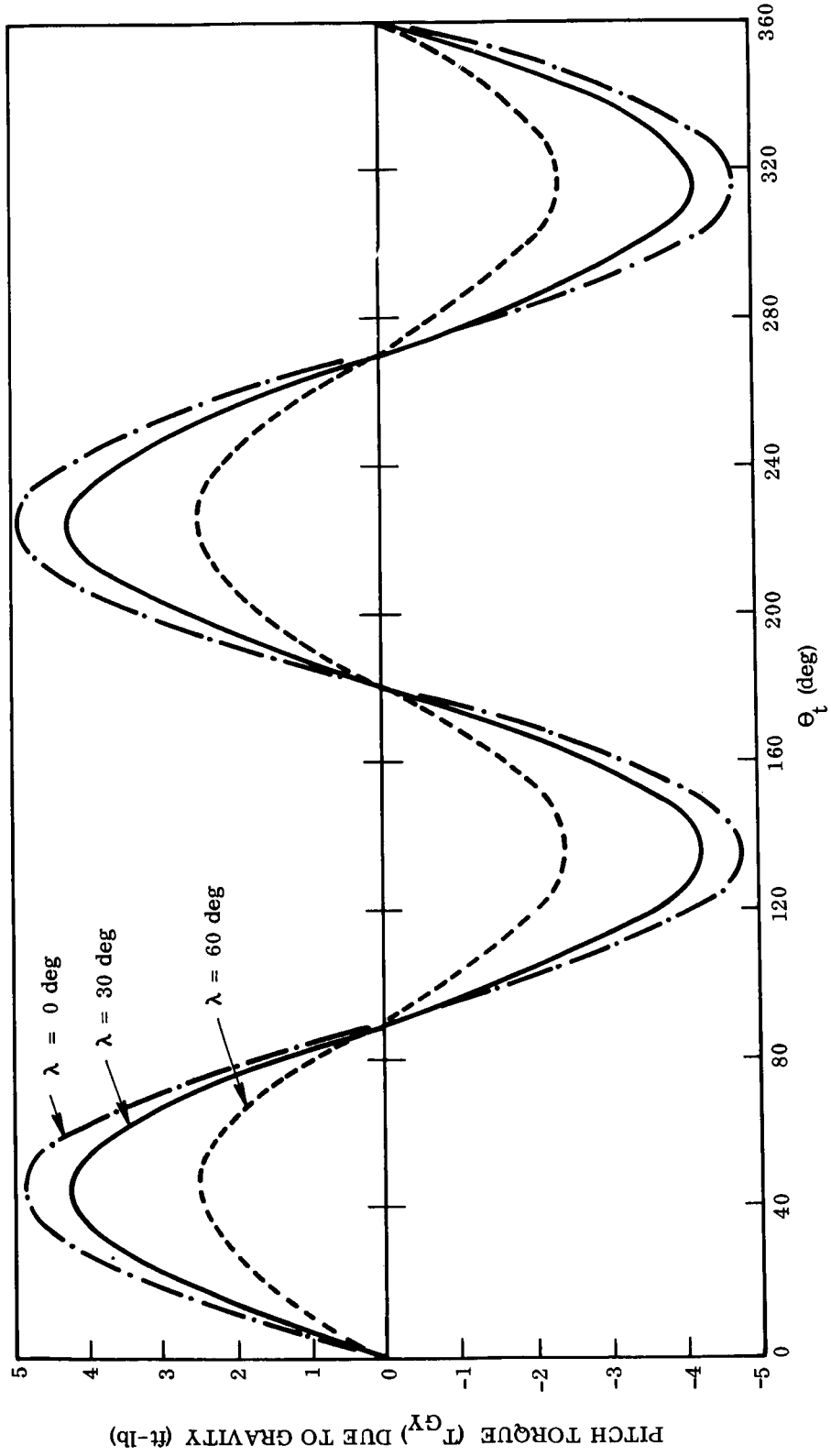
Fig. II-9 Pitch Torque T_{AY} due to Gravity vs. θ_t for Ideal Orientation

LOCKHEED MISSILES & SPACE COMPANY
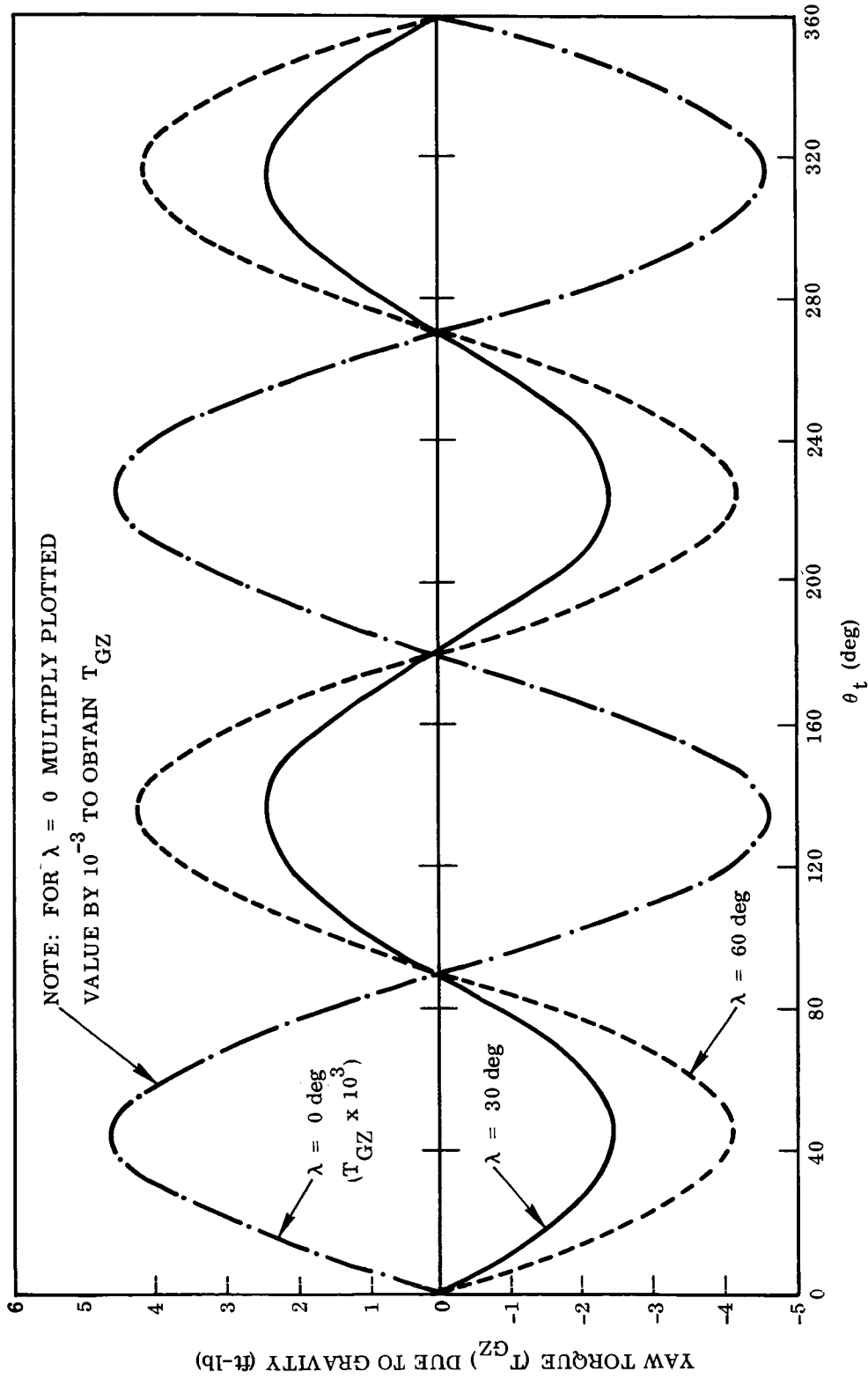
Fig. II-10 Yaw Torque T_{GZ} due to Gravity vs. θ_t for Ideal Orientation

For $\lambda = 0$ the Y-axis is normal to the orbit plane and the complete gravity torque is given by

$$T_{GY} = \frac{3\Omega_o^2}{2} (J - J_1) \sin 2 \theta_t$$

This situation is illustrated in Fig. II-9. Figures II-8 and II-10 show that T_{GX} and T_{GZ} are not identically zero because of the slight difference between J_2 and J_3. However, their amplitudes are at least two orders of magnitude less than T_{GY}. As λ varies between its limits of ± 52-deg the magnitude of the gravity torque is not significantly altered, but the components in the body fixed geometric coordinate system vary.

The effects of pitch and roll misalignment of the geometric axes with respect to the sun reference axes can be observed in Figs. II-8 through II-10. A constant roll error (about the X_1-axis) produces the same results as changing the value of λ by the value of the error. A constant pitch error (about the Y_1-axis) is equivalent to a phase angle to be added to θ_t. The effect of a yaw error (about the Z_1-axis) cannot be obtained from the nominal orientation data but must be determined from the complete equations of Ref. II.4 which allows for misalignments between the geometric and sun-referenced systems. This was done for a yaw error of $\alpha_3 = 15$-deg for $\lambda = 0$ and the results are plotted in Fig. II-11. The importance of keeping the X-axis of the vehicle in the orbit plane is illustrated in this figure. When the axis is allowed to drift out of the orbit plane, a large noncyclic torque is created which requires the application of a large continuous control torque.

II.6 EQUATIONS OF MOTION

In subsections II.4 and II.5 it was pointed out that both the gravity torque and the aero torque are essentially normal to the orbit plane so that the most significant deviations from the nominal orientation can be expected to occur in the orbit plane. In addition,
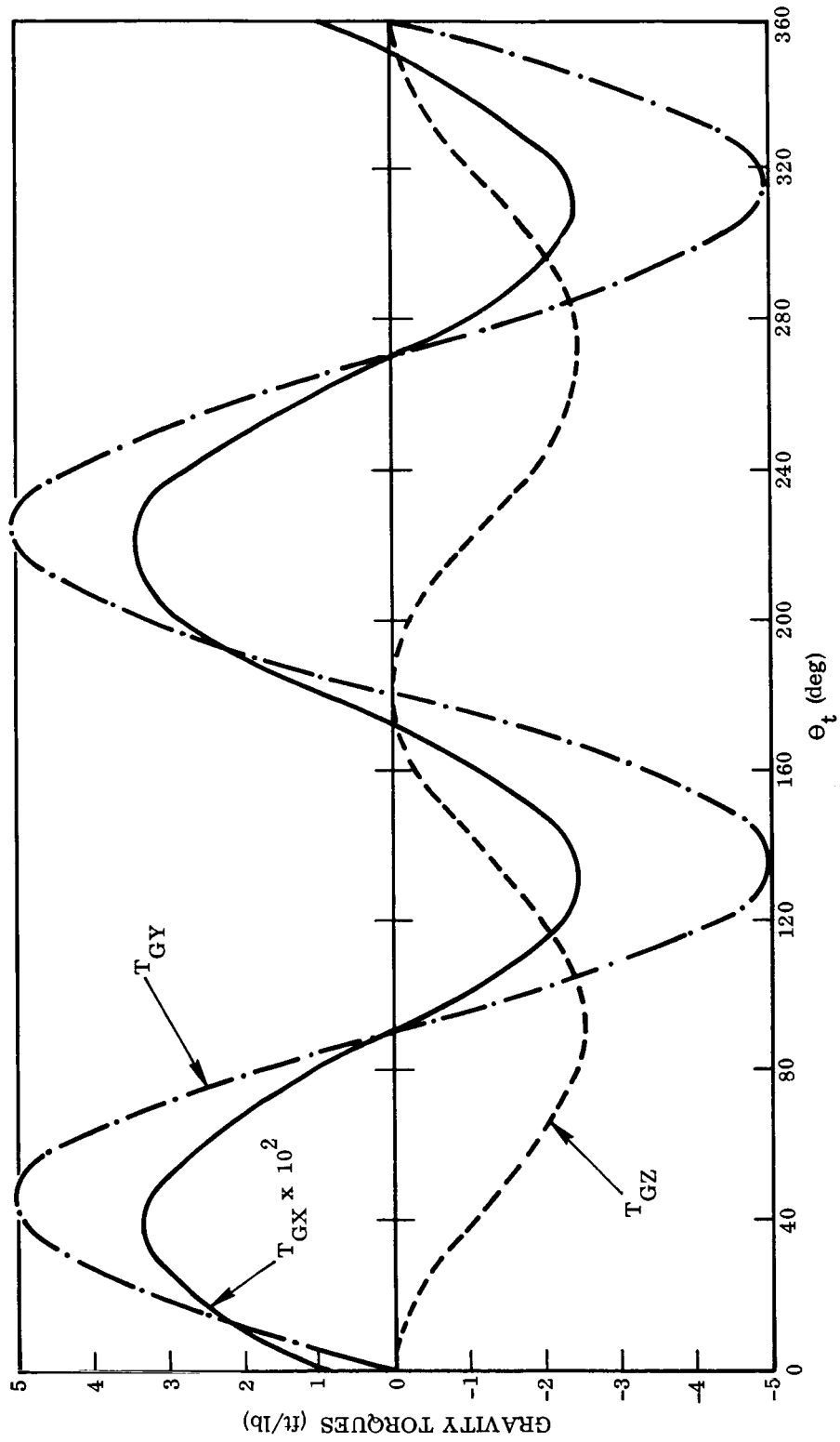
Fig. II-11 Gravity Torques vs. θ_t for 15-deg Yaw (Z) Misalignment

LOCKHEED MISSILES & SPACE COMPANY

when expressed in the orbital system, the disturbance torques were found to be only weak functions of the parameter λ so that treatment of a single value of λ should lead to results which are generally applicable. Since for $\lambda = 0$ the orbital axes and the sun-referenced axes coincide, the analysis will be based on this case.

Neglecting the small X and Z torques and approximating the moment of inertia about the Y-axis by the average of J_2 and J_3, the equation of motion of the vehicle becomes

$$J \ddot{\alpha}_2 = T_{GY} + T_{AY}$$

where $J \triangleq (J_2 + J_3)/2$ and T_{GY} and T_{AY} are the Y-components of the gravity and aero torques, respectively. Both T_{GY} and T_{AY} are functions of α_2 as well as time, but if it is assumed that α_2 remains small, then T_{AY} and T_{GY} may be approximated by the results obtained in subsections II.4 and II.5. The gravity torque may thus be written

$$T_{GY} = G \sin 2\theta_t$$

where

$$G \triangleq \frac{3\Omega_o^2}{2}(J - J_1) = 4.88 \text{ ft-lb}$$
$$\theta_t = \Omega_o t$$

The aero torque was approximated analytically by

$$T_{AY} \approx A \sin \theta_t + B$$

where

A = 0.676 ft-lb
B = 0.148 ft-lb

II-22

This analytical model is based on a 25 percent overestimate of the aerodynamic moment arm, increasing the amplitude of the total disturbance torque by approximately 3 percent. The total disturbance torque, $T_Y = T_{AY} + T_{GY}$, is plotted in Fig. II-12.

With the approximations discussed above, the final form of the differential equation for α_2 becomes

$$\ddot{\alpha}_2 = \frac{B}{J} + \frac{A}{J} \sin \Omega_o t + \frac{G}{J} \sin \Omega_o t$$

The solution to this equation is discussed in subsection II.7.

II.7 UNCONTROLLED MOTION

In subsection II.6, the differential equation of motion of a simplified system was derived. The form is such that it can be integrated directly leading to

$$\dot{\alpha}_2 = \left(\frac{B}{\Omega_o J}\right) \theta_t - \left(\frac{A}{\Omega_o J}\right) \cos \theta_t - \left(\frac{G}{2\Omega_o J}\right) \cos 2\theta_t + C_1 \tag{II.4}$$

$$\alpha_2 = \left(\frac{B}{2\Omega_o^2 J}\right) \theta_t^2 - \left(\frac{A}{\Omega_o^2 J}\right) \sin \theta_t - \left(\frac{G}{4\Omega_o^2 J}\right) \sin 2\theta_t + \left(\frac{C_1}{\Omega_o}\right) \theta_t + C_2 \tag{II.5}$$

where

$\quad B/\Omega_o J \quad = 50.5321 \times 10^{-6}$ deg/sec/deg

$\quad A/\Omega_o J \quad = 13.1950 \times 10^{-3}$ deg/sec

$\quad G/2\Omega_o J \quad = 47.6806 \times 10^{-3}$ deg/sec

$\quad B/2\Omega_o^2 J \quad = 3.7880 \times 10^{-4}$ deg/sec^2

$\quad A/\Omega_o^2 J \quad = 11.3346$ deg

$\quad G/4\Omega_o^2 J \quad = 20.4790$ deg
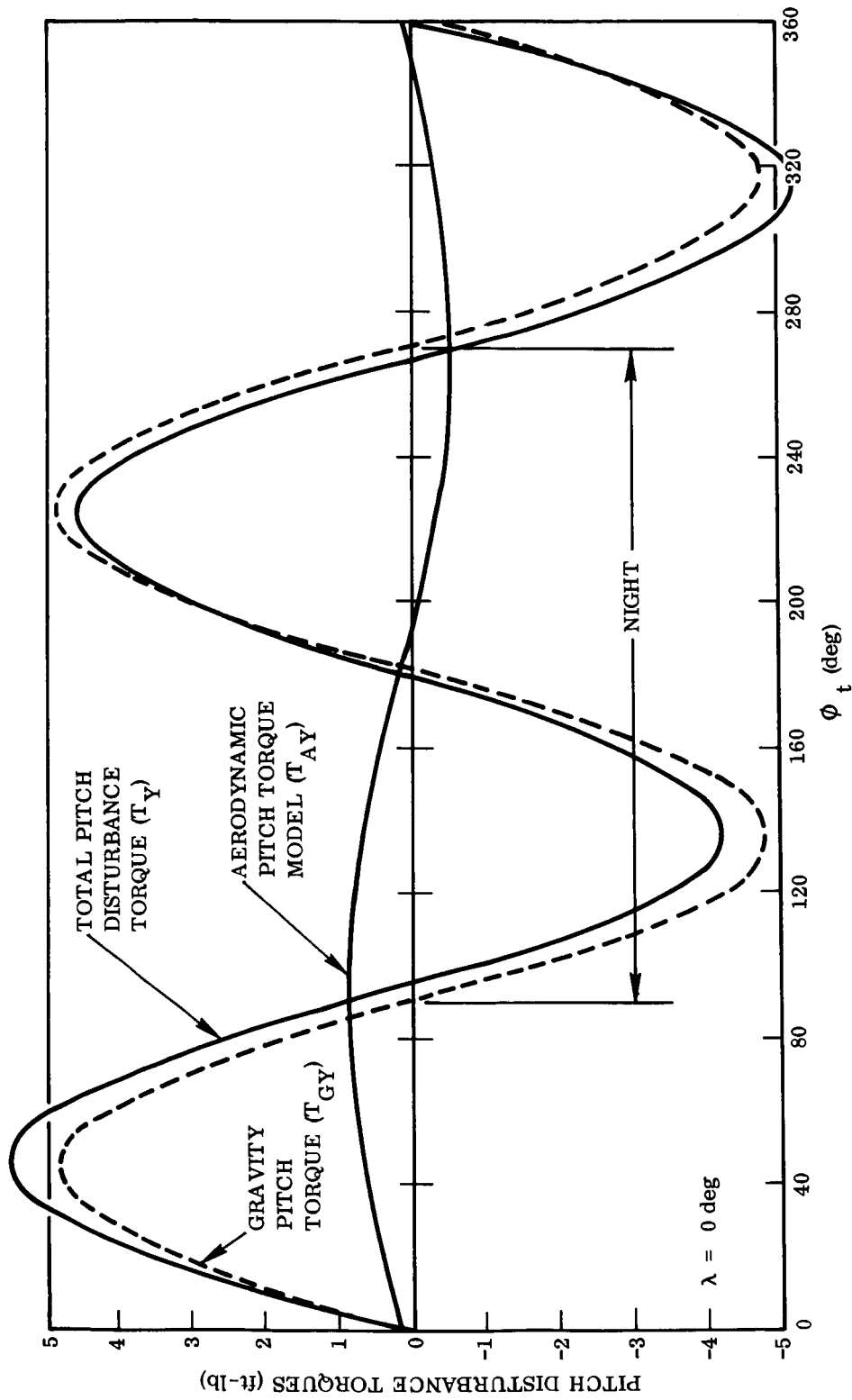
Fig. II-12 Pitch Disturbance Torques T_Y Vs. θ_t for Ideal Orientation

and C_1 and C_2 are constants of integration. In Figs. II-13 and II-14, $\dot{\alpha}_2$ and α_2 are plotted vs. θ_t for the special case of $C_1 = C_2 = 0$.

Figure II-14 shows that the aerodynamic bias torque if uncontrolled, leads to a pitch angle of 50-deg in one orbit. While the consequences of reaching a 50-deg angle would probably require a modification of the aerodynamic characteristics it is nonetheless clear that this bias torque may be the most significant disturbance requiring control.

The next notable feature is the interaction of the gravity gradient and aerodynamic torques. Although the amplitude of the cyclic portion of the aero torque is less than 15 percent of the gravity torque, the amplitude of the corresponding oscillation is greater than 50 percent of that due to gravity because the period of the aero torque is twice as long as that of the gravity torque. The net result is a 30-deg maximum pitch angle (ignoring the contribution of the aerodynamic bias torque).

If the aerodynamic bias torque is ignored, then Eq. (II.5) shows that the motion is periodic, if $C_1 = 0$. For any other value there will be a monotonically increasing angle. We assume hereafter that $C_1 = 0$.

If the motion is uncontrolled, then the energy actually acquired during each orbit is given by Eq. (II.6).

$$E = \dot{E} \int \cos \alpha_2 (t) \, dt \qquad (II.6)$$

where

$\dot{E}$ = power collected for $\alpha_2 = 0$-deg

$\alpha_2 (t)$ = deviation from LOS (e.g., see Fig. II-14)
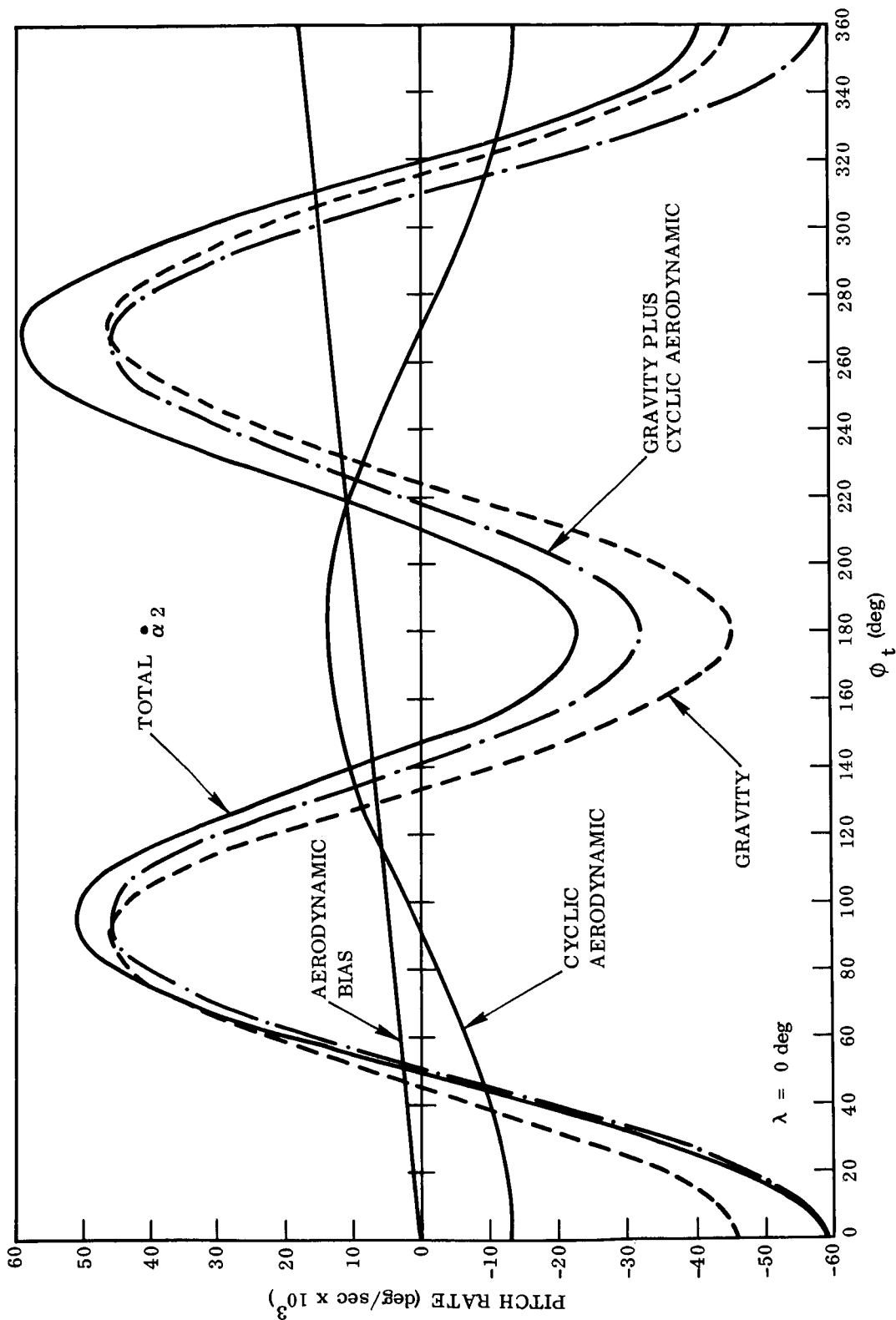
Fig. II-13 Uncontrolled Pitch Rate Components Vs. $\dot{\theta}_t$ During First Orbit
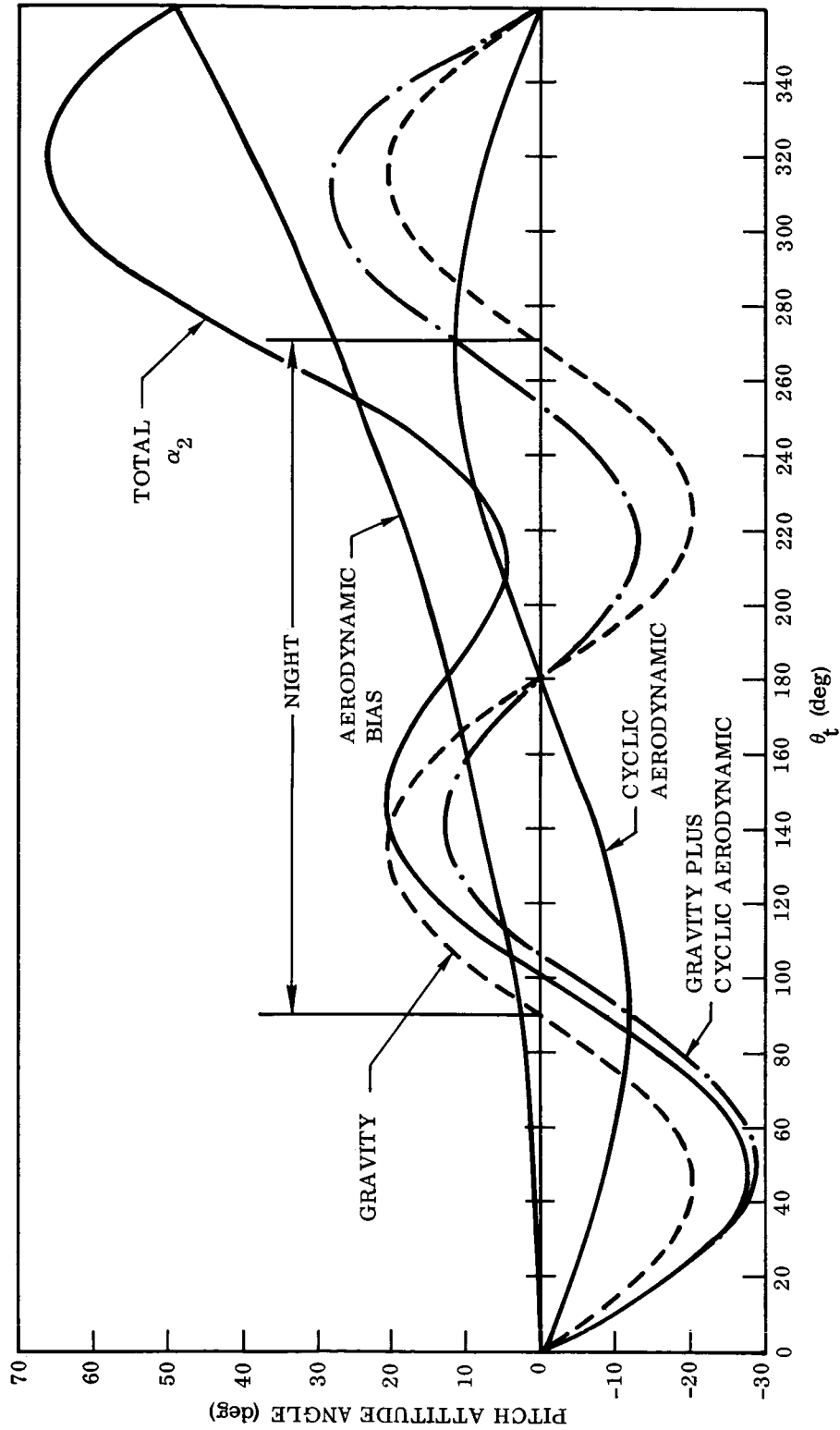
Fig. II-14 Uncontrolled Pitch Attitude Components Vs. θ_t During First Orbit

Ignoring the effects of the aerodynamic bias, the motion is shown by Fig. II-14 to be symmetric about the orbit. Integrating graphically* over 90 deg of the daylight portion of the orbit gives a value for the integral of

$$E/\dot{E} = 1310 \text{ sec} \qquad (\text{II-7})$$

If the attitude (α_2) had been zero throughout, i.e., had there been no deviation from LOS, then the value of the integral would have been 1410 sec (a quarter of the orbit period). Then, the energy loss is

$$\frac{E_{max} - E_{actual}}{E_{max}} = \frac{1410 - 1310}{1410} = 7.1\% \qquad (\text{II-8})$$

If a control system were to hold the vehicle to a maximum α_2 of ± 20 deg, but otherwise not affect its motion, then the integral of Eq. (II-6) has the value of

$$E/\dot{E} = 1344 \text{ sec} \qquad (\text{for } \alpha_{2max} = \pm 20 \text{ deg}) \qquad (\text{II-9})$$

In this case the energy loss is

$$\frac{E_{max} - E_{actual}}{E_{max}} = \frac{1410 - 1344}{1410} = 4.7\% \qquad (\text{II-10})$$

While a control system with a 20 deg deadband would doubtless alter the motion significantly from that shown in Fig. II-14, it is nonetheless clear that only modest reductions in the energy loss can be expected to be achieved through the use of a control system to limit the oscillatory pitch motion.

---

*See Appendix B for details of the integration.

LOCKHEED MISSILES & SPACE COMPANY

II. 8 IMPULSE REQUIREMENTS FOR PERFECT CONTROL

When perfect control is applied to the vehicle, the body fixed geometric axes remain aligned with the sun-reference system at all times. Under these conditions, the disturbance torques calculated in subsections II. 4 and II. 5 are exact. In order to maintain perfect control, it is necessary to apply control torques continuously that are equal and opposite to the disturbance torques. The required torque impulse per orbit is given by the integral of the absolute value of the disturbance torque over one orbit period. Ignoring the aerodynamic bias torque and assuming $C_1 = 0$ the control impulse for one orbit is

$$I_{control} = \int (G \sin 2\Omega_o t + A \sin \Omega_o t) \, dt \qquad (II. 11)$$

During a quarter of the orbit, the aerodynamic torques aid the gravity-gradient torques and oppose them in the succeeding quarter. In this fashion the impulse contribution of the aerodynamic torques is cancelled out and Eq. (II. 11) reduces to the time integral of the gravity gradient torques.

$$I_{control} = \frac{4G \dfrac{\cos 2\Omega_o t}{-2\Omega_o}}{\dfrac{\pi}{2\Omega_o}} = 19,400 \text{ ft-lb-sec/orbit} \qquad (II-12)$$

If the control force is located in the OWS engine area (Sta. 1225 has been used) a control moment arm of 50 ft is realized giving a control impulse required of

$$I_c = 388 \text{ lb-sec/orbit} \qquad (II-13)$$

For a period of 94 min there are 15. 3 orbits per day giving --

$$I_c = 388 \times 15.3 = 5950 \text{ lb-sec/day} \qquad (II. 14)$$

To estimate a propellant weight we assume a specific impulse of 276 lb_f-sec/lb_m (CSM RCS)

$$W_p = \frac{5950}{276} = 21.6 \text{ lb/day} \tag{II.15}$$

For a 28-day mission this leads to a propellant weight of 604 lb. While continuous control is not required, this value provides a limiting case against which more realistic situations may be evaluated.

In subsections II.4 and II.5 it was pointed out that the magnitude of the disturbance torque vector is not a strong function of the parameter λ. The control torque impulse necessary to cancel the disturbance torque, however, does depend on λ because the body-fixed thrusters must cancel the components of the disturbance torque individually. Consequently, if the thrusters are aligned with the vehicle geometric axes, the impulse required to cancel the disturbance for $\lambda = 45$ deg will be approximately $\sqrt{2}$ times that required for $\lambda = 0$.

II.9 DISCONTINUOUS CONTROL

In subsection II.7 it was shown that without the bias in the aero torque, the uncontrolled pitch motion is cyclic with a maximum amplitude of approximately 29 deg. For a dead band greater than 29 deg, therefore, it is necessary to supply only enough control impulse to compensate for the aero bias. For smaller dead bands additional impulse will be required. The impulse required to limit the maximum amplitude of the oscillation is strongly dependent on the manner in which it is applied. If a continuous control torque cancelling the cyclic aero torque were applied, the maximum amplitude would be reduced by approximately 8 deg at a cost in impulse of 1.4×10^6 ft-lb-sec. To effect a similar reduction in maximum amplitude by attenuating the gravity torque response would require approximately 8/20 of the total gravity impulse or 3×10^6 ft-lb-sec.

In reality the control impulse will probably be applied in a discontinuous fashion with the control system actuated by an attitude error sensing device. In addition, if a sun

sensor is used for actuation, control can be applied only during the daylight portion of the orbit. In order to assess the behavior of such a system, a model with the following characteristics has been analyzed.

(1) Impulses I_1 and I_2 are applied in opposition to the disturbance torques in the first and fourth quadrants of θ_t, respectively.

(2) I_1 is larger than I_2 by the magnitude of the aero bias impulse of a single orbit period so that the total impulse (algebraic) applied to the vehicle over one orbit is zero.

(3) The initial conditions are selected so that α_2 and $\dot{\alpha}_2$ are the same at the beginning and the end of the orbit.

The system is illustrated schematically in Fig. II-15. The resulting equation for α_2 during the first orbit period is

$$\alpha_2 = \left(\frac{B}{2\Omega_o^2 J}\right)\theta_t^2 - \left(\frac{A}{\Omega_o^2 J}\right)\sin\theta_t - \left(\frac{G}{4\Omega_o^2 J}\right)\sin 2\theta_t - \frac{I_1}{J\Omega_o}(\theta_t - \Omega_o t_1)\, U(\theta_t - \Omega_o t_1)$$

$$+ \frac{I_2}{J\Omega_o}(\theta_t - \Omega_o t_2)\, U(\theta_t - \Omega_o t_2) + \frac{C_1}{\Omega_o}\theta_t + C_2$$

where U is the unit step function occurring at the zero value of its argument. Condition (2) leads to

$$I_1 - I_2 = 2\pi B/\Omega_o$$

Assuming that the vehicle is initially aligned ($C_2 = 0$), condition (3) leads to

$$\frac{C_1}{\Omega_o} = \frac{2\pi B}{J\Omega_o^2}\left(\frac{1}{2} - \frac{\Omega_o t_1}{2\pi}\right) + \frac{I_2}{J}\frac{\Omega_o(t_2 - t_1)}{2\pi}$$
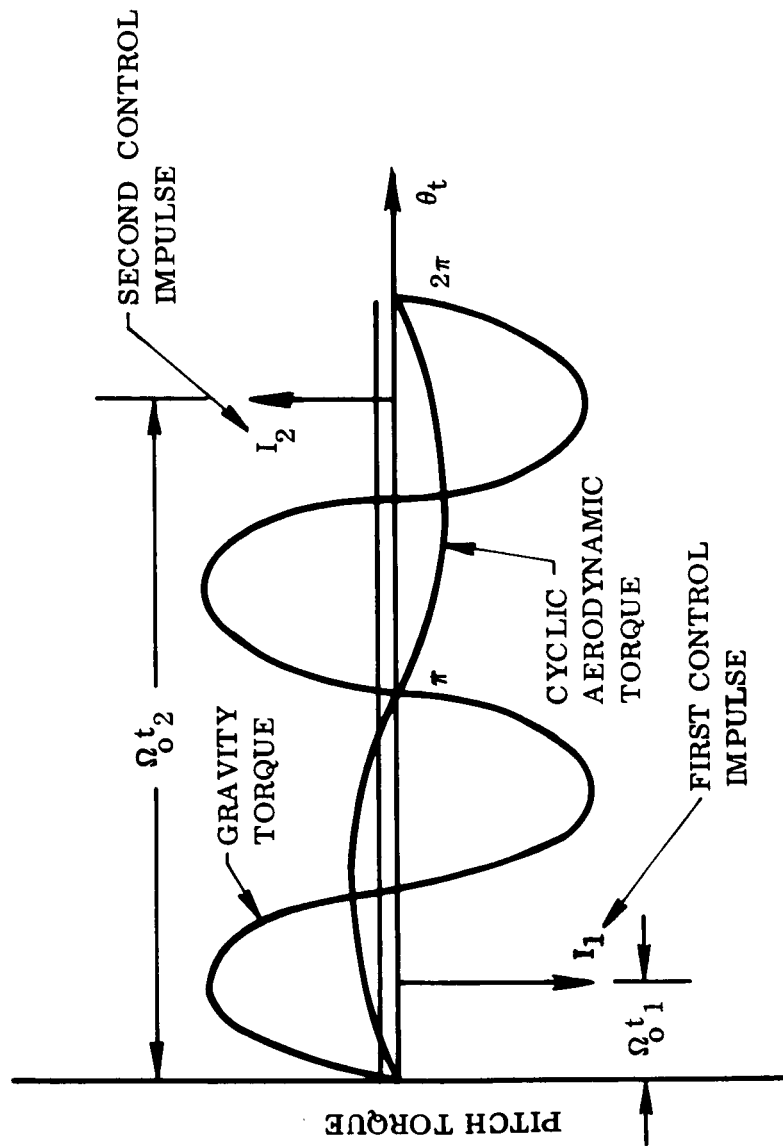
Fig. II-15 Schematic of Impulsive Control Model

LOCKHEED MISSILES & SPACE COMPANY

These equations have been solved for several values of I_2 for the special case of $\Omega_o t_1 = \pi/4$ and $\Omega_o t_2 = 7\pi/4$ and the results are plotted in Fig. II-16. The parameter k is the value of I_2 normalized with the gravity impulse by the following equation:

$$k \triangleq I_2/(G/\Omega_o) = \frac{I_2}{498 \text{ ft-lb-sec}}$$

The trajectories in Fig. II-16 indicate that for the assumed control system the smallest value of maximum amplitude is approximately 21-deg which occurs for k = 0.1. As k increases above that value, the maximum amplitude increases again. The important effect, however, is that for k > 0.1, the maximum amplitudes occur during the dark portion of the orbit. The maximum values of α_2 attained during the daylight portion of the orbit continue to decrease until α_2 reaches a value of 7.8-deg for k = 0.4. Since the primary purpose of the attitude control system is to keep the solar panels pointed at the sun, only the daylight portion of the orbit is of interest. A plot of impulse requirement vs. maximum daylight α_2 is presented in Fig. II-17.

II.10 ACQUISITION

On entering the earth's shadow the solar reference is lost and must be reacquired on leaving the shadow. Since no solar energy can be acquired in the shadow there is no reason to attempt to hold a specified attitude unless the propellant needed to reacquire the sun should exceed that needed to hold a specified attitude.

Assuming that the vehicle is at the maximum possible attitude error of 30-deg from the LOS, the control impulse to reacquire the sun — ignoring the disturbing torques — is
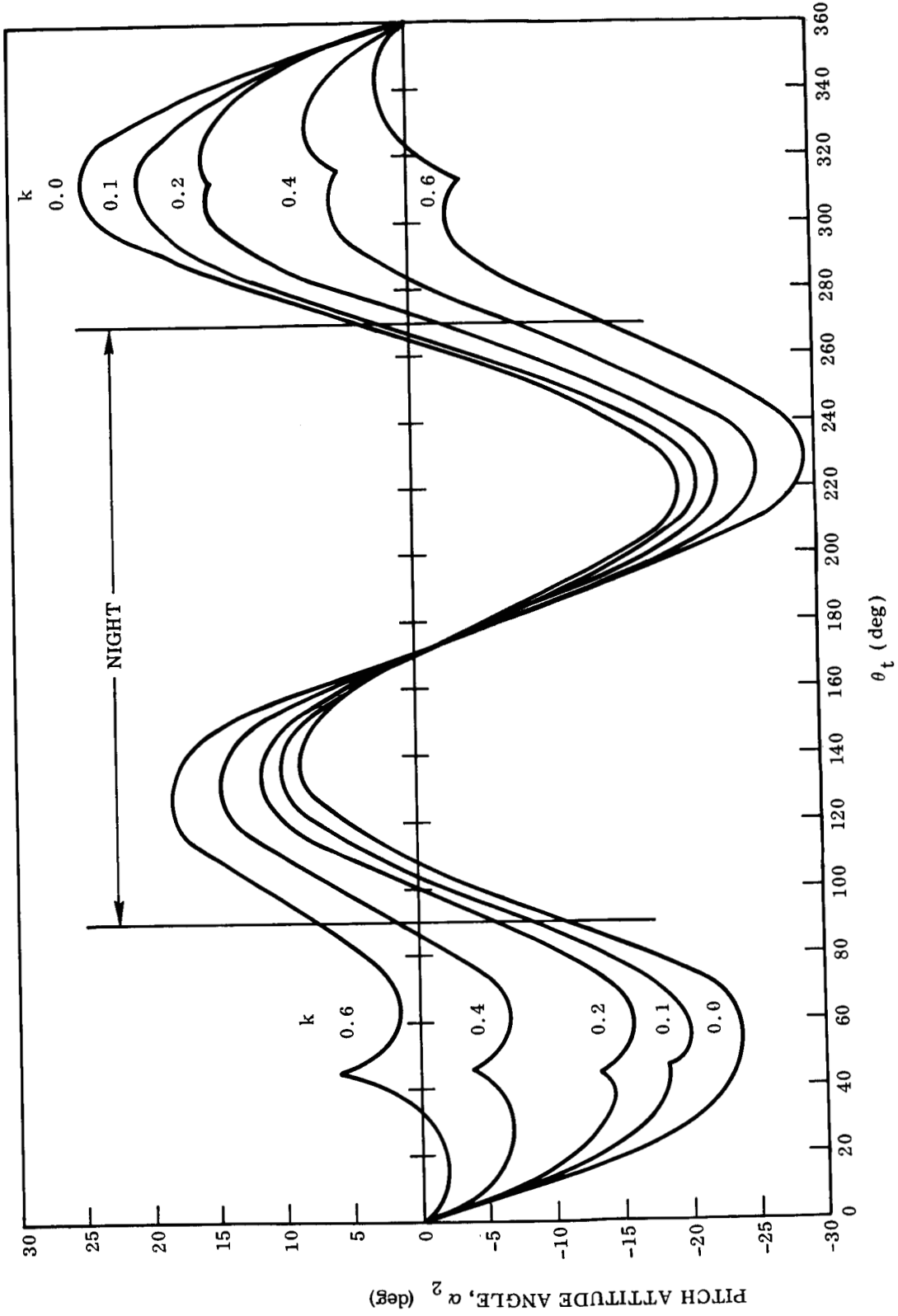
Fig. II-16 Pitch Attitude Angle α_2 Vs. θ_t for Impulsive Control
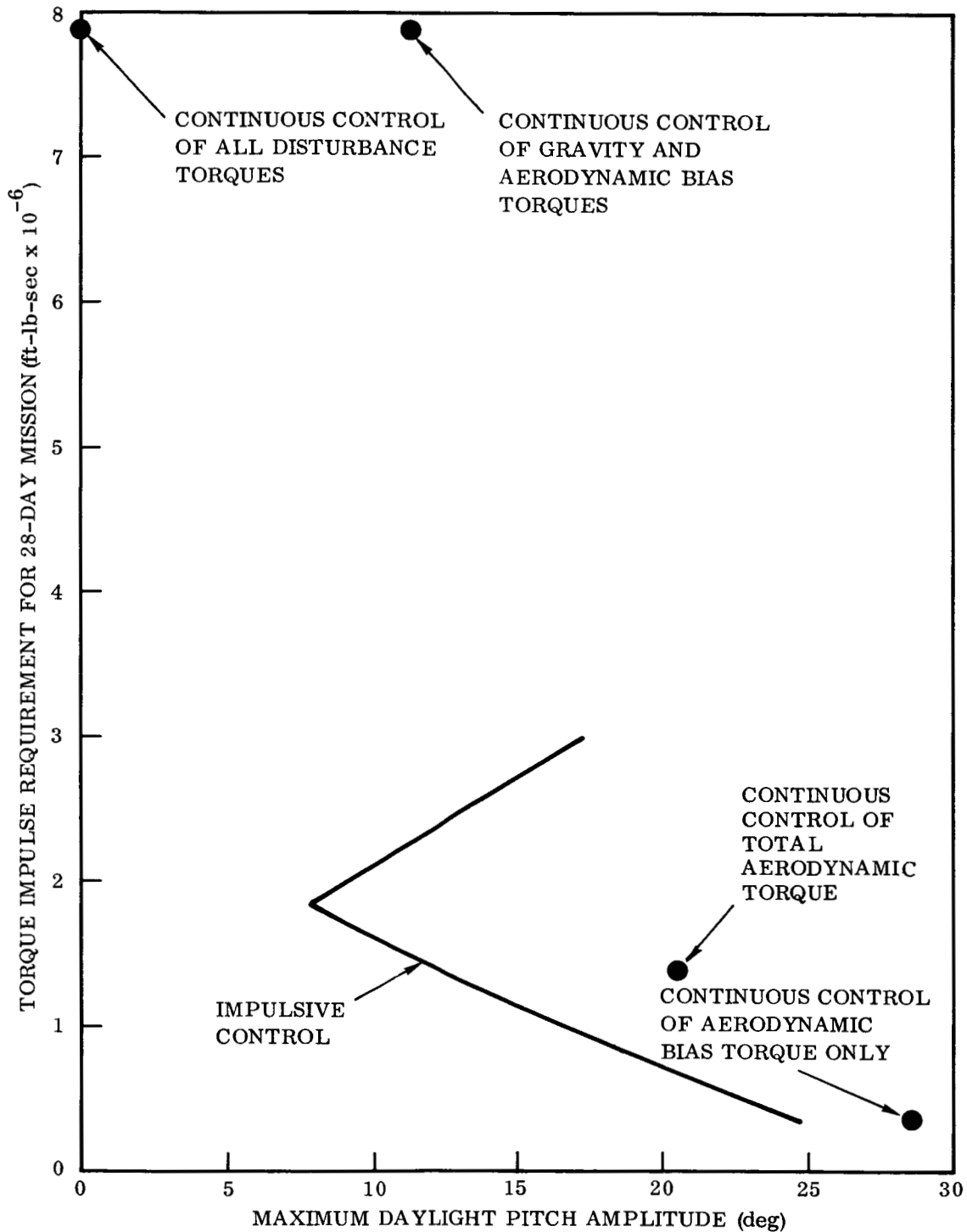
Fig. II-17 Torque Impulse Requirements vs. Maximum Daylight Pitch Amplitude
for Several Types of Control (28-Day Mission)

- $Ft = 2 \left| \dfrac{\alpha_{20} J}{t\ell} \right|$

  where α_{20} = initial error 30-deg

   J_2 = vehicle moment of inertia, 2.5×10^6 slug-ft^2

   t = time to reacquire and also time of control action

   ℓ = control moment arm, 50 ft

   F = control force

Our model assumes that the vehicle is accelerated through half of θ_o and decelerated through the second half to stop aligned to the LOS to the sun with no error and no pitch rate. For the given values and for $t = 5$ min (300 sec).

- $Ft = 2664 \dfrac{\text{lb-sec}}{\text{day}}$

For a specific impulse of 276 sec (because the firing is continuous no degradation of specific impulse is taken) we get a propellant weight of

- $W_p = \dfrac{Ft}{I_{sp}} = \dfrac{2664}{276} = 9.67$ lb/day

For a 28-day mission this leads to a propellant weight of 270 lb. If the time of acquisition is raised to 10 min, this weight drops by half to 135 lb.

An estimate may be made of the collected energy loss in this operation by assuming perfect control following reacquisition and an energy loss proportional to the $\cos \alpha_{20}/2$ during the acquisition period.

- $E_{actual}/E_{max} = 1 - \dfrac{t}{55} \left| 1 - \cos \dfrac{\alpha_{20}}{2} \right|$

  where τ = time when $\alpha_2 \equiv 0$

   t = time when $\alpha_2 \neq 0$

   $t + \tau$ = time in sunlight (min)

For $t = 10$ min and $\alpha_{20} = 30$-deg

LOCKHEED MISSILES & SPACE COMPANY

- $E_{actual}/E_{max} = 1 - \frac{10}{55} (1 - \text{Cos } 15°) = 0.9936$

    Thus, a 10-min reacquisition period will lead to an energy loss of well under 1 percent.

II. 11 ATTITUDE DETERMINATION

To meet the operational requirements of aligning the solar panels normal to the LOS requires determination of the LOS. This need is most directly met with a sun sensor. The sun sensor will establish, in terms of pitch and roll angles, the LOS to the sun. Rotations in yaw, i.e., about the LOS, do not affect the energy collected by the solar panels. However, rotations in yaw will, in general, lead to increases in both the gravity gradient and aerodynamic torques. If unopposed they could conceivably tumble the vehicle. Thus, yaw rotations must be controlled although they do not directly affect the solar energy collected.

To measure yaw angles two basic means are available – gyroscopic and star sightings (basically geometric). If the CM platform is operative, it can directly supply the yaw angle; if not operative, a separate gyroscope can be used. To compensate for gyro drift, they can be realigned each orbit with data supplied by star sightings. Star sightings can be used directly in conjunction with an ephemeris, orbit elements, and a computer (presumably the CM computer). This last approach is covered in greater detail in Ref. II.6.

II. 12 CONTROL SYSTEMS

The analysis of the previous sections has established the impulse requirements to limit the amplitude of the deviation of the solar panels from the LOS for different modes of control. It has also made estimates of the collected solar energy loss for different deviations. These impulse requirements may be met in two basic ways:

- Aerodynamic bias control
- Amplitude control

The most basic consideration in selecting a particular system is weight. Figure II-16 shows the impulse required to constrain α_2 to various amplitudes for both continuous and discontinuous control. From this figure we construct Fig. II-18 where the impulse is converted to control propellant weight (assuming an RCS) using a control moment arm of 50-ft and a specific impulse of 200 sec. If cold gas were to be considered, a specific impulse of 70 sec would be used and the weight figures may be scaled up accordingly. The 50-ft moment arm implies an auxiliary RCS located in the OWS engine area. If the CSM RCS is used, the moment arm is 30 ft and the specific impulse is 276, and the weights of Fig. II-18 must be scaled up accordingly.

II.12.1 Aerodynamic Bias Control

If only the aerodynamic bias is controlled, a control propellant weight of about 30 lb is required for a 28-day mission (see Fig. II-18). In this mode, the pitch and roll angles will be measured directly with a sun sensor and when they exceed ±30-deg the CSM RCS will be activated. The activation may be done either automatically or manually. If done manually, a display must be made for the crew who will have to take action once about every 70 min. (Figure II-14 shows it takes about 70 min for α_2 to reach 30-deg.) Operated in this mode the collected energy loss is 7 percent of the theoretical maximum that could be collected. An elementary block diagram of the system is shown in Fig. II-19 where the deadband is to be understood as set at ±30-deg.

II.12.2 Amplitude Control

Strictly speaking this system is the same as one for aerodynamic bias control shown in Fig. II-19. The difference lies in the magnitude of the amplitude of α_2 that is permitted. If α_2 is limited to ±30-deg, Fig. II-18 shows a control propellant weight of 75-lb is required for a 28-day mission. Operated in this mode, the collected energy loss is about 5 percent of the theoretical maximum that could be collected.

If continuous control is attempted in order to hold α_2 to, or near, zero, a control propellant weight of 790-lb is required for a 28-day mission. Allowing for inerts (if an auxiliary system were used) the flight weight would be on the order of 1100 lb. In this
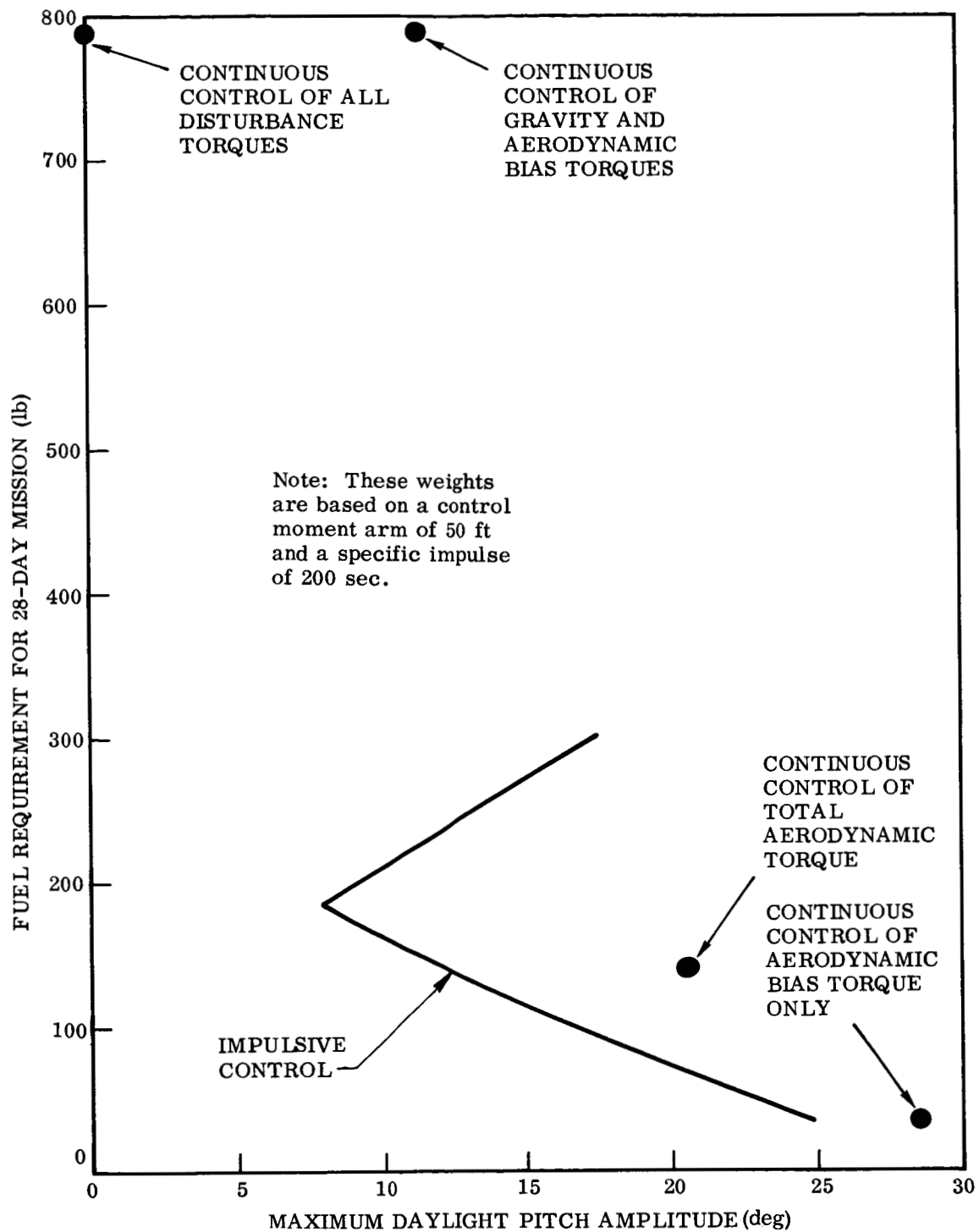
Fig. II-18 Fuel Requirements vs. Maximum Daylight Pitch Amplitude for Several
Types of Control (28-Day Mission)

DEADBAND

CANOPUS
TRACKER

CSM
CONTROL
JETS

CONTROL
TORQUES

OWS/OSM

ψ

CSM
CONTROL
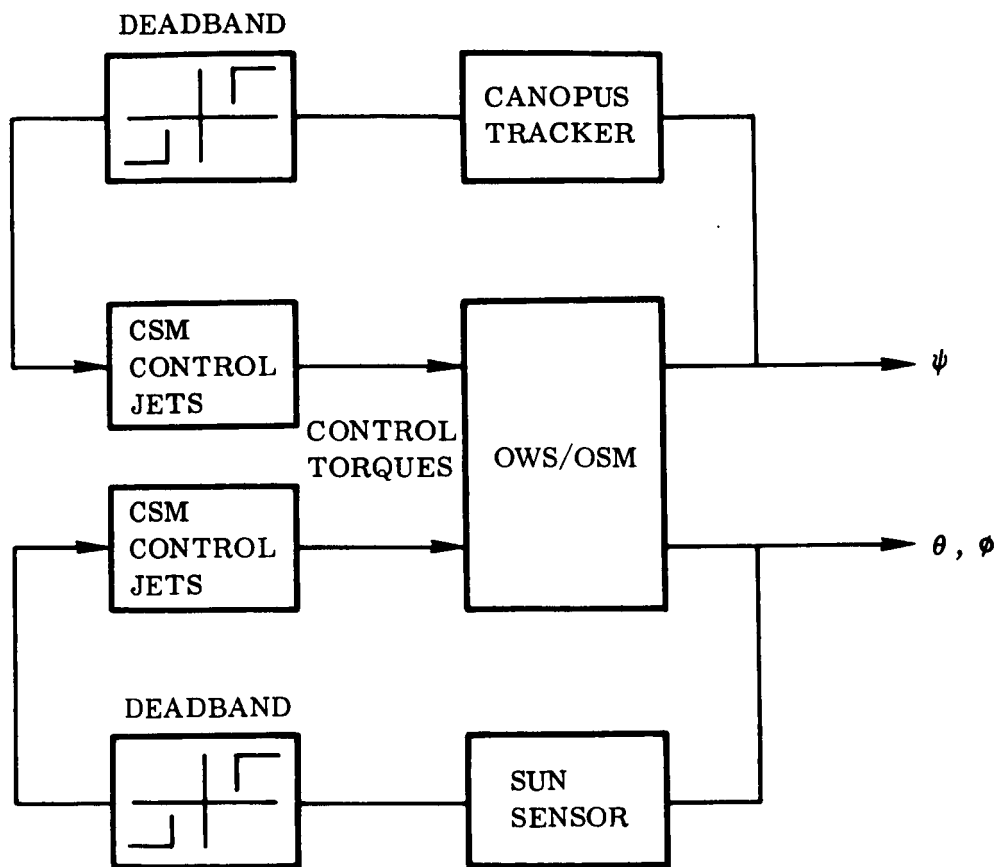JETS

θ , ϕ

DEADBAND

SUN
SENSOR

Fig. II-19 LOS Attitude Control System Block Diagram

mode of operation, the collected energy loss would be essentially zero. It should be noted that continuous control here means not only that the disturbance torques are continuously opposed but that this is done on the dark as well as the daylight side of the orbit. Since energy loss as such is not meaningful on the dark side of the orbit, the control propellant weight could be materially reduced by not controlling there. This case has not been analyzed, and to do so one must reconsider the biases and re-acquisition, but this would clearly lead to a control propellant weight on the order of 400 to 500 lb and flight weights of 600 to 700 lb rather than the 800-lb and 1100-lb weights noted above.

II.13 CONCLUSIONS AND RECOMMENDATIONS

The most notable conclusions of the analysis are as follows:

- Aerodynamic bias torques exist which, if uncontrolled, can lead to pitch angles of 50-deg within one orbit.
- The aerodynamic and gravity-gradient torques interact to produce a pitch angle 50 percent greater than that due to gravity gradient alone, although the aerodynamic torques are 12 percent of the gravity gradient torques.
- If only the aerodynamic bias torques are controlled, the collected energy loss is only 7 percent of the theoretical maximum that could be collected.
- Controlling the pitch angle to reduce its maximum to ±20-deg from ±30-deg (controlling only the bias torques) reduces the energy loss from 7 to 5 percent.
- Controlling the aerodynamic bias torques requires about 30-lb of control propellant (I_{sp} = 200, moment arm = 50-ft) for a 28-day mission.
- Controlling the pitch angle to a maximum of ±20-deg requires about 75 lb of control propellant for a 28-day mission.
- Controlling the pitch angle continuously to reduce the energy loss to zero requires 800 lb of control propellant if controlled through the orbit, and about 400 to 500 lb if controlled only on the daylight side of the orbit, both for a 28-day mission.

The recommendations are as follows:

- Control only the aerodynamic biases and pitch angle using the CSM RCS. This will require 30 lb of RCS propellant.
- If the 5 percent energy loss associated with the previous item is not acceptable, then conduct a more extensive analysis to determine the control weight associated with a given energy loss to aid in selecting an acceptable operating point.

II.14 REFERENCES

II.1 National Aeronautics and Space Administration, Mass Characteristics for the Cluster Mission, R-P&VE-VAW-67-66, NASA MSFC, 8 May 1967

II.2 Lockheed Missiles & Space Company, Free Molecule Flow Theory and Its Application to the Determination of Aerodynamic Forces, by Lee H. Sentman, LMSC-448514, Sunnyvale, Calif., 1 Oct 1961

II.3 -----, Orbital Aerodynamic Data for the S/AA Docked Configuration of the OWS-M&SS-LM/ATM-RM, LMSC/HREC-A784066, Org. No. 54/20, 15 Mar 1967

II.4 National Aeronautics and Space Administration, Theoretical Models for the Solar-Cycle Variation of the Upper Atmosphere, by Isadore Harris and Wolfgang Priester, NASA PND-1444, Aug 1962

II.5 Lockheed Missiles & Space Company, Final Report for ATM and Cluster Systems Analyses, Augmentation Task Nos. 1 and 19, LMSC-A842251, Sunnyvale, Calif., 17 Jul 1967

II.6 -----, Conceptual Design and Analysis of Control System for Apollo Telescope Mount, LMSC-A842157, 17 Mar 1967

II.7 -----, User's Manual: Apollo Telescope Mount Simulation (ATOMS), LMSC-A842251-1, Jun 1967

II.15 NOMENCLATURE

T_r	reflected molecular temperature
T_i	incident molecular temperature
T_w	vehicle surface temperature
S	molecular speed ratio
α	thermal accommodation coefficient
θ_t	true anomoly
(X_o, Y_o, Z_o)	orbit-referenced axes
(X_1, Y_1, Z_1)	sun-referenced axes
(X, Y, Z)	geometric body-fixed axes
(x, y, z)	Saturn IB body-fixed axes
F_{AX}, F_{AY}, F_{AZ}	aerodynamic force components in geometric body-fixed coordinates
$\alpha_1, \alpha_2, \alpha_3$	roll, pitch, and yaw angles about positive X-, Y-, and Z-axes, respectively
T_{AX}, T_{AY}, T_{AZ}	aerodynamic roll, pitch, and yaw torques referenced to vehicle C.G. and geometric body-fixed axes
t	time
I_c	control impulse
W_p	propellant weight per day
E	energy from solar arrays
F	control force
ℓ	control moment arm
I_{sp}	specific impulse

J_x, J_y, J_z	moments of inertia for Saturn IB axes (for C.G.)
J_{xy}, J_{xz}, J_{yz}	products of inertia for Saturn IB axes (for C.G.)
J_1, J_2, J_3	principal moments of inertia for C.G.
J_{xp}, J_{yp}, J_{zp}	principal moments of inertia for C.G.
J	average of two maximum principal moments of inertia
ν	angle of rotation from geometric to principal axes (about X)
T_{GX}, T_{GY}, T_{GE}	components of gravity torque in geometric system
Ω_o	mean orbital rate
λ	angle between earth-sun line and orbital plane
A	amplitude of cyclic portion of aerodynamic torque model
B	magnitude of constant portion (bias) of aerodynamic torque model
G	amplitude of gravity torque model
C_1, C_2	constants of integration
I_1, I_2	torque impulses used in discontinuous control
t_1, t_2	times of application of impulses in discontinuous control
k	scaled magnitude of impulses in discontinuous control

Appendix A

AERODYNAMIC FORCE COMPONENTS REFERENCED TO BODY-FIXED AXES

θ_t (deg)	$\lambda = \alpha_1 = \alpha_2 = \alpha_3 = 0$			$\lambda = 30\text{-deg}, \alpha_1 = \alpha_2 = \alpha_3 = 0$			$\lambda = \alpha_1 = \alpha_2 = 0, \alpha_3 = 15\text{-deg}$			$\lambda = 30\text{-deg}, \alpha_2 = 15\text{-deg}, \alpha_1 = \alpha_3 = 0$			$\lambda = 30\text{-deg}, \alpha_2 = 15\text{-deg}, \alpha_1 = \alpha_3 = 0$		
	$10\,F_{AX}$ (lb)	F_{AY} (lb)	$10\,F_{AZ}$ (lb)	$10\,F_{AX}$ (lb)	$10\,F_{AY}$ (lb)	$10\,F_{AZ}$ (lb)	$10\,F_{AX}$ (lb)	$10\,F_{AY}$ (lb)	$10\,F_{AZ}$ (lb)	$10\,F_{AX}$ (lb)	F_{AY} (lb)	$10\,F_{AZ}$ (lb)	$10\,F_{AX}$ (lb)	$10\,F_{AY}$ (lb)	$10\,F_{AZ}$ (lb)
0	8.9	0	0	8.9	0	0	11.1	-3.2	0	8.6	0	0	8.6	0	0
15	14.4	0	4.3	13.8	2.0	3.6	15.8	-4.4	4.8	14.2	0	4.3	13.6	2.0	3.5
30	20.1	0	12.3	19.1	5.7	10.2	20.3	-5.6	12.8	20.4	0	12.4	19.3	5.8	10.3
45	21.0	0	21.8	19.3	9.8	17.4	20.4	-5.6	22.0	21.8	0	22.6	20.0	10.2	18.0
60	16.6	0	29.6	15.2	13.3	23.6	16.1	-4.4	29.7	17.6	0	31.4	16.1	14.1	25.0
75	8.7	0	33.3	7.9	14.9	26.4	8.4	-2.3	33.3	9.4	0	36.0	8.6	16.1	28.6
90	0	0	32.2	0	14.4	25.4	0	0	32.2	0	0	35.6	0	15.9	28.1
105	-7.3	0	28.0	-6.7	12.6	22.2	-7.1	1.9	28.0	-8.3	0	31.7	-7.6	14.3	25.1
120	-11.5	0	20.6	-10.5	9.3	16.4	-11.4	3.1	21.0	-13.2	0	23.7	-12.2	10.7	18.9
135	-12.3	0	12.8	-11.4	5.8	10.3	-12.0	3.3	12.9	-14.3	0	14.8	-13.2	6.7	11.9
150	-10.1	0	6.2	-9.4	2.8	5.0	-10.2	2.8	6.4	-11.7	0	7.2	-10.9	3.2	5.8
165	-6.5	0	2.0	-6.3	0.9	1.7	-6.9	1.9	2.1	-7.4	0	2.3	-7.2	1.0	1.9
180	-3.8	0	0	-3.8	0	0	-4.6	1.3	0	-4.2	0	0	-4.2	0	0
195	-5.2	0	-1.6	-5.0	-0.7	-1.3	-5.5	1.5	-1.7	-5.4	0	-1.7	-5.2	-0.7	-1.3
210	-6.8	0	-4.1	-6.4	-1.9	-3.4	-6.8	1.9	-4.3	-6.6	0	-4.0	-6.2	-1.8	-3.3
225	-7.3	0	-7.6	-6.8	-3.5	-6.2	-7.2	1.9	-7.7	-6.7	0	-6.9	-6.2	-3.2	-5.6
240	-6.5	0	-11.7	-6.1	-5.3	-9.4	-6.4	1.7	-11.7	-5.7	0	-10.2	-5.3	-4.6	-8.2
255	-4.2	0	-16.0	-3.8	-7.3	-12.9	-4.1	1.1	-16.0	-3.6	0	-13.8	-3.3	-6.3	-11.2
270	0	0	-19.3	0	-8.8	-15.5	0	0	-19.3	0	0	-16.7	0	-7.6	-13.4
285	5.6	0	-21.4	5.2	-9.7	-17.2	5.4	-1.5	-21.4	4.9	0	-18.6	4.5	-8.4	-14.9
300	11.6	0	-20.7	10.8	-9.3	-16.7	11.2	-3.0	-20.7	10.3	0	-18.3	9.6	-8.2	-14.8
315	16.0	0	-16.6	15.1	-7.6	-13.4	15.6	-4.2	-16.8	14.5	0	-15.0	13.7	-6.9	-12.1
330	16.8	0	-10.2	15.9	-4.7	-8.5	16.9	-4.6	-10.7	15.5	0	-9.4	14.7	-4.3	-7.9
345	13.1	0	-3.9	11.9	-1.8	-3.3	14.4	-4.0	-4.4	12.4	0	-3.7	11.2	-1.7	-3.1
360	8.9	0	0	8.9	0	0	11.1	-3.2	0	8.6	0	0	8.6	0	0

Appendix B

The solar energy is given by

$$E = \dot{E} \int \text{Cos } \alpha_2 (t) \, dt \qquad \text{(B.1)}$$

where

$\dot{E}$　　　= power collected with solar panels normal to the LOS

$\alpha_2 (t)$ = is given by Fig. II-14

For graphical integration

$$E/\dot{E} = \sum \left(\text{Cos } \alpha_2 \right)_{\text{avg}} \frac{\Delta \Omega_o t}{\Omega_o} = \frac{1}{\Omega_o} \sum \left(\text{Cos } \alpha_2 \right)_{\text{avg}} \Delta \Omega_o t \qquad \text{(B.2)}$$

where

$\Delta \Omega_o t$ = increment in orbit angle, taken here as 5-deg

Ω_o　　= orbit rate

α_2 = average value of α_2 in the $\Delta \Omega_o t$ interval
avg

At 250 mi, the period is about 94 min giving

$$\Omega_o = \frac{2\pi}{94 \times 60} = \frac{\pi}{2820} \text{ Rad/sec} \qquad \text{(B.3)}$$

II-47

LOCKHEED MISSILES & SPACE COMPANY

Using Eq. (B.3) , (B.2) is evaluated in Table B-1. Equation (B.2) is expressed in times of seconds and may be interpreted as giving the equivalent time of exposure of the full panels, undeflected, from the LOS.

For example, if α_2 were zero through a quarter of the orbit, the maximum energy possible to collect is collected and the equivalent time is one-fourth of the orbit period, i.e., 1410 sec. If the panels were deflected from the LOS by 45-deg throughout the same period the equivalent time of exposure would simply be

$$E/\dot{E} = \int_0^{\frac{\tau}{4}} \cos 45° \, dt = 0.707 \frac{\tau}{4} = 996 \text{ sec} \tag{B.4}$$

In this example the energy loss is 30 percent. From Table B-1 the equivalent time is found to be 1310 sec and the energy loss is

$$\text{Energy loss} = \frac{1410 - 1310}{1410} \times 100\% = 7.1\% \tag{B.5}$$

If a control system were to limit α_2 to ±20-deg but otherwise not affect the motion then the energy loss is computed using the data of Table B-1 for the periods when $\alpha_2 \leq$ 20-deg and $\alpha_2 =$ 20-deg for the remaining time.

$$E/\dot{E} = \frac{1}{\Omega_o} \left[\sum \left(\cos \alpha_2 \right)_{\text{avg}} \Delta \Omega_o t \right] + \left(\frac{\cos 20°}{\Omega_o} \right) \int_{\Omega_o t_1}^{\Omega_o t_2} d(\Omega_o t) \tag{B.6}$$

where $\Omega_o t_1$ and $\Omega_o t_2$ are the orbit angles where $\alpha_2 >$ 20-deg

Table B-1

NUMERICAL EVALUATION OF E/Ė

$\Delta\Omega_0$ (deg)	α_2 avg (deg)	Cos α_2 avg	$\Delta\Omega$/rad	Ω_0 Cos α_2 avg
0–5	2.5	0.99905	0.08727	0.08719
5–10	7.5	0.99144	0.08727	0.08652
10–15	11.75	0.97905	0.08727	0.08544
15–20	15.5	0.96363	0.08727	0.08410
20–25	19.25	0.94409	0.08727	0.08239
25–30	22.5	0.92554	0.08727	0.08077
30–35	24.75	0.90814	0.08727	0.07925
35–40	27.00	0.89101	0.08727	0.07776
40–45	28.5	0.87882	0.08727	0.07669
45–50	29.00	0.87462	0.08727	0.07633
50–55	28.75	0.87673	0.08727	0.07651
55–60	28.25	0.88089	0.08727	0.07688
60–65	27.00	0.89101	0.08727	0.07776
65–70	25.00	0.90631	0.08727	0.07909
70–75	23.00	0.92050	0.08727	0.08033
75–80	20.25	0.93819	0.08727	0.08188
80–85	17.25	0.95502	0.08727	0.08334
85–90	13.25	0.97338	0.08727	0.08495
				1.45718

$E = 0.42564$

$$\frac{E}{\dot{E}}$$

$$\frac{0.16829}{0.59393}$$

From Table B-1 we evaluate Eq. (B.6) as

$$E/\dot{E} = \frac{0.59393}{\pi} + 0.94 \times \frac{2820}{\pi} \left(\frac{55}{57.3}\right) = 531 + 810 = 1341 \text{ sec} \qquad (B.7)$$

The energy loss is

$$\frac{1410 - 1341}{1410} \times 100\% = 4.9\% \qquad (B.8)$$

Part III

AAP SOLAR ARRAY SYSTEM POWER STUDY

III.1 SUMMARY

This study was performed to determine the power available from the AAP Solar Array System mounted on the S-IVB OWS. Results were obtained for the solar arrays in the sun-oriented mode as well as for the arrays in various locations in the gravity-gradient (storage) mode. The maximum total power available during one orbit was found to be 10,490 w-hr.

Solar Array Power Program

Solar array power is dependent upon the following:

- Vehicle configuration parameters
- Thermodynamic parameters
- Space geometric variables
- Temporal variables

The primary temporal variable is the degradation of performance with time of the solar array due to the effect of the space environment. This variable is independent of the other parameters.

The space geometric variables are the vehicle's position with respect to the sun and earth. They depend upon the orbit inclination; launch date, time, and site; and orbit altitude and eccentricity. However, for the AAP mission, the space geometry variables also depend upon the astronaut controlling the vehicle to make it sun-oriented or to place in a gravity-gradient storage mode.

III-1

The main thermodynamic parameters are the array's solar absorptivity (α_s) and emissivity (ϵ) both on the cell side and backside, its thermal capacity, and its orientation to the sun, vehicle, and earth. These parameters are greatly dependent array design and space geometry.

The primary vehicle configuration parameters are the position of the solar arrays on the vehicle and the orientation of the vehicle with respect to its orbital path.

For a given solar array area in a constant solar flux, the power output of the array equals the product of the variables e (solar cell efficiency) and ϵ_{sa} (array effectivity). The effectivity ϵ_{sa} is the cosine of the angle between the earth-sun line and the normal to the solar cell (i.e., a surface perpendicular to the sun has an effectivity of one and is dependent on the space geometry and vehicle configuration. The efficiency e of a solar cell is dependent on the temperature and temporal effects. A typical efficiency curve is shown in Fig. III-1. Note that efficiency decreases as temperature increases. From this it can be concluded that a sun-oriented solar array at 80°F or below would supply maximum power. However, the solar array's temperature is also a function of the array's effectivity, with the temperature increasing as the effectivity increases.

III.2 METHOD OF ANALYSIS

To obtain the solar array power, the computer program* was modified. This computer program is versatile in that it can be used for up to 64 separate solar array panels on a satellite in a circular orbit. The inputs to the program are the space geometry variables, the vehicle and solar array configurations, the thermodynamic properties, and the solar array efficiency.

The space geometry variables are input with respect to a right-handed geocentric inertial system, with one axis directed toward the vernal equinox, the third axis directed toward the north pole, and the second axis chosen to complete the triad. The

---

*Lockheed Missiles & Space Co., "Program 461 Solar Array Power Study." LMSC-A319781. Sunnyvale, Calif., 25 Feb 1963
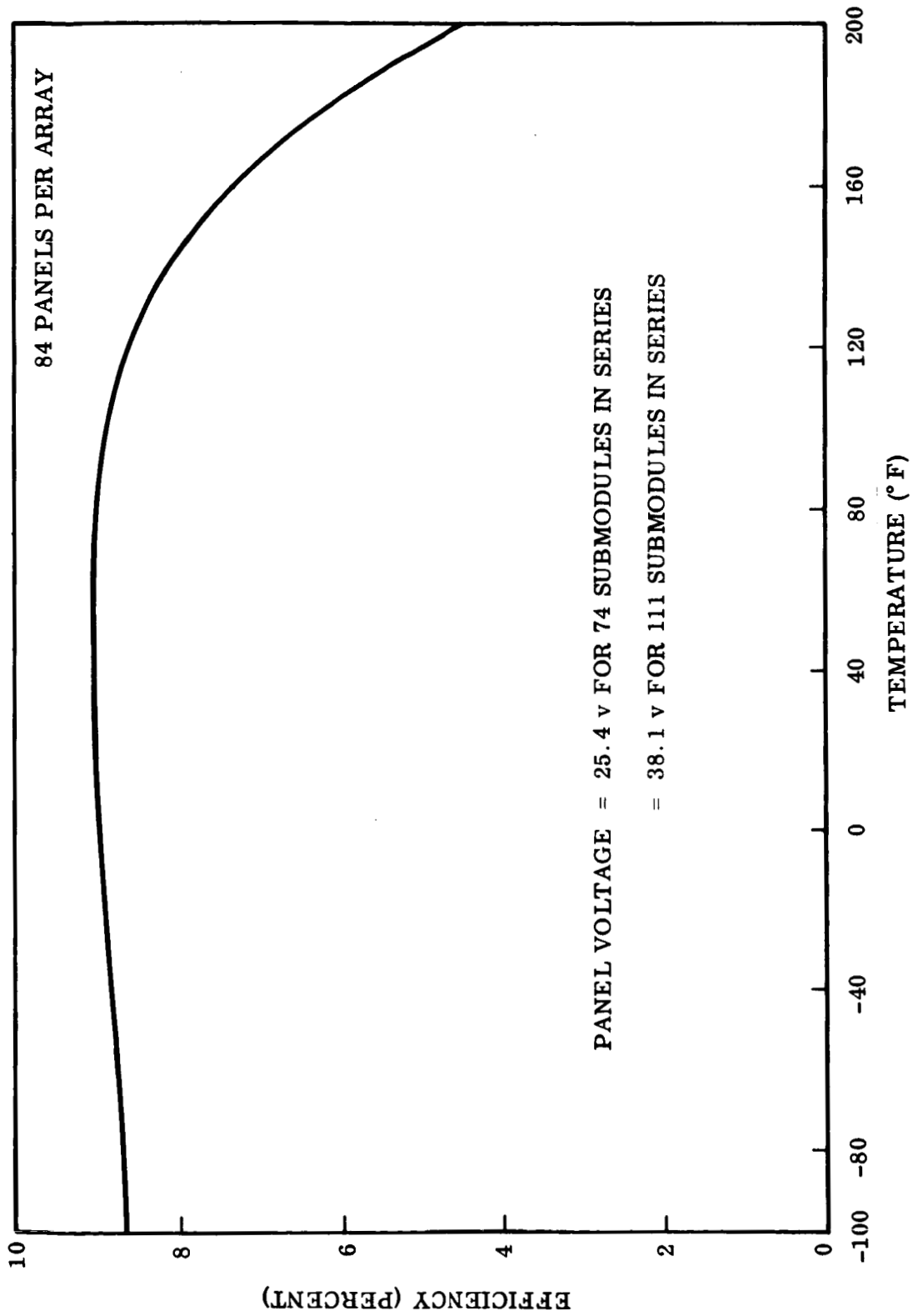
Fig. III-1 Solar Array Efficiency vs. Temperature

LOCKHEED MISSILES & SPACE COMPANY

satellite moves in a plane at some inclination to the equatorial plane. The input consists of the initial position of the sun, initial right ascension of the ascending mode, initial position of the satellite in the orbit plane, inclination of the orbit plane, angular velocity of the sun and satellite, and the radius of the orbit. With this information the vehicle position in the orbit can be determined as well as the earth-shadow points.

The configuration input consists of describing the vehicle and solar arrays with respect to a vehicle coordinate system. The vehicle can be described by either one or two right circular cylinders. The solar arrays are described as rectangular plane sections located at specified points and at specified rotations from the vehicle's axis. There are no restrictions on the array positions.

The thermodynamic properties that are input are the cell side and back side solar absorptivity and emissivity, the solar constant, the thermal capacity, the thermal radiation to the vehicle (assumed to be a constant over the orbit), an earthshine variable, and the albedo variable.

III.3 RESULTS

Initial studies were made with 6 arrays having 63 panels and 2 arrays having 44. Each array was described by one temperature calculation method. Analyses were performed by beta angles of 0 deg (noon orbit) and 52 deg for the sun-oriented mode and 0 deg ±25 and ±52 deg for two gravity-gradient modes. [The beta angle is defined as the acute angle between the earth-sun line and orbit plane, and is positive if an increase in orbit position angle produces a counterclockwise motion when the orbit plane is viewed from the sun.]

In the sun-oriented cases, all the solar arrays are normal to the sun. In the gravity-gradient cases, the solar arrays are oriented as shown in Figs. III-2 and III-3. In Fig. III-2 the middle solar arrays are in the plane of motion so that in a noon orbit they would always be parallel to the sun's rays. In minus beta angles, they would

receive solar energy on the cell side, while in positive beta angles the back side would receive solar energy. The end arrays were rotated ±65 deg from the other arrays in a position to receive energy even when the other arrays were parallel to the sun's rays, Fig. III-3 shows the arrays on the ±Y sides of the vehicle with the end arrays rotated at the same angles as in Fig. III-2. For the orientation of Fig. III-2 computer runs for beta angles of 0 deg, ±25 deg, and ±52 deg were made, while the orientation of Fig. III-3, only runs of 0 deg, +25 deg and +52 deg were made since the minus beta results are the same as the plus beta results.

The back side of the arrays were assumed white (solar absorptivity = 0.22, emissivity = 0.90) and the solar cell cover glass was assumed to have a solar absorptivity of 0.76 and emissivity of 0.79. (These values were used on previous programs and the predictions matched the flight data quite well). The total power for the various cases is given in Table III-1. Figures III-4 through III-12 show the orbital power variation and Fig. III-13 shows the β = 52 deg sun-oriented temperature variation.

Later studies were performed with each of the all eight solar arrays having 84 panels. Each solar array was divided into two temperature nodes, one close to the vehicle and one away from the vehicles. By dividing each array into two nodes, the array's temperature was obtained more accurately than before since the effect of shading was taken over a smaller area and the difference in the radiation heat transfer from the vehicle to the different parts of the array could be considered. (The same thermal coefficients assumed in the initial studies were used.) The results are shown in Table III-2 and Fig. III-14 through III-24.

The results show that the maximum power is obtained in the β = 52 deg sun-oriented mode in which the arrays are in the sun for the longest period of time. In this mode, the increase of panels brought a proportional increase in power.

With the arrays on the ±Y sides of the vehicle in the gravity-gradient mode, the maximum power is in the β = 0 deg orbit and decreases as the beta angle decreases. For

VIEW FROM Z DIRECTION
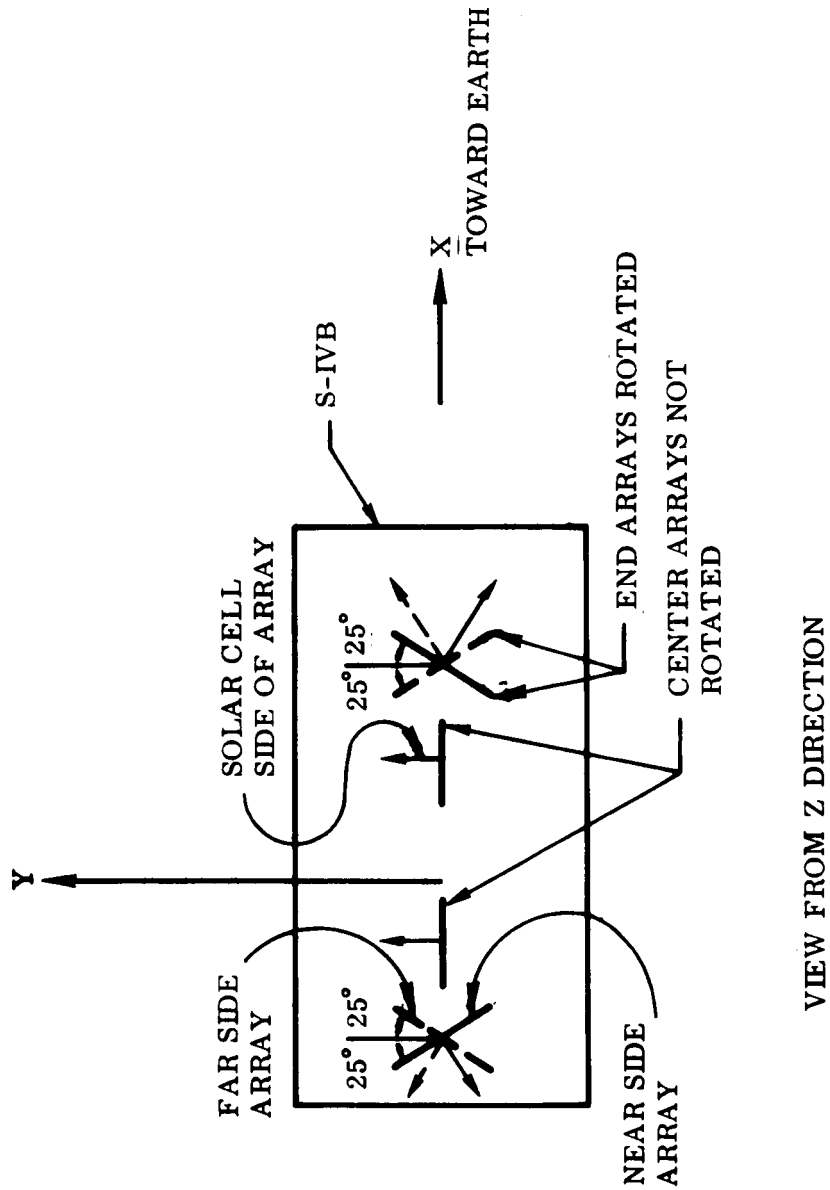
Fig. III-2 Gravity-Gradient Orientation, Arrays on Z Side
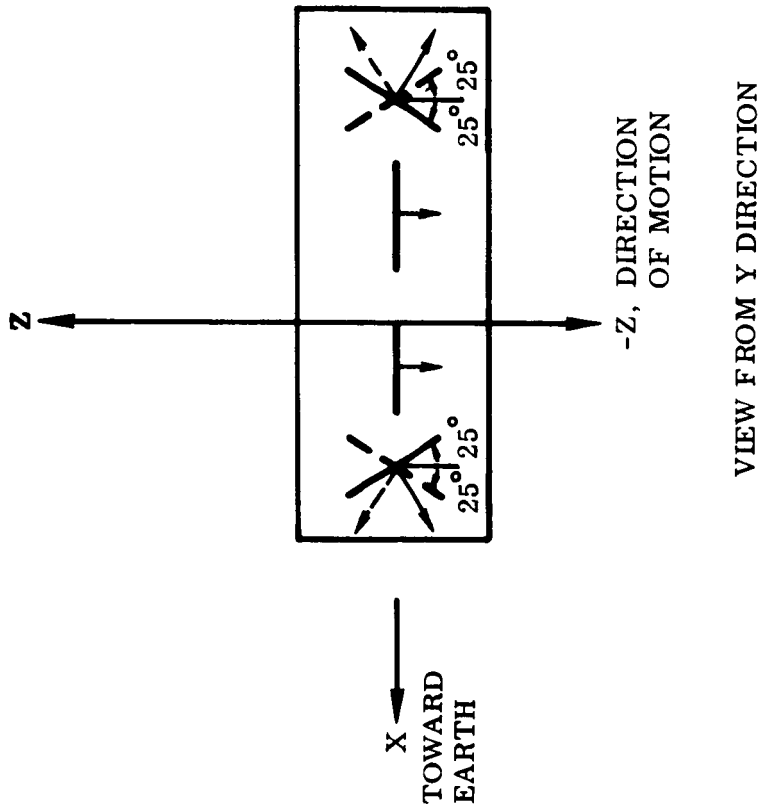
Fig. III-3 Gravity-Gradient Orientation, Arrays on Y Side

this condition, the larger arrays have more than a proportional increase in power since the larger arrays have more panels further from the vehicle that are not shaded.

With the arrays on the ±Z sides, the maximum power was in the β = -52 deg orbit. The power decreased as the beta angle increased until it reached a minimum at β = 0 deg and slowly increased as the beta angle increased. The reason for the large variation in power with beta angle is that the middle arrays receive more energy as the beta angle decreases away from β = 0. As with the arrays on the ±Y sides, the 84 panel arrays had more than a proportional increase in power due to lower temperatures at the outside end of the arrays. The maximum power for the gravity-gradient mode was with the arrays on the ±Y sides and β = 52 deg while the minimum power was also for the arrays on the ±Y sides and for β = 0 deg.

Table III-1

TOTAL SOLAR ARRAY POWER, 63- AND 44- PANEL ARRAYS

Orientation	Figure Number	Angle	Total Power Generated Per Orbit (kwh)
Sun	III-4	0	6.70
Sun	III-4	52	7.28
Gravity Gradient, ±Y Sides	III-5	0	2.23
Gravity Gradient, ±Y Sides	III-6	25	1.87
Gravity Gradient, ±Y Sides	III-7	52	1.08
Gravity Gradient, ±Z Sides	III-8	0	.43
Gravity Gradient, ±Z Sides	III-9	+25	.54
Gravity Gradient, ±Z Sides	III-10	+52	.62
Gravity Gradient, ±Z Sides	III-11	-25	1.66
Gravity Gradient, ±Z Sides	III-12	-52	3.76
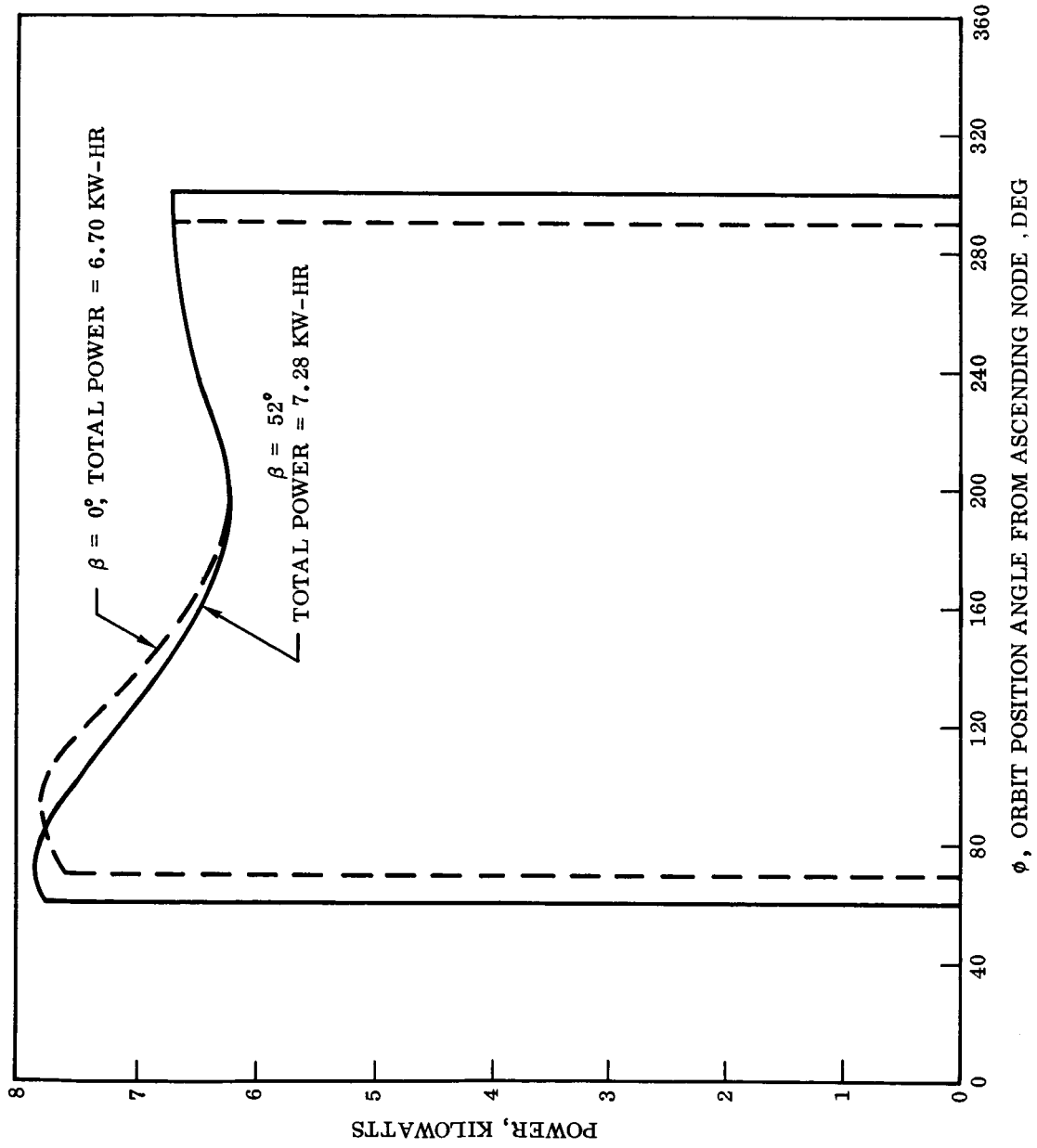
Fig. III-4 Solar Array Power, β = 0 and 52-deg, Sun-Oriented Mode

LOCKHEED MISSILES & SPACE COMPANY
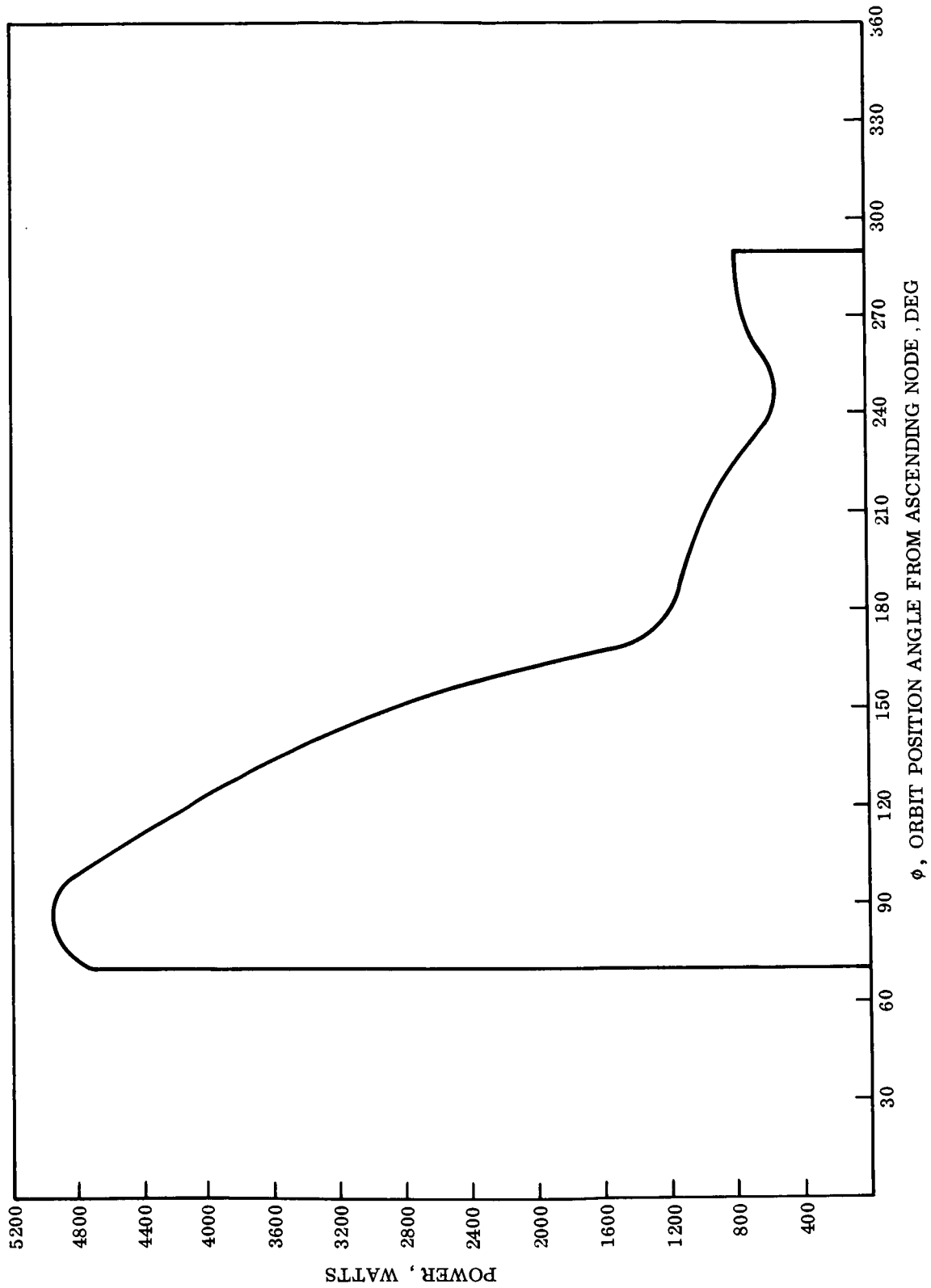
Fig. III-5 ASAP Power, $\beta = 0$, Arrays on $\pm$Y Sides, Integrated Power = 2.23 kwh
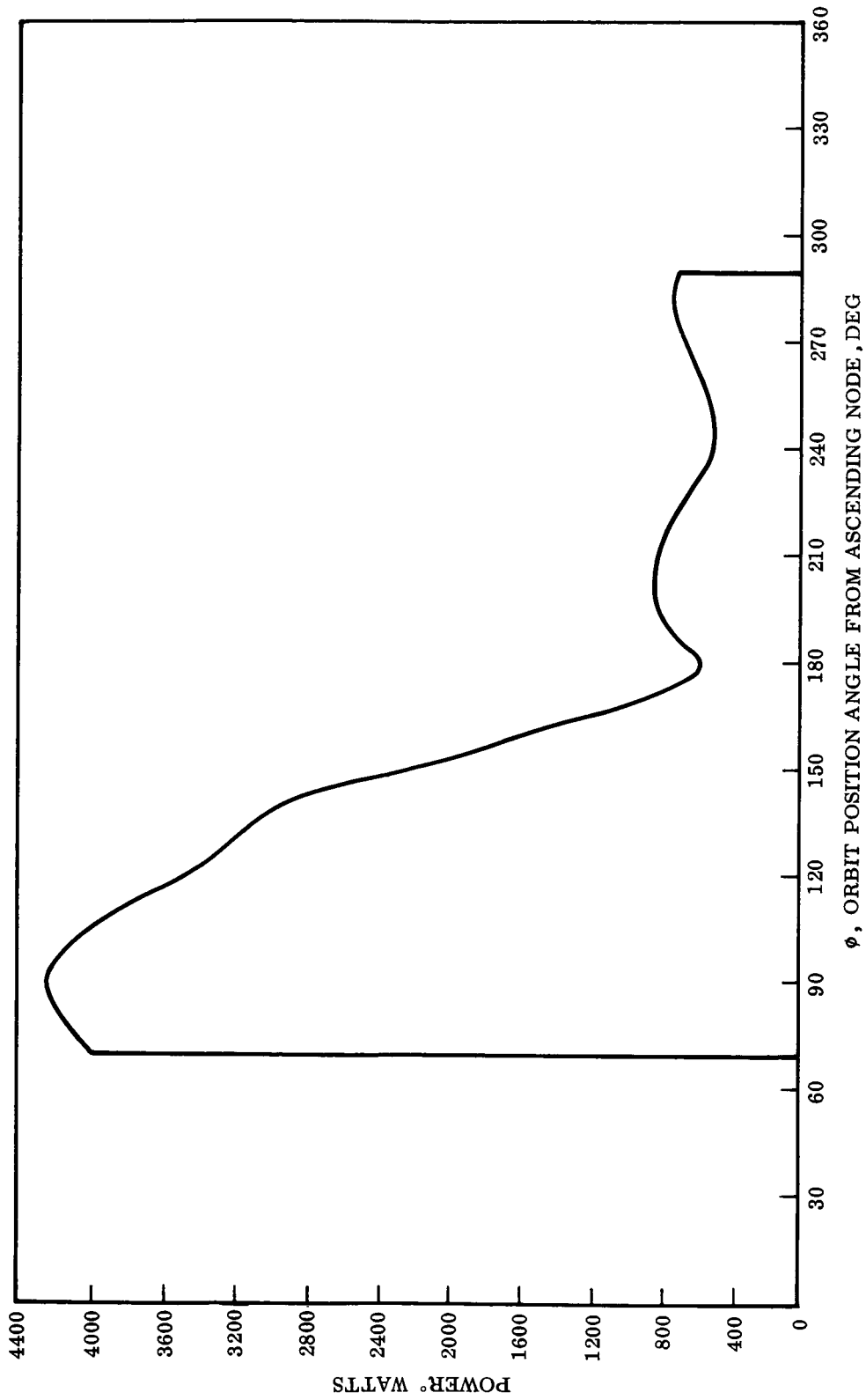
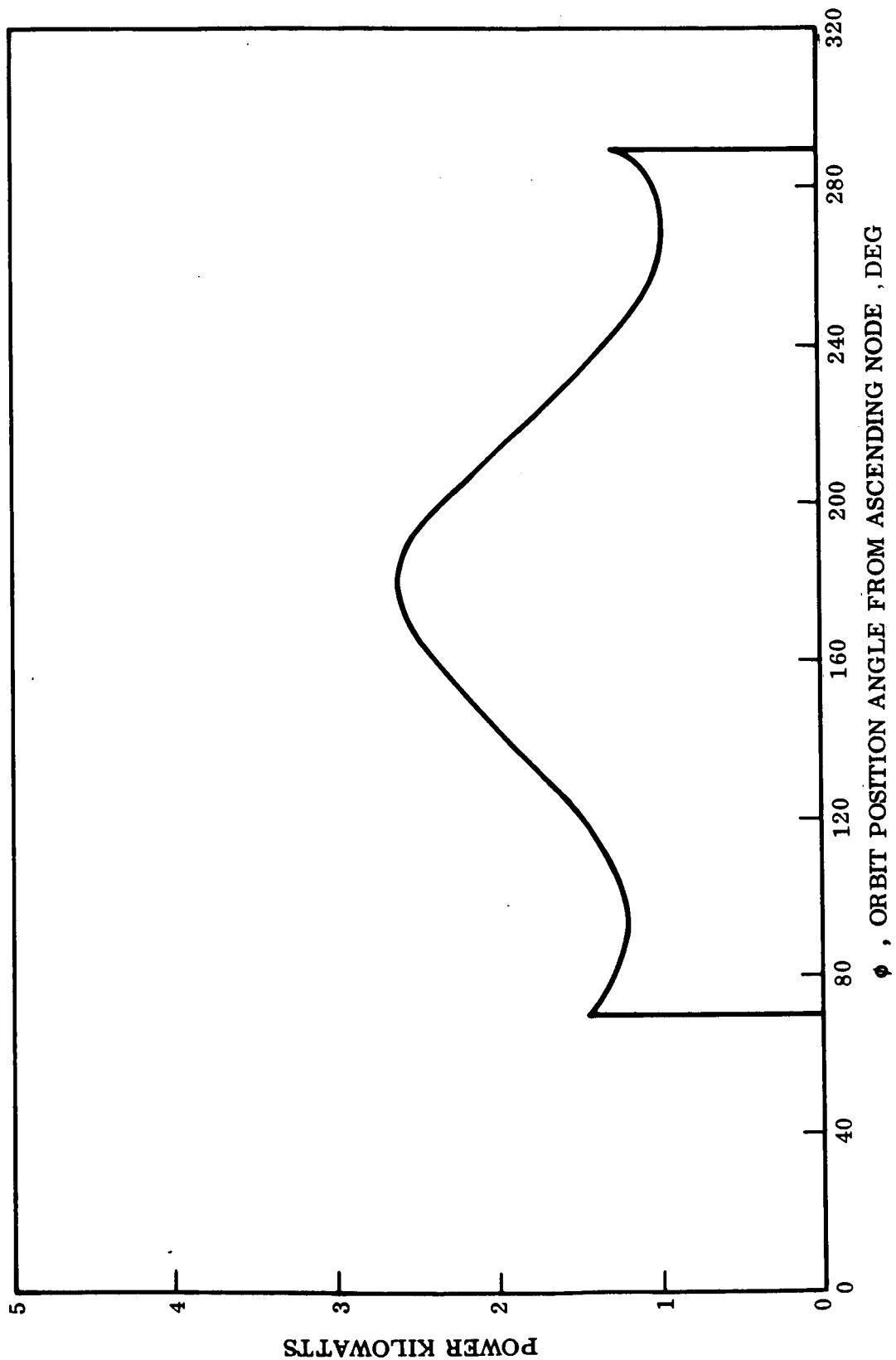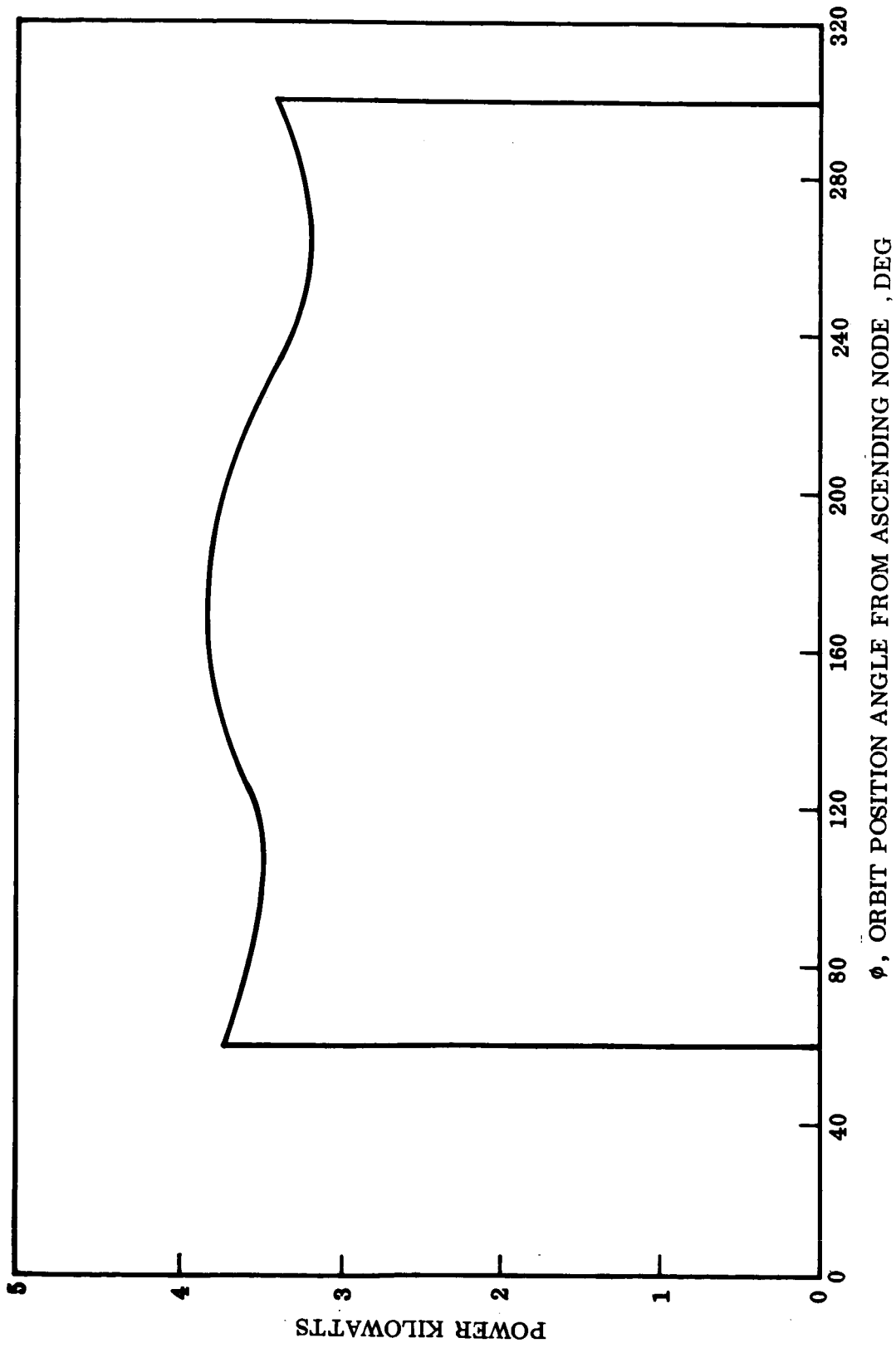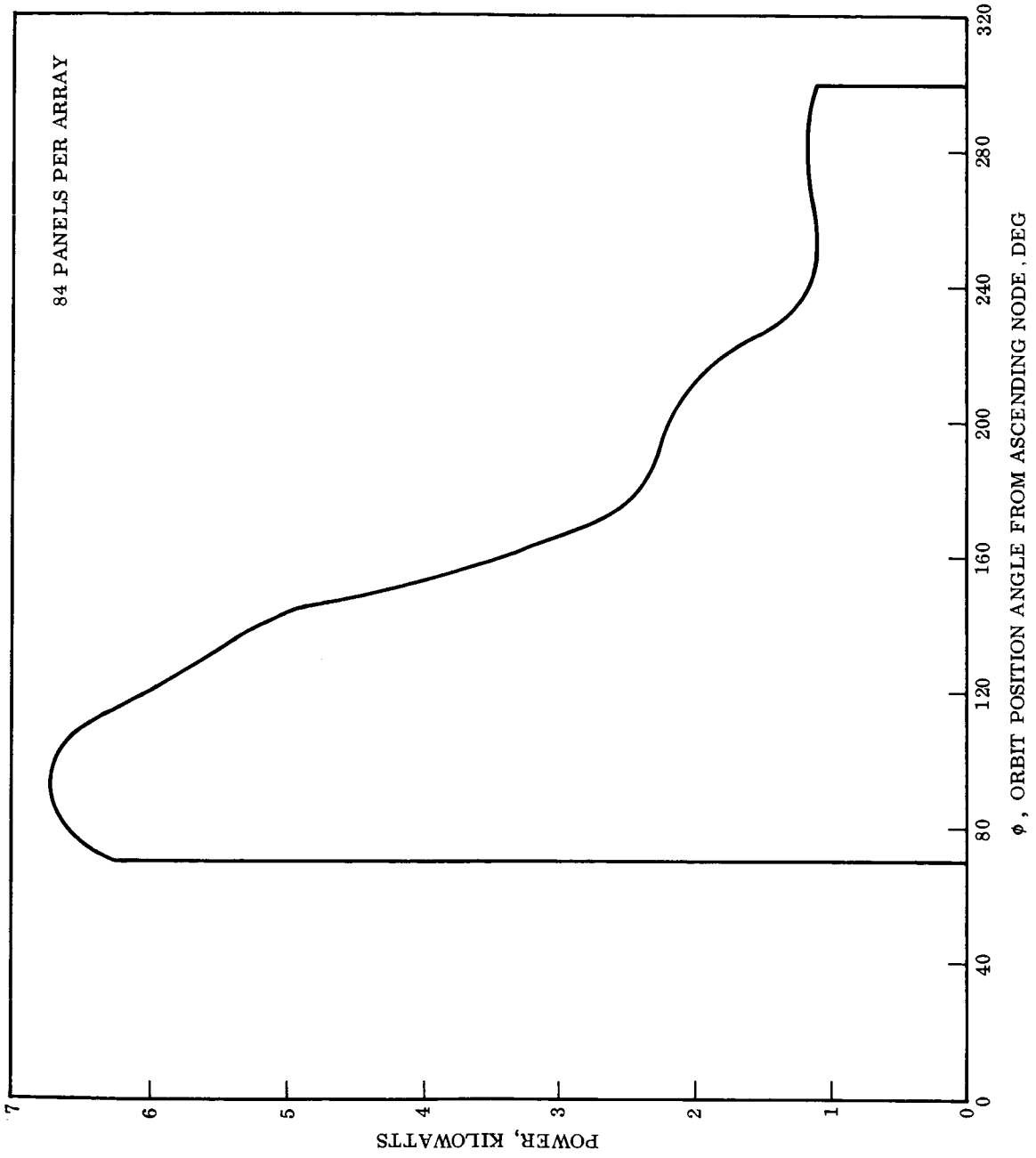Fig. III-6 ASAP Power, $\beta = 25$, Arrays on $\pm Y$ Sides, Integrated Power = 1.87 kwh

LOCKHEED MISSILES & SPACE COMPANY
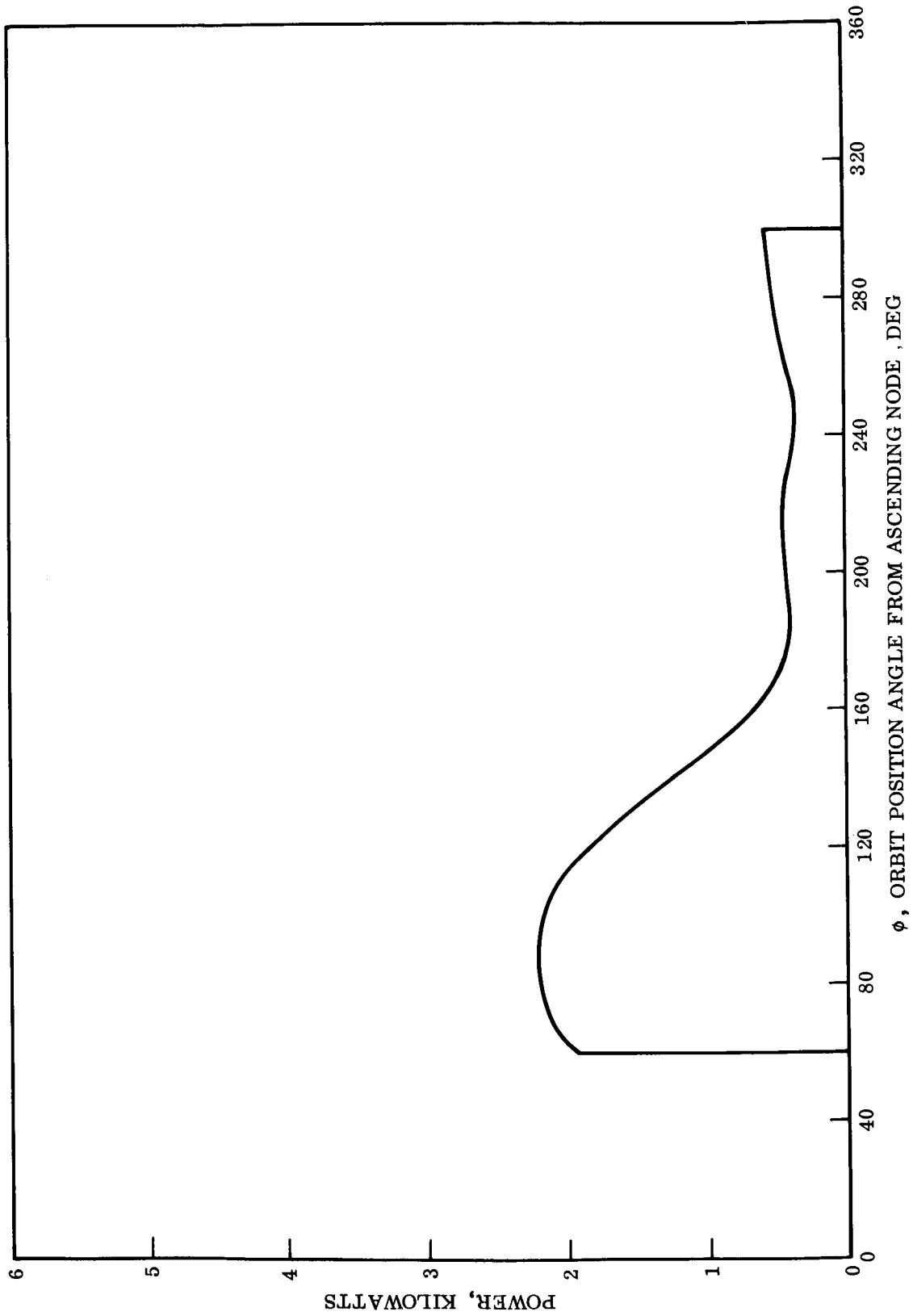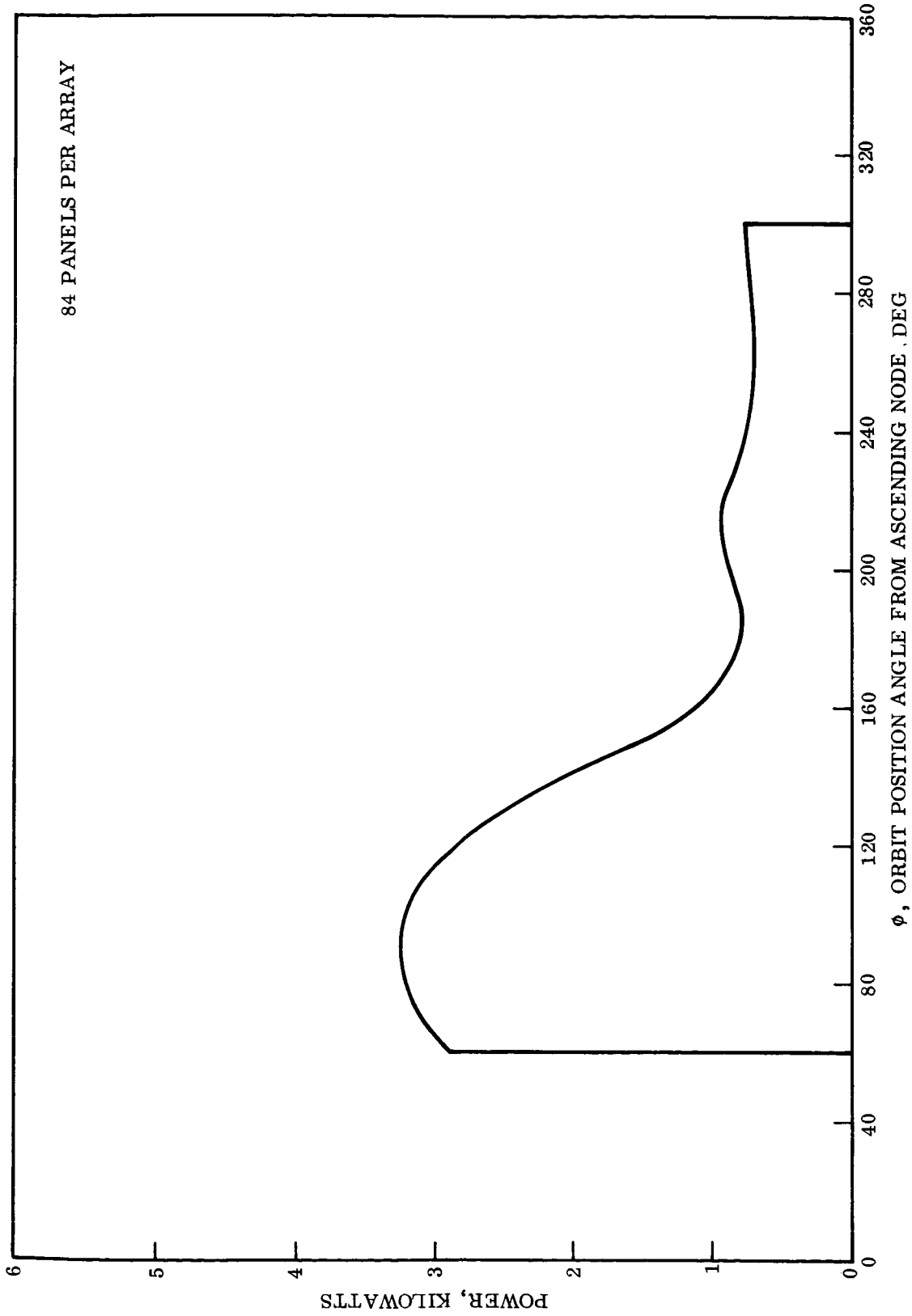
Fig. III-7 ASAP Power, $\beta = 52$, Arrays on $\pm Y$ Sides, Integrated Power = 1.08 kwh
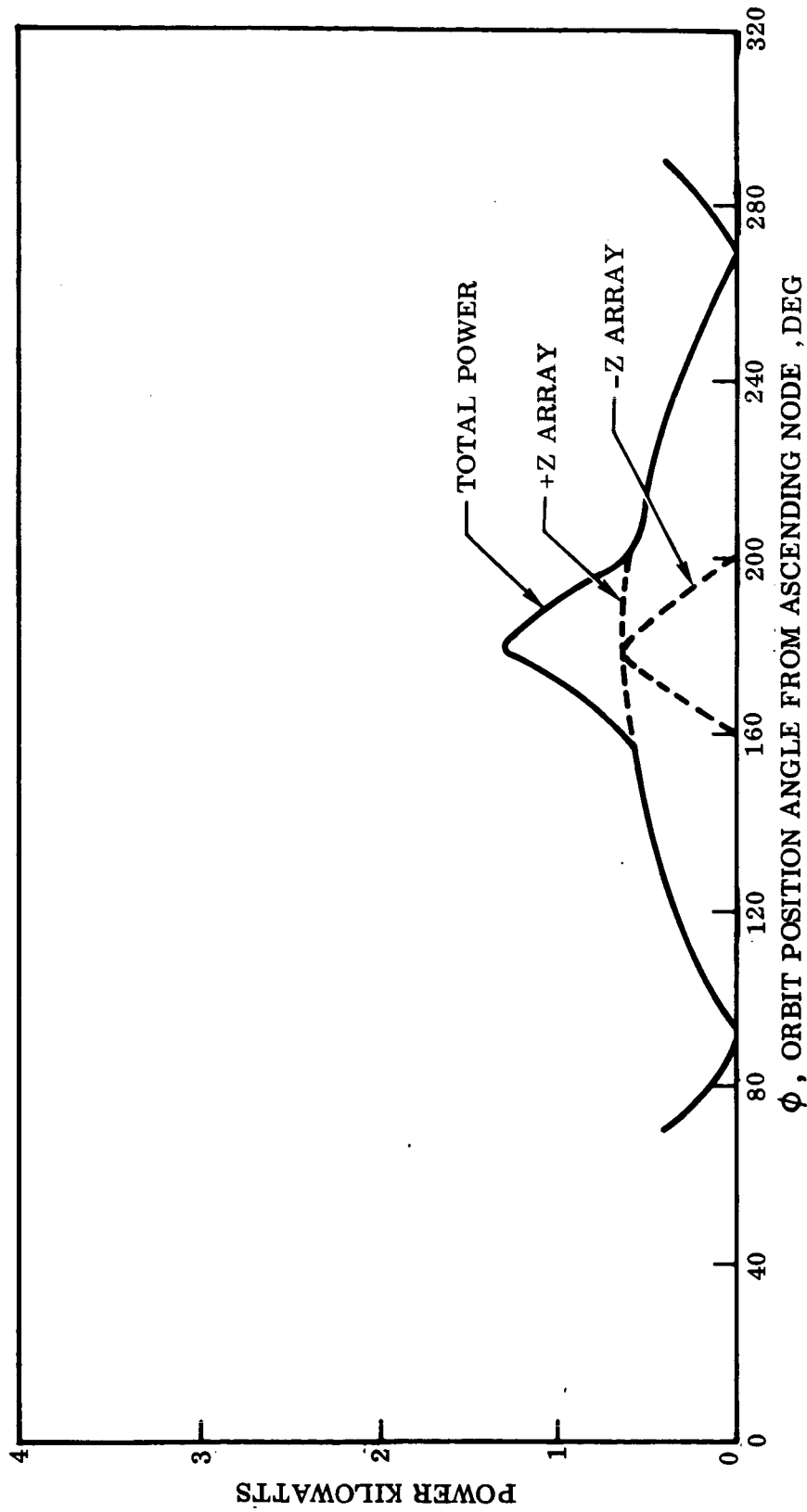
Fig. III-8 ASAP Power, $\beta = 0$, Arrays on $\pm$Z Sides, Integrated Power = 0.43 kwh

LOCKHEED MISSILES & SPACE COMPANY
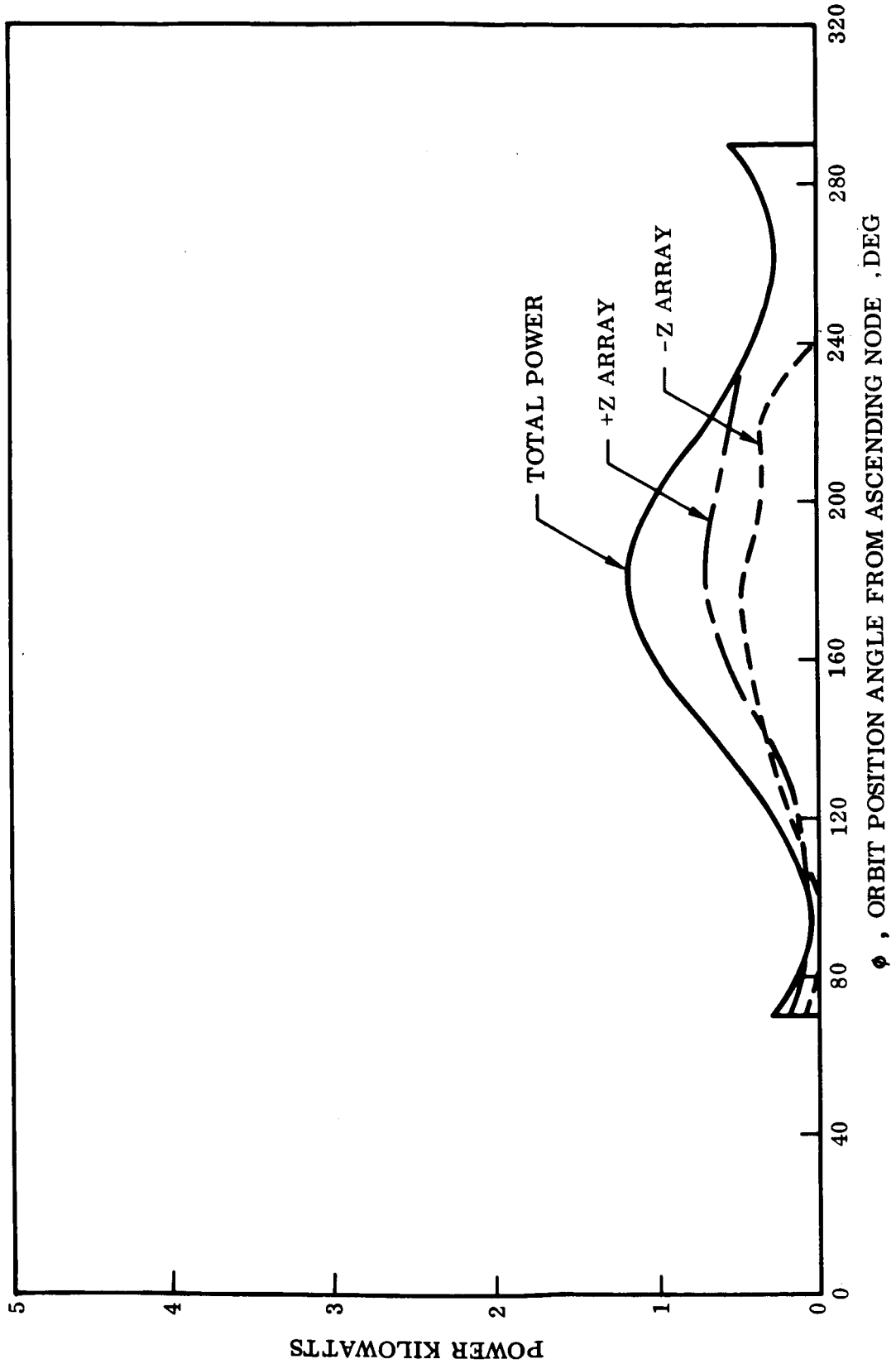
Fig. III-9 ASAP Power, β = 25, Arrays on ±Z Sides, Integrated Power = 0.54 kwh
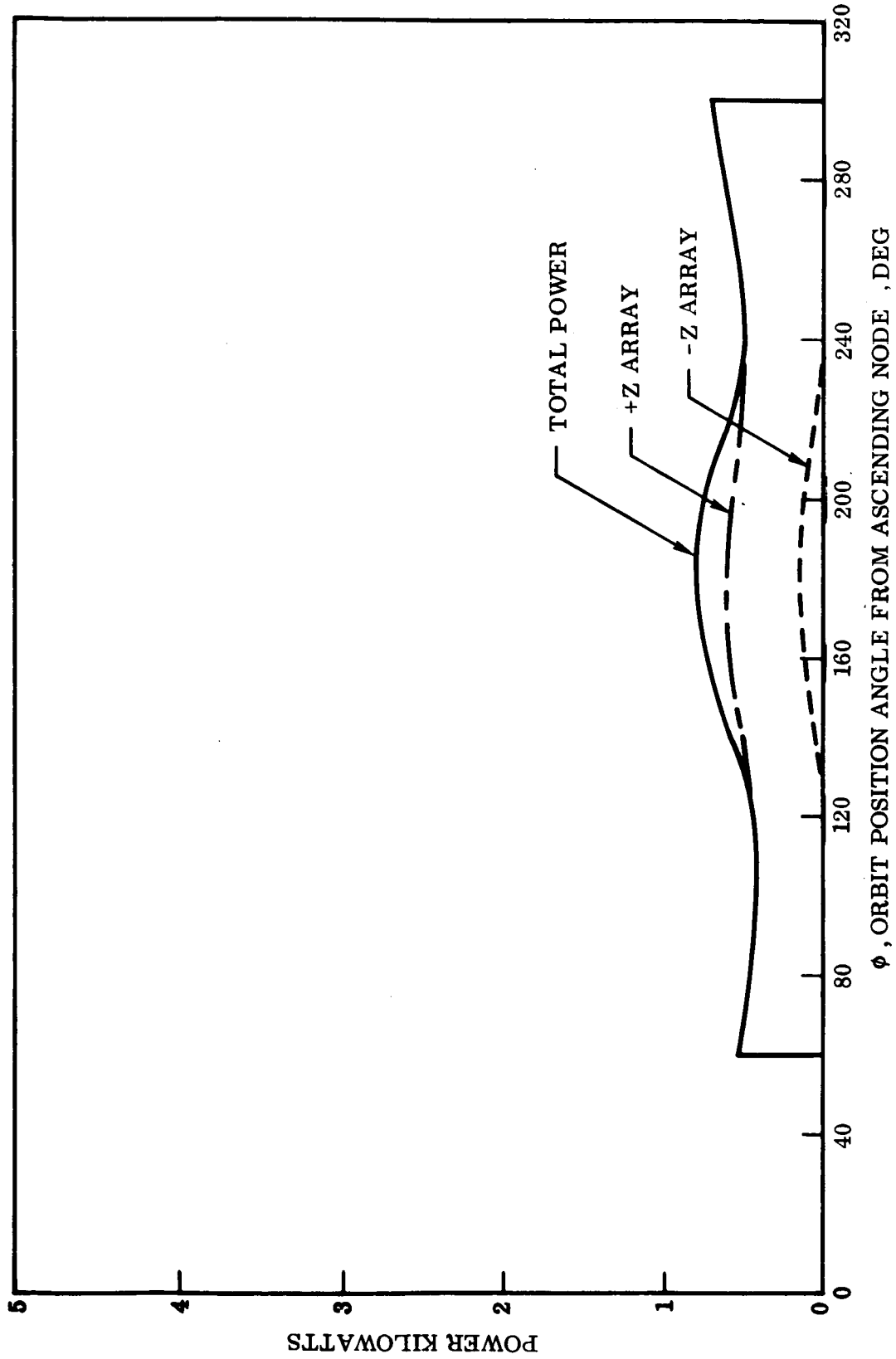
Fig. III-10 ASAP Power, β = 52, Arrays on ±Z Sides, Integrated Power = 0.62 kwh

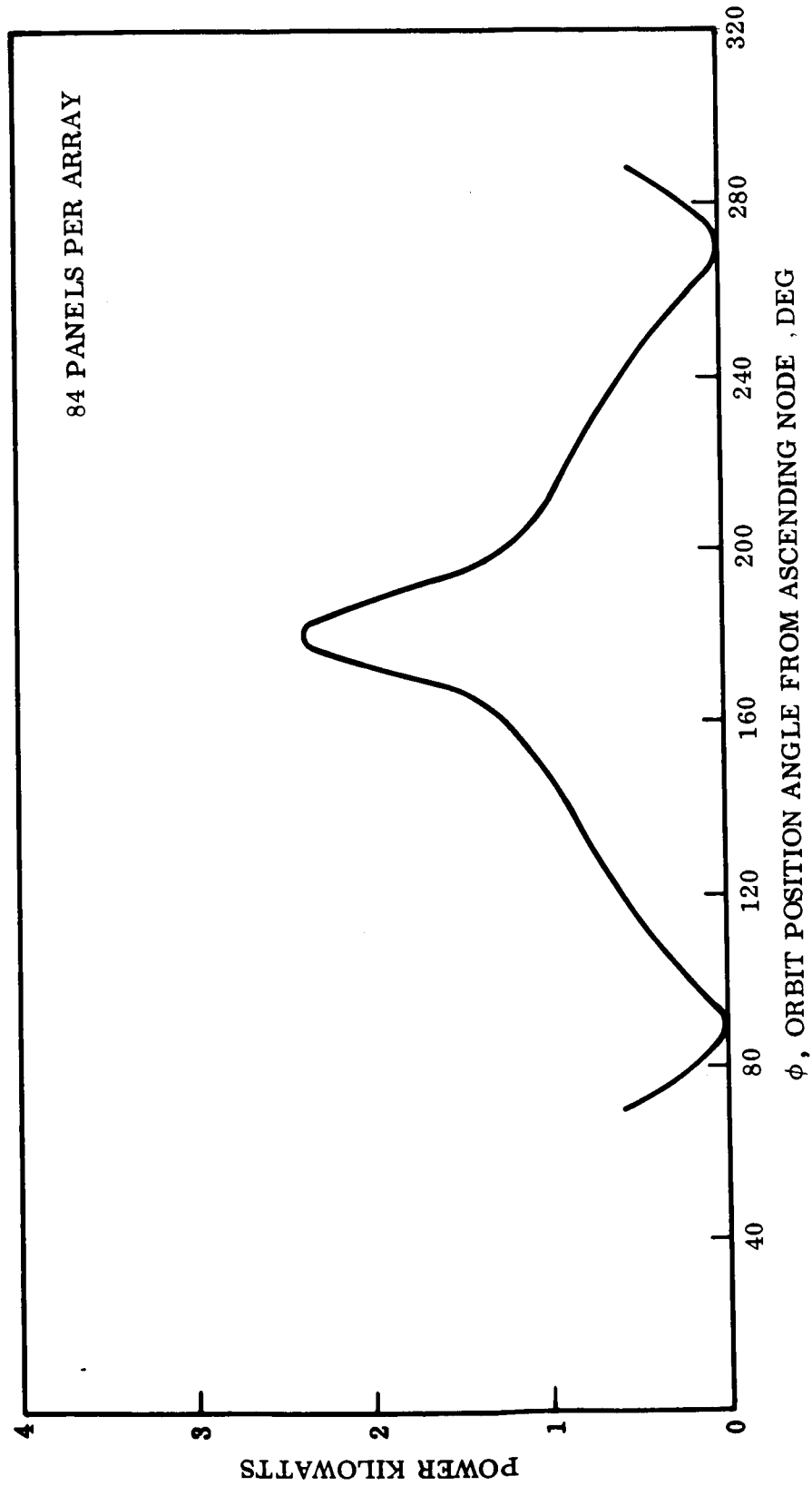Fig. III-11 ASAP Power, β = 25 Deg, Arrays on $\pm Z$ Sides, Integrated Power = 1.66 kwh

LOCKHEED MISSILES & SPACE COMPANY

Fig. III-12 ASAP Power, β = -52 Deg, Arrays on ±Z Sides, Integrated Power = 3.76 kwh
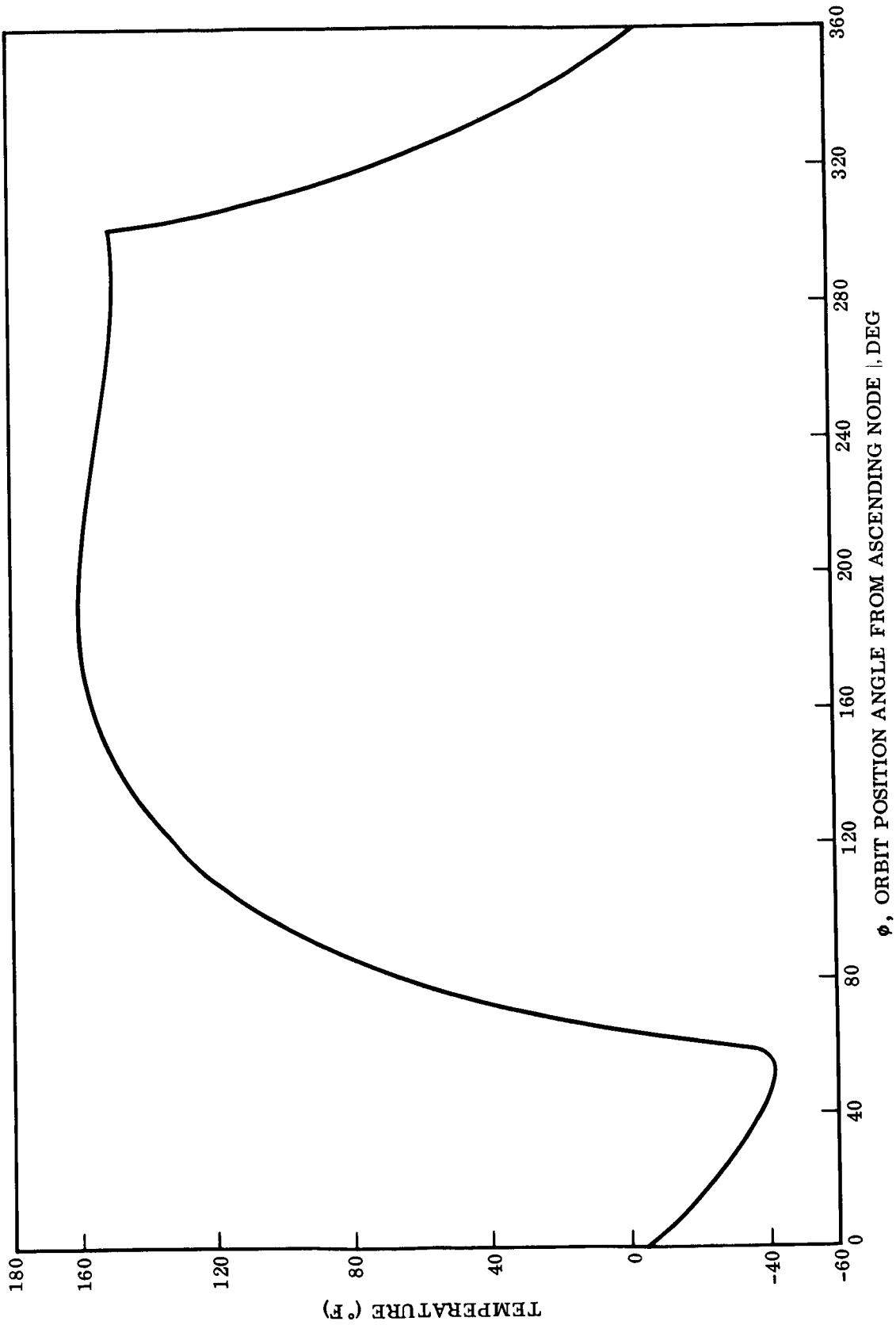
Fig. III-13   Solar Array Temperature, β = 52 Deg, Sun-Oriented Mode

Table III-2

TOTAL SOLAR ARRAY POWER, 84-PANEL ARRAYS

Orientation	Figure Number	Beta Angle	Total Power Generated Per Orbit (kwh)
Sun	14	0	9.63
Sun	14	52	10.49
Gravity Gradient, ±Y Sides	15	0	3.39
Gravity Gradient, ±Y Sides	16	25	2.86
Gravity Graident, ±Y Sides	17	52	1.72
Gravity Gradient, ±Z Sides	18	0	0.78
Gravity Gradient, ±Z Sides	19	+25	0.99
Gravity Gradient, ±Z Sides	20	+25	1.05
Gravity Gradient, ±Z Sides	21	-25	2.65
Gravity Gradient, ±Z Sides	22	-52	5.32
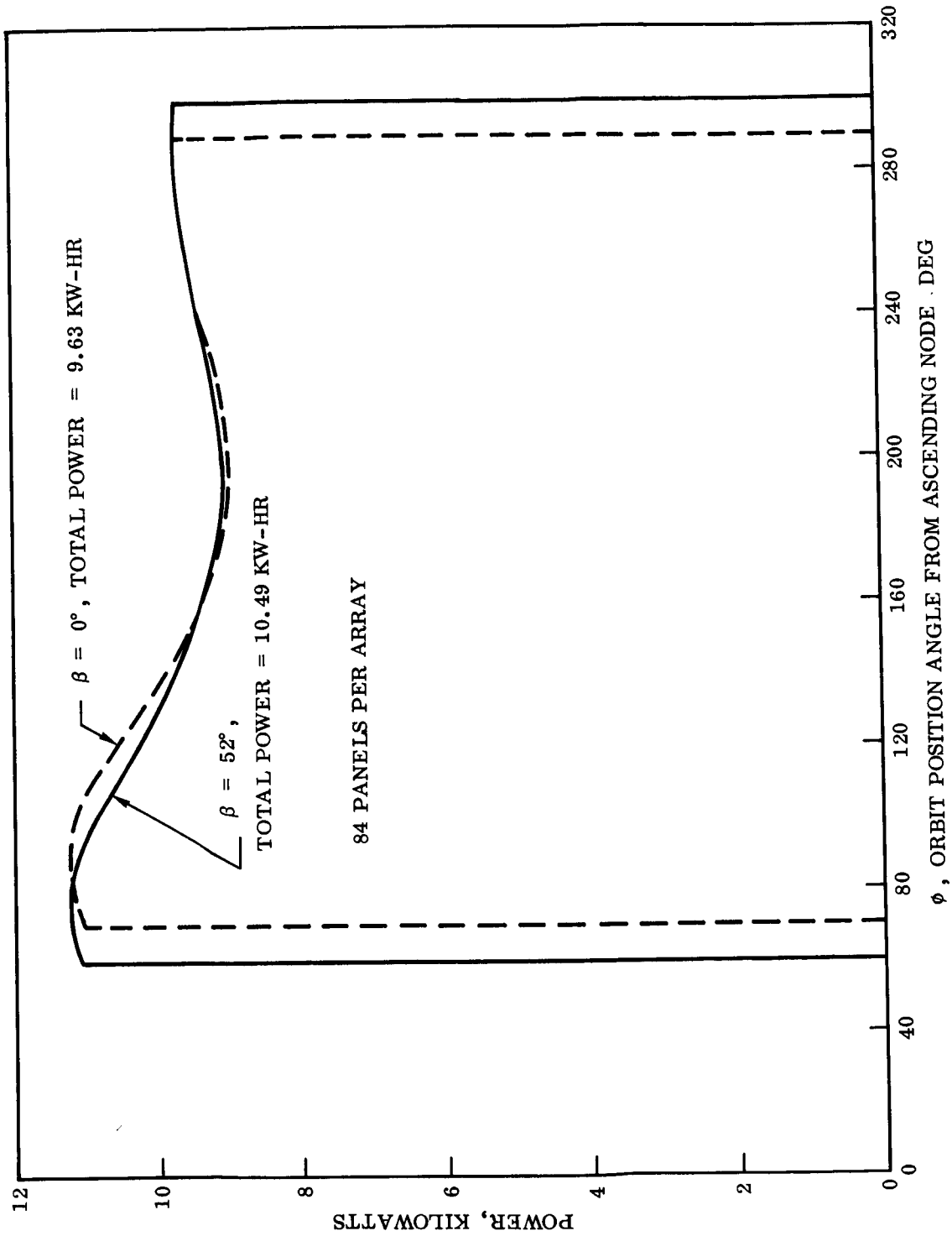
Fig. III-14 Solar Array Power, $\beta = 0$ Deg and 52 Deg, Sun-Oriented Mode

LOCKHEED MISSILES & SPACE COMPANY
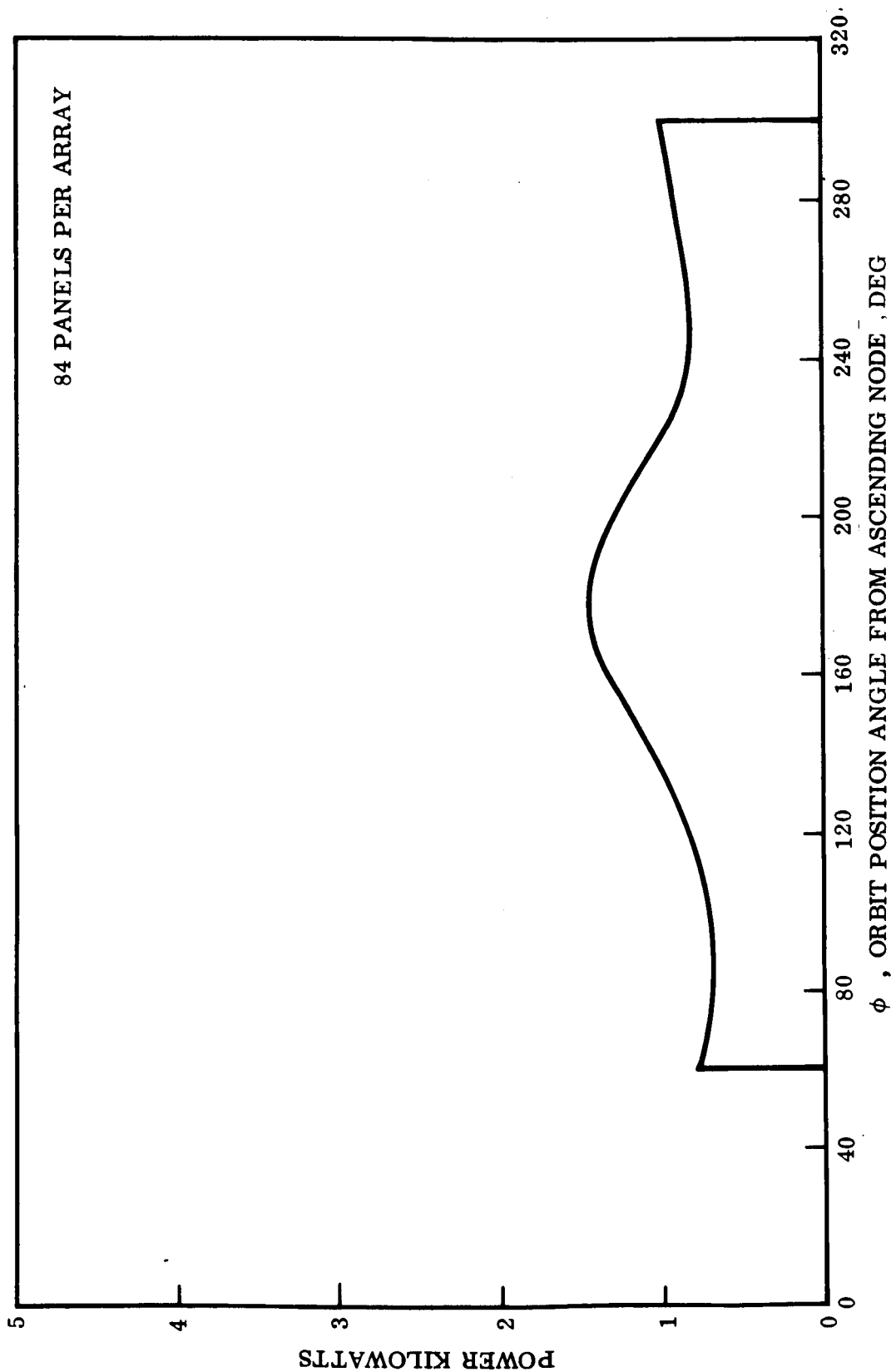
Fig. III-15 ASAP Power, $\beta = 0$ Deg, Arrays on $\pm$Y Sides, Integrated Power = 3.39 kwh
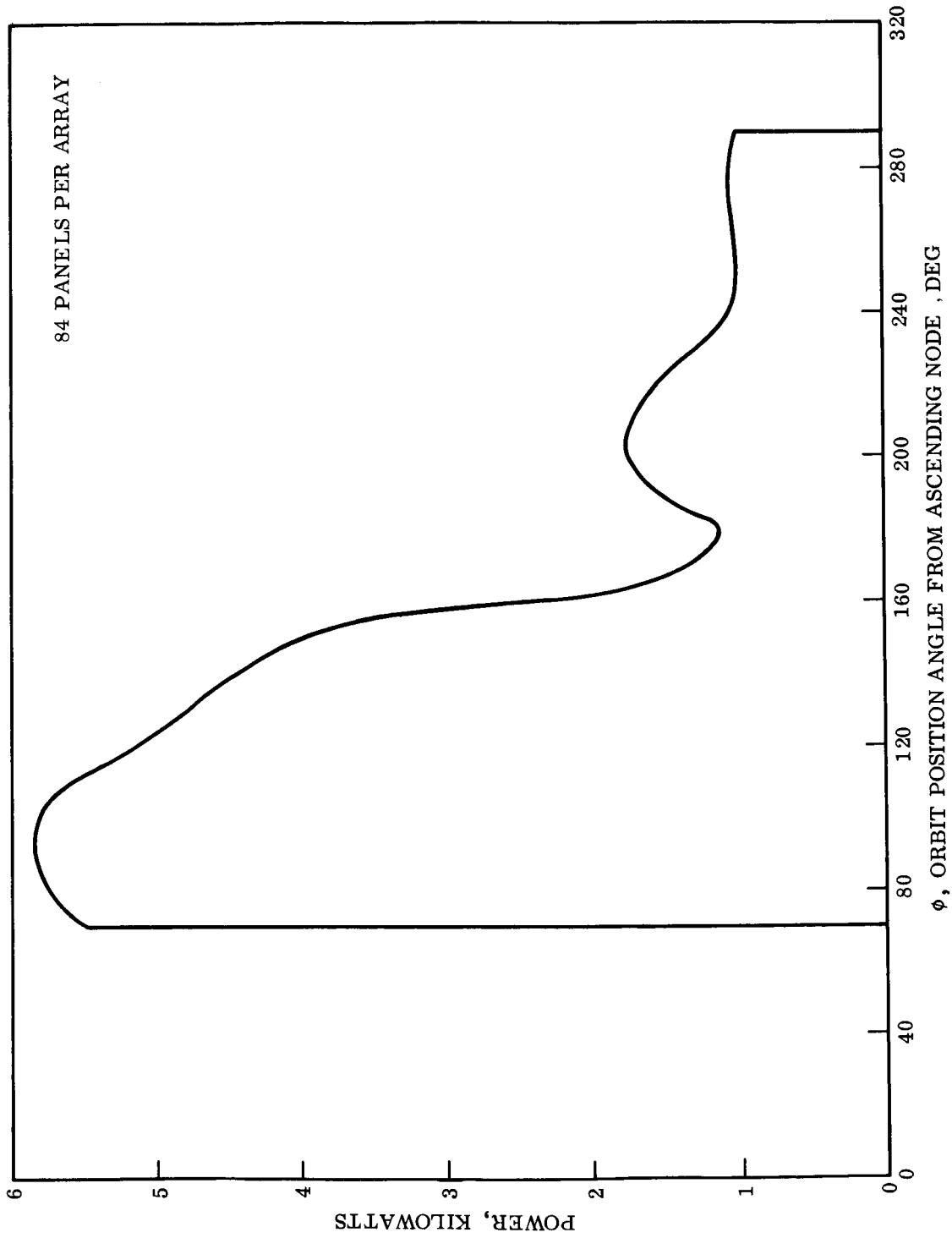
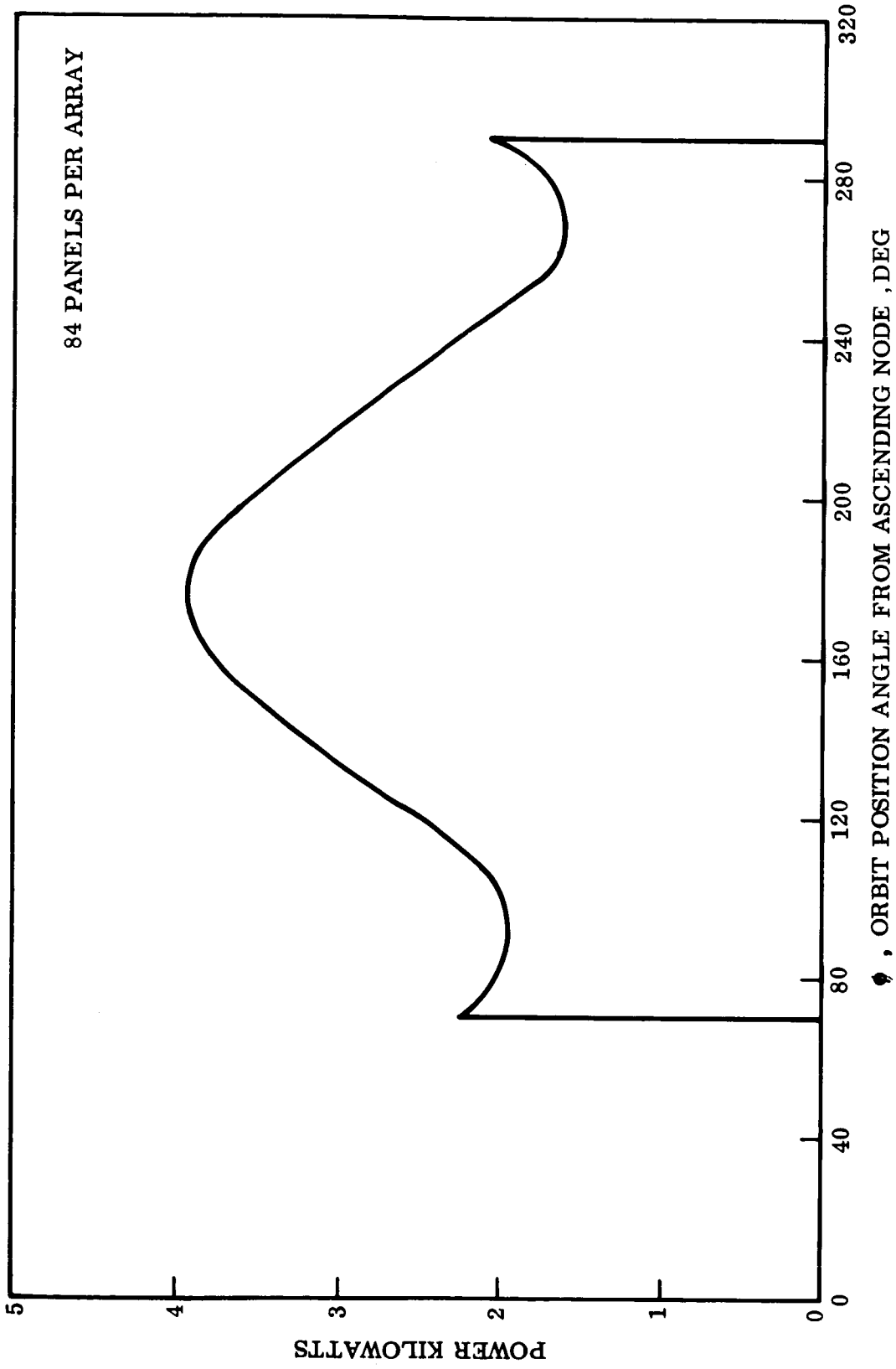Fig. III-16 ASAP Power, $\beta = 25$ Deg, Arrays on $\pm$Y Sides, Integrated Power = 2.86 kwh

LOCKHEED MISSILES & SPACE COMPANY

Fig. III-17 ASAP Power, β = 52 Deg, Arrays on $\pm$Y Sides, Integrated Power = 1.72 kwh

LOCKHEED MISSILES & SPACE COMPANY

Fig. III-18 ASAP Power, β = 0 Deg, Arrays on $\pm$Z Sides, Integrated Power = 0.78 kwh
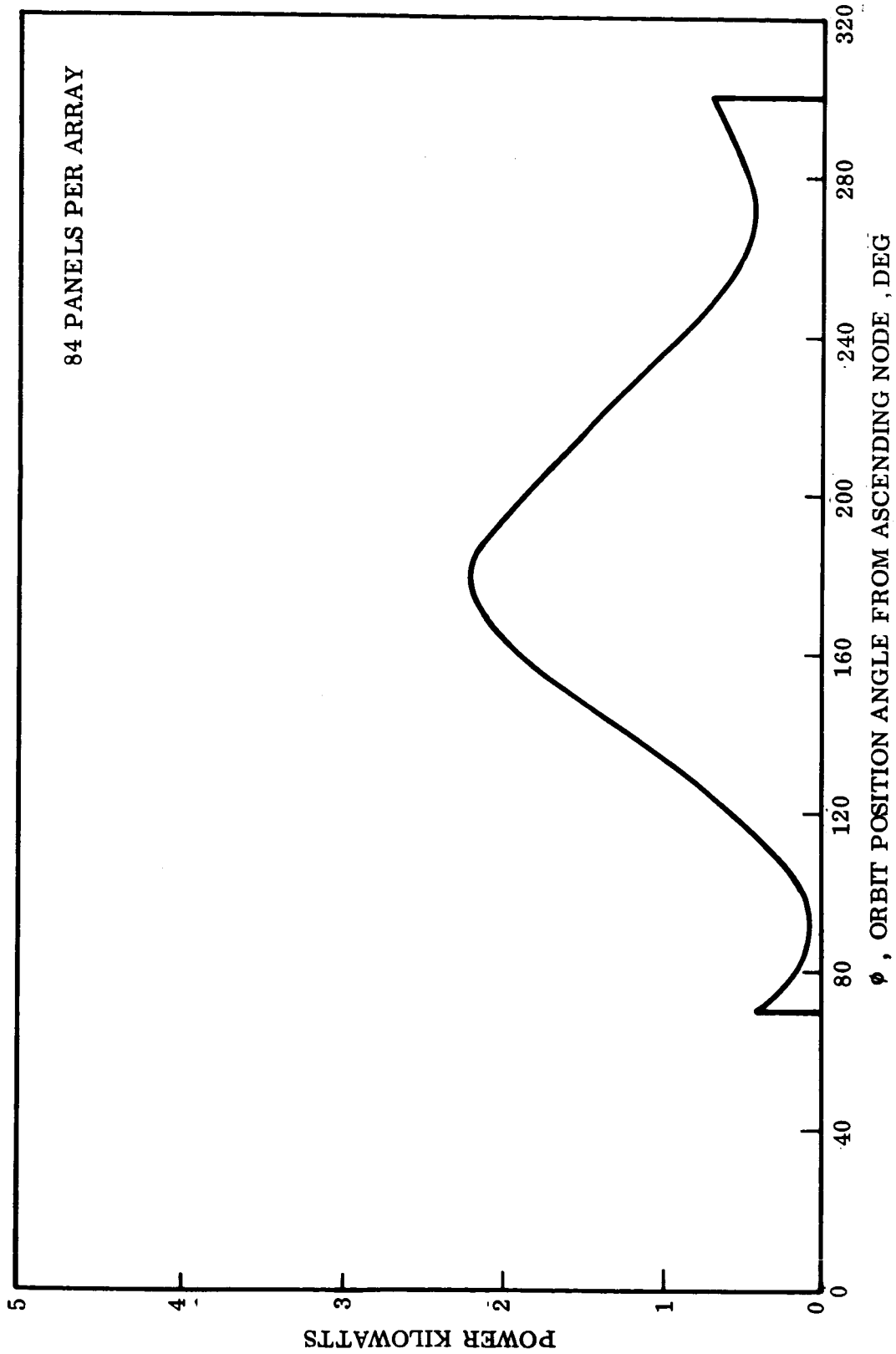
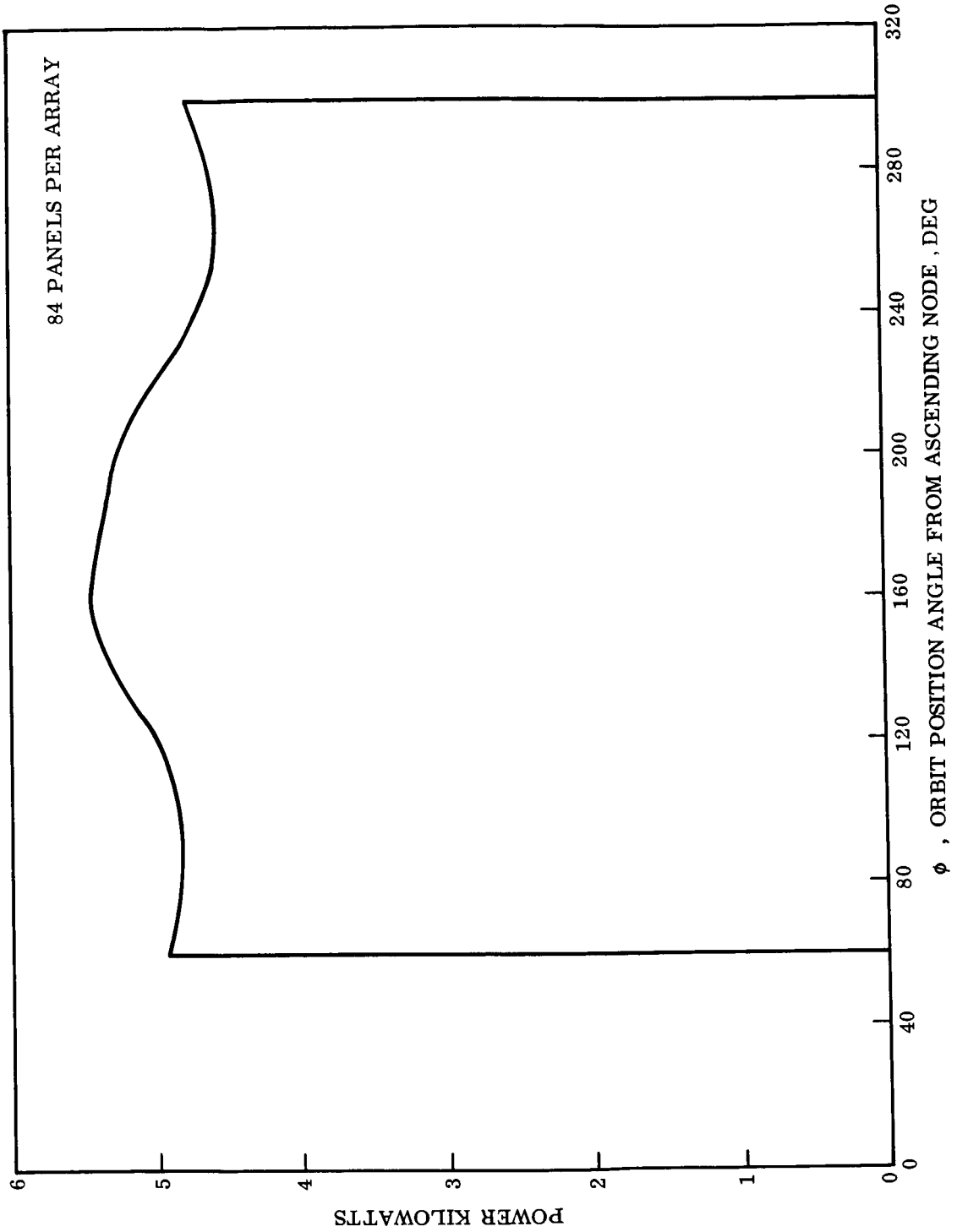Fig. III-19 ASAP Power, β = 25 Deg, Arrays on $\pm$Z Sides, Integrated Power = 0.99 kwh

Fig. III-20 ASAP Power, β = 52 Deg, Arrays on ±Z Sides, Integrated Power = 1.05 kwh

LOCKHEED MISSILES & SPACE COMPANY

Fig. III-21 ASAP Power, β = -25 Deg, Arrays on ±Z Sides, Integrated Power = 2.65 kwh

LOCKHEED MISSILES & SPACE COMPANY

Fig. III-22 ASAP Power, β = -52 Deg, Arrays on ±Z Sides, Integrated Power = 5.32 kwh

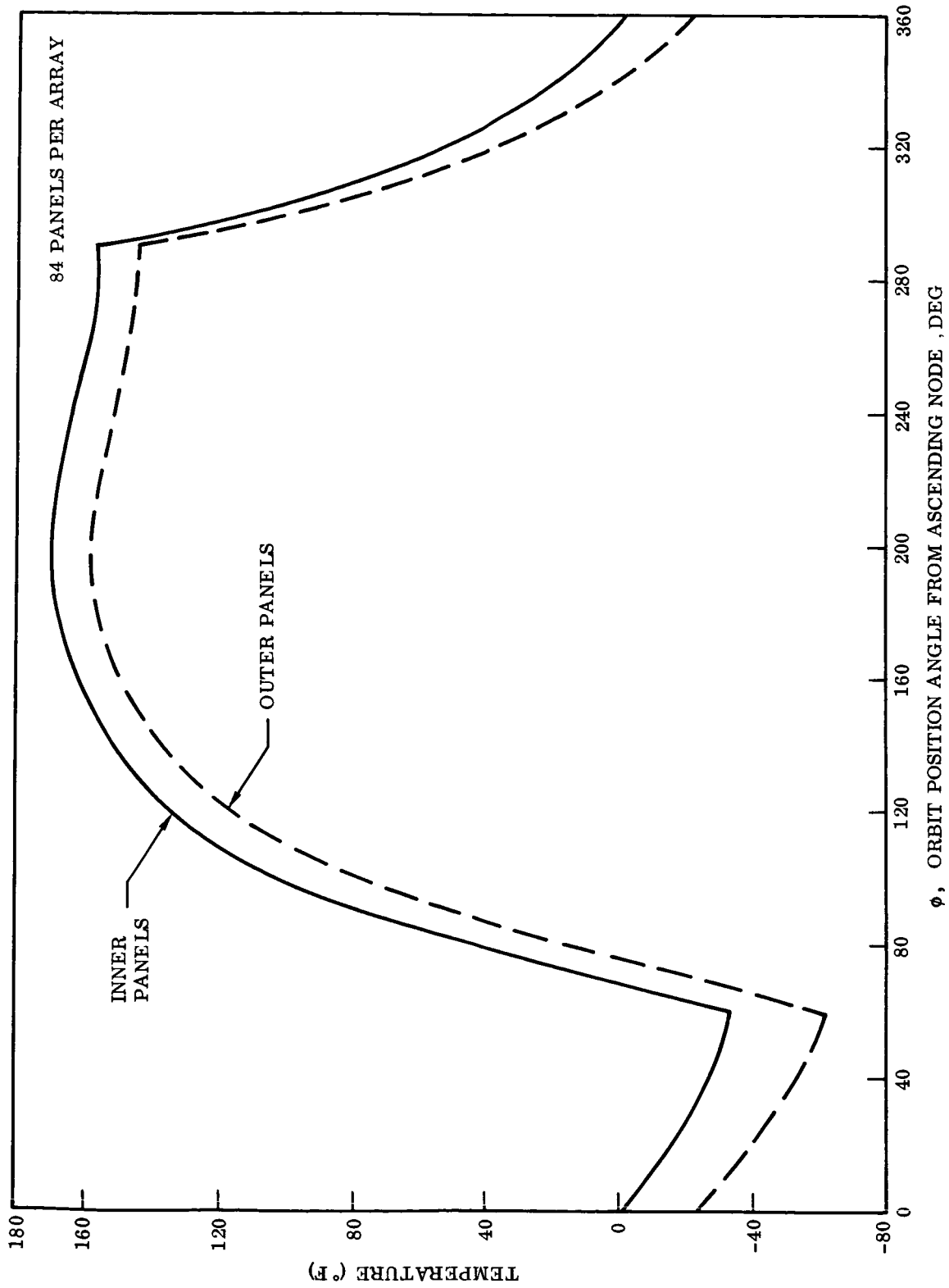LOCKHEED MISSILES & SPACE COMPANY

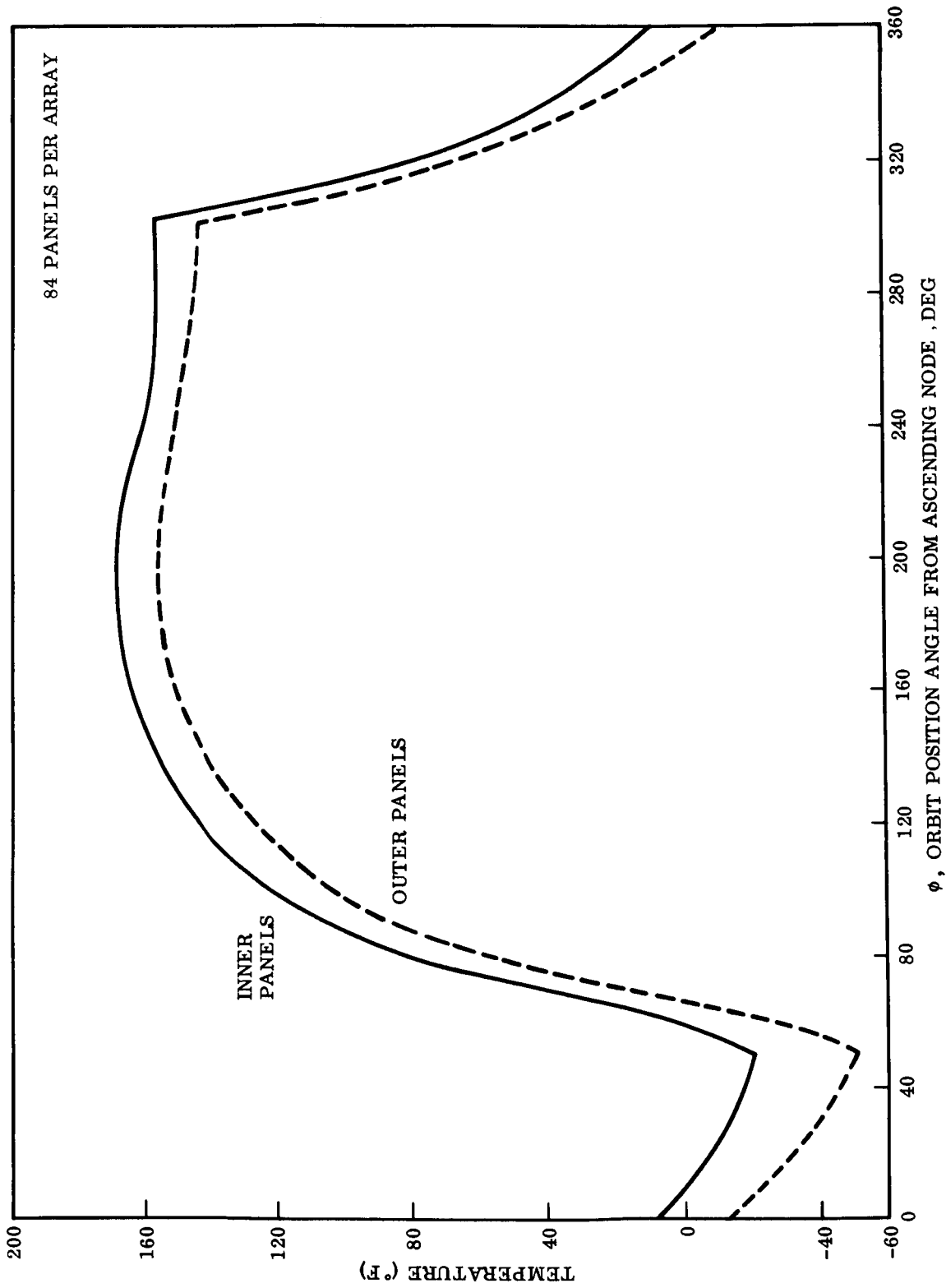Fig. III-23 Solar Array Temperature, $\beta = 0$ Deg, Sun-Oriented Mode

Fig. III-24 Solar Array Temperature, β = 52 Deg, Sun-Oriented Mode

LOCKHEED MISSILES & SPACE COMPANY